SDC-91-128

SDC
SOLENOIDAL DETECTOR NOTES

CONCEPTUAL DESIGN REPORT FOR THE STRAW-FIBER TRACKING SYSTEM FOR SDC

November 8, 1991

A.T. Goshaw, S. Oh, W. Robertson, M.Yin
Duke University

V. Hagopian, E. Hernandez, K. Hu, K. Johnson
Florida State University

Y. Arai, H. Ikeda
KEK, Tsukuba

J. Dainton
Liverpool University

J. Chapman, A. Dunn, J. Mann
University of Michigan

G. Alverson, A. Grimes, M. Glaubman, L. Leedom, S. Reucroft, T. Yasuda
Northeastern University

G. Alley, H. Brashear, C.L. Britton, Jr., M. Emory, T. Gabriel, R.M. Leitch, T. Ryan, D. Vandergriff
Oak Ridge National Laboratory

W.L. Dunn, M. van Haaren, F. O'Foghludha, A.M. Yacout
Quantum Research Services, Inc.

M. Edwards
Rutherford Appleton Laboratory

M. Corden, M. Mermikides, D. Xiao
Supercomputer Computations Research Institute

W. Fraszer, R. Henderson, R. Openshaw, M. Salomon
TRIUMF

M. Newcomer, R. van Berg, H.H. Williams
University of Pennsylvania

SDC-91-128

Conceptual Design Report for the Straw-Fiber Tracking System for SDC

Submitted to the

Solenoidal Detector Collaboration

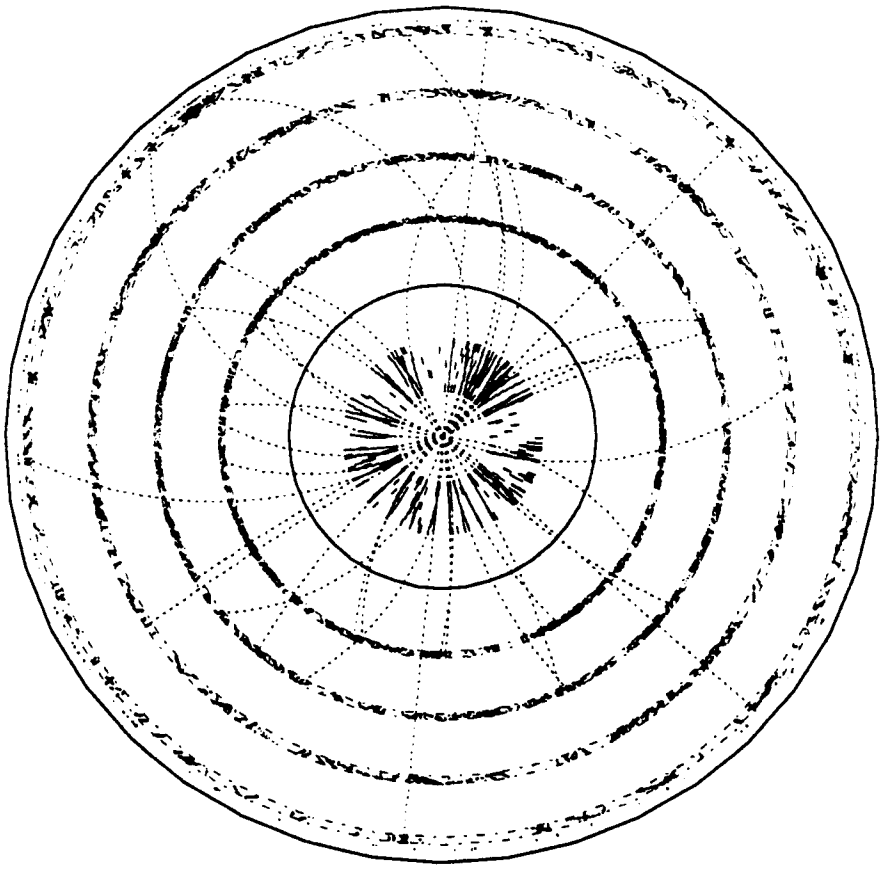

8 November 1991

Contributors*

A.T. Goshaw, S. Oh, W. Robertson, M. Yin
Duke University

V. Hagopian, E. Hernandez, K. Hu, K. Johnson
Florida State University

Y. Arai, H. Ikeda
KEK

J. Dainton
Liverpool University

J. Chapman, A. Dunn, J. Mann
University of Michigan

G. Alverson, A. Grimes, M. Glaubman,
I. Leedom, S. Reucroft, T. Yasuda
Northeastern University

G. Alley, H. Brashear, C.L. Britton, Jr., M. Emory
T. Gabriel, R.M. Leitch, T. Ryan, D. Vandergriff
Oak Ridge National Laboratory

W.L. Dunn, M. van Haaren, F. O'Foghludha, A.M. Yacout
Quantum Research Services, Inc.

M. Edwards
Rutherford Appleton Laboratory

M. Corden, M. Mermikides, D. Xiao
Supercomputer Computations Research Institute

W. Fraszer, R. Henderson, R. Openshaw, M. Salomon
TRIUMF

M. Newcomer, R. van Berg, H.H. Williams
University of Pennsylvania

Contacts: A.T. Goshaw and S. Reucroft

* We acknowledge the efforts of the following: S. Majewski, C. Zorn, *CEBAF*; S. Blake, T.S. Elleman, J. Paulos, *North Carolina State University*; H. Dautet, R. McIntyre, *EG&G, Canada*; C. Hurlbut, *Bicron*; F. Amirani, *Mitsui*; T. Shimizu, *Kurary*.

Straw-Fiber Tracking System for SDC

Abstract

This Conceptual Design Report (CDR) provides a comprehensive account of the feasibility, design, performance, integrability, upgradability, and cost of a straw-fiber tracking system that offers significant advantages for incorporation as the central tracker in the Solenoidal Detector Collaboration (SDC) detector. The straw-fiber tracking system capitalizes on the best features of both straw-tube drift cells – *e.g.*, excellent single-track resolution, low cost, and good r,ϕ coverage with modest channel count – and plastic scintillating fibers – *e.g.*, good two-track resolution, ease of stereo operation, and low occupancy; it does so in a robust way that also minimizes construction and operation difficulties. The straw-fiber tracking system does not push the limits of either straw-tube or fiber technology, the number of channels is optimized for the various purposes, and construction techniques are kept simple. The result is that the cost of the straw-fiber tracking system is less than or comparable to either all-straw or all-fiber options. Cost estimates by ORNL based upon a detailed Work Breakdown Structure are $28.8 M exclusive of straw electronics, or $38.5 M inclusive.

The straw-fiber approach *naturally* accommodates upgrading and staging requirements and thus long-term costs are also minimized. Detailed simulations – which account for time-of-flight and drift/wire propagation times, event pileup, dead time, time spectra and cuts, and dead space – demonstrate excellent physics performance of the straw-fiber system when used in conjunction with the silicon tracker. The system described in this report utilizes single straws (with modular electronics) but the straw-fiber approach can accommodate either single- or modular-straw construction techniques. The fiber superlayers require only a modest number of readout channels (54k initially) and do not place severe restriction on the per channel cost of the readout device (VLPC or APD). This CDR demonstrates that the straw-fiber approach offers significant advantages in performance without compromising cost. It permits a straightforward and inexpensive upgrade to accommodate higher than design luminosity and is a flexible option for central tracking in the SDC detector.

Conceptual Design Report for the Straw-Fiber Tracking System for SDC

	Page
1. Introduction	1
1.1 Overview of proposed design	1
1.2 Physics performance	5
1.3 Technical and engineering feasibility	5
1.4 Cost and schedule	7
1.5 Report organization	8
2. Design of barrel tracker	9
2.1 Optimized superlayer structure	9
2.2 Straw tube superlayers	10
2.3 Scintillating fiber superlayers	17
2.4 Mechanical support structures	21
2.5 Electronics and utilities	37
2.6 Material in SFTS	41
3. Physics performance	45
3.1 Simulation procedure	45
3.2 Pattern recognition	48
3.3 Single isolated track resolution	49
3.4 Higgs $\rightarrow Z^0Z^0 \rightarrow$ 4 leptons performance	52
3.5 Tracks in jets	52
3.6 Matching to outer detectors	52
3.7 High luminosity	52
3.8 Implications of further descoping	56
3.9 Interdependence of inner and outer trackers	56
4. Trigger capability	61
4.1 The single superlayer trigger	62
4.2 Simulation of the superlayer trigger	64
4.3 Chip performance	67
4.4 Trigger modularity and data flow	69
4.5 Summary	70
5. Integration with other systems	71
5.1 Overview	71
5.2 Silicon tracker	71
5.3 Intermediate tracker	73
5.4 Calorimeter	73
5.5 Barrel Toroid	75

Conceptual Design Report for the
Straw-Fiber Tracking System for SDC (continued)

	Page
6. Other factors	77
6.1 Staging and upgrade	77
6.2 Maintenance and repairs	78
6.3 Radiation hardness	78
7. Cost	81
7.1 Methodology	81
7.2 Breakdown	83
7.3 Work breakdown structure	86
7.4 Shell cost analysis	91
8. Schedule and milestones	93
8.1 Schedule summary	93
8.2 Critical R&D	93
8.3 Risk considerations	98
9. Conclusions	101
10. References	107

Appendices
A. Bicron ribbon cost estimate
B. Schedule Detail

Cover: *The cover shows a simulated event of the type Higgs* $\rightarrow Z^0Z^0 \rightarrow$ *4 muons. The simulation inluded four straw superlayers, an outer fiber superlayer, and a full silicon system.*

1. Introduction

1.1. Overview of proposed design

The straw-fiber tracking system (SFTS) described in this document takes advantage of the natural strengths of the alternate tracking technologies. Straw tubes yield excellent single track resolution while plastic scintillating fibers of the appropriate diameter yield good two track resolution. A straw tube system has fewer channels than a comparable fiber system. Straw tubes can be readily used parallel to the beam line to give high precision azimuthal track measurements but only with some difficulty to give stereo information. Fibers on the other hand are natural stereo detectors but require a prohibitive number of precisely aligned channels in order to attain the azimuthal precision and pattern recognition capabilities of straw tubes. At a given radius, fibers have lower occupancy than straw tubes.

The SFTS has been designed to cover the radial region from 50 to 170 cm and the pseudorapidity range $|\eta| < 1.6$. The detection elements – 4 mm diameter straw tube drift cells and 1.0 and 1.5 mm diameter scintillating fibers – are laid in superlayers on the outer surfaces of concentric support cylinders whose axes coincide with that of the colliding beams. These stable base cylinders span the length of the tracking region with no support structures or other mechanical frames within the barrel tracking volume. The detection elements are split at $\eta = 0$ and read out at the ends of the superlayers. The structure and location of the superlayers has been selected to allow a fast level-one trigger and to provide reliable pattern recognition and precise momentum resolution for charged tracks when taken in conjunction with complementary information provided by the silicon tracker and a preliminary version of the gas microstrip intermediate tracker.

Figure 1.1 illustrates the superlayer configuration of the straw-fiber tracking system. Straw tubes are used for precision azimuthal tracking and scintillating fibers are used for stereo tracking (at large radius) and for all tracking at small radius where high-luminosity occupancy limits the usefulness of straws. The detailed structure of each of the six superlayers is presented in Table 1.1. The basic logic behind this design is simple. It attempts to maximize the strengths of straw tubes and scintillating fibers while minimizing total cost.

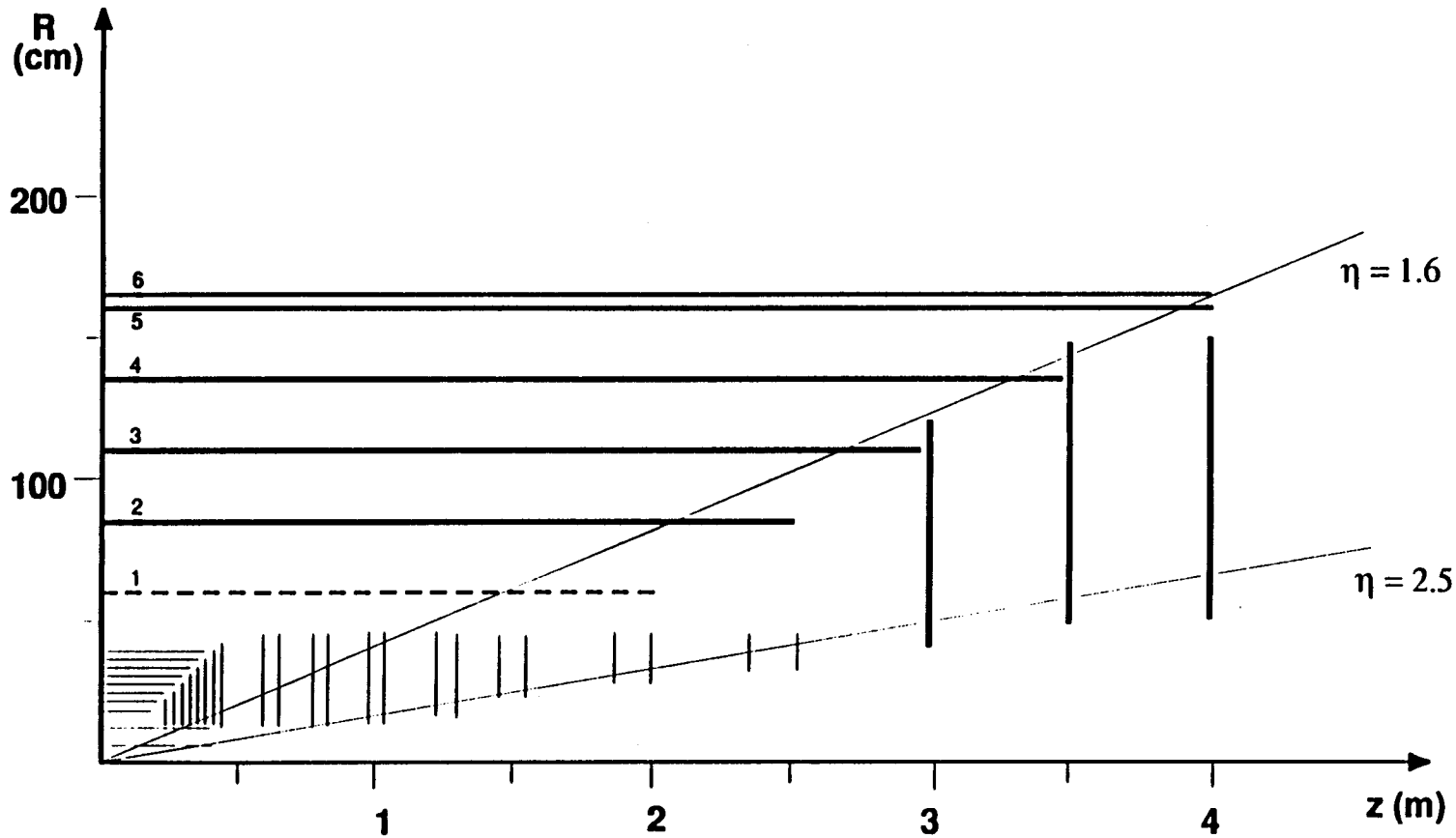

FIG. 1.1. Profile of one-quarter of the straw-fiber tracking system including one possible silicon and intermediate tracker architecture. Superlayer 1 consists of 2z 1-mm fibers separated by 4 cm from 2z 2u 2v 1-mm fibers; superlayers 2 and 3 consist of 6z 4-mm straws; superlayers 4 and 5 consist of 8z 4-mm straws; and superlayer 6 consists of 2u 2v 1.5-mm fibers. Superlayers 2-6 form the inital tracker; superlayer 6 is a staging option.

TABLE 1.1

Straw-fiber barrel tracking system summary

Superlayer	Radius (cm)	Length (m)	Pseudorapidity Range	Structure	Readout Channels	Radiation Length at $\eta = 0$ ($\%X_0$)
1 (staged)	60	4	± 1.9	1 mm fibers 2z (4 cm gap) 2z 2u 2v ± 5° stereo	62.1k	2.2
2	85	5	± 1.8	4 mm straws 6z	15.3k	0.7
3	110	6	± 1.7	4 mm straws 6z	19.9k	0.7
4	135	7	± 1.7	4 mm straws 8z	32.5k	0.8
5	160	8	± 1.6	4 mm straws 8z	38.5k	0.8
6	165	8	± 1.6	1.5 mm fibers 2u 2v ± 5° stereo	54.2k	1.5

Total number of readout channels:

Initial 106.2k straws plus 54.2k fibers
Staged 106.2k straws plus 116.3k fibers

Comments:

1. Superlayers 1, 2, 3, 4 and 5 provide pattern recognition and P_t measurement in the r-ϕ plane.
2. Superlayers 1 and 5-6 provide vector track segments localized in r-ϕ-z.
3. Superlayers 4 and 5 provide the level 1 P_t trigger.
4. This CDR assumes the "high luminosity" superlayer 1 will be staged and reports performance based upon superlayers 2-6 only.
5. Since superlayer 6 is at 165 cm radius and superlayer 1 is staged, the material budget of 3.0% includes only superlayers 2-5.

Straw Tube Superlayers

The four straw tube superlayers are constructed of 4 mm diameter straw tubes with axial sense wires. This is the simplest mechanical configuration for straw tubes since they can be supported directly by the stable base cylinder and the tubes pack hermetically. The same construction technique can be used for all four superlayers (see Section 2.2 for details). Superlayers 2 and 3 are six straw tubes deep and superlayers 4 and 5 are eight straw tubes deep, for a total of 105.3k straw channels. The four superlayers provide pattern recognition in the r-ϕ plane and, in conjunction with the silicon tracker, precise P_t measurements for $|\eta| < 1.6$ (see Section 3). Uniformity of tube placement within a superlayer also provides the simplest (and fastest) pattern recognition for track segments. Superlayers 4 and 5 provide the stiff track information needed for the level one high P_t trigger. This design optimizes the efficiency of the trigger by placing the trigger layers 4 and 5 at the maximum radius (see Section 4).

Scintillating Fiber Superlayers

Superlayers 1 and 6 are constructed of scintillating fibers. The design of these superlayers takes advantage of the ability of scintillating fibers to handle high luminosities and to easily provide stereo information. Superlayer 6 uses 54.2k readout channels of 1.5 mm diameter fibers to make $\pm$ 5° stereo measurements (see Table 1.1). Superlayers 5 and 6 thus provide a charged particle track segment, localized in r-ϕ-z, as close as possible to the barrel calorimeter. The innermost superlayer (number 1 at radius 60 cm) is composed of 62.1k readout channels of 1 mm diameter scintillating fibers. This superlayer forms a track segment localized in r-ϕ-z as described in Table 1.1. The necessity of this "high luminosity" superlayer depends on detailed trade offs between the construction of the outer and silicon barrel trackers.

For the purpose of this Conceptual Design Report we include superlayer 1 as a staged or upgrade option in the mechanical design of the barrel tracker and carry out our performance evaluation using only superlayers 2 to 6. This system, then, has 106.2k straw tube and 54.2k scintillating fiber readout channels. The radiation length at $\eta = 0$, including support structure, is 3.0% (see Table 1.1 for details). This excludes the 1.5% X_0 thickness of superlayer 6 which is adjacent to the coil. The most uncertain part of this barrel tracker design is the interface with the intermediate tracker, although our system can readily accommodate all of the

intermediate tracker alternatives presently under active consideration. Figure 1.1 illustrates that continuous tracking coverage out to $|\eta| = 2.5$ can be obtained. The physics performance of this system when used in conjunction with the silicon tracker is summarized below.

1.2. Physics performance

Section 3 contains a detailed description of the procedure used to simulate the behavior of the SDC tracking system. The results presented are based upon the initial stage of the straw-fiber barrel (superlayers 2-6) plus a version of the silicon tracker with eight barrel layers. Although the procedure is still being developed and improvement work is in progress, it is already sophisticated enough to allow us to make some important conclusions:

- Track finding efficiency is high even above design luminosity. For example, the efficiency for reconstructing high-P_t muons (≥200 GeV/c) is greater than 99% at design luminosity and greater than 95% at 5×10^{33} $cm^{-2}s^{-1}$. A low statistics high luminosity run indicated that the efficiency is never less than 75% even at a luminosity of 10^{34} $cm^{-2}s^{-1}$.
- The momentum resolution for high-P_t muons (200 GeV/c) is ~2.5% at design luminosity and degrades slowly as the luminosity increases, being ~4.5% at 5×10^{33} $cm^{-2}s^{-1}$.
- The outer fiber stereo superlayer is important. Even with a silicon inner tracking working perfectly, it reduces the error on the reconstructed dip angle significantly and produces a high resolution ϕ-z measurement of tracks as they leave the tracking system and enter the calorimeter ($\sigma_z \sim 3$ mm).
- The innermost fiber superlayer is crucial at high luminosity. At design luminosity it will reduce the need of the outer tracker for a fully operational inner tracker.

1.3. Technical and engineering feasibility

The straw-fiber barrel tracker is a robust system which is feasible because it optimizes with respect to the two contributing technologies thereby avoiding the technologically difficult aspects of each. The proposed stable-base cylinder approach employs simple straw and fiber superlayer construction techniques; straws are glued axially in successive layers onto high-precision cylinders (although straw modules are allowed they are not required) and fibers are installed in ribbons (both axial and in stereo) which assure interfiber registration. Specifically, the SFTS reduces the

technical and engineering difficulties associated with straw-tube drift cells and scintillating fibers because of the following:

- all straws are axial, permitting simple and uniform construction
- quarter-fiber overlapping techniques are not needed
- the number of fiber channels is minimized (54.2k)
- since the fibers are large (1.5 mm diameter), light output is relatively high and fiber electronics requirements are modest; alternative readout devices (APD's, VLPC's, or even PMT's) are possible and the same fiber readout technology can be used for the SFTS as for the Shower Maximum Detector.

With respect to triggering, the SFTS allows multiple 8-straw superlayers for redundancy. In the system as proposed, two 8-layer straw superlayers are planned. A distinguishing feature of the SFTS is that two other straw superlayers could be used for triggering, since none are needed for stereo. If triggering considerations indicate that three 8-straw superlayers are particularly advantageous (as has been suggested by Chapman), one of the remaining 6-layer superlayers could be upgraded at minimum cost to contain 8 layers.

As discussed in Section 8.2, there are few critical R&D issues associated with the SFTS. Radiation damage testing indicates that both straws and fibers will likely be sufficiently rad-hard for central tracking purposes. The central tracking volume is subject to lower doses and fluences than portions of the calorimeter and the intermediate tracking volumes. All of the remaining issues – *e.g.*, lowering the operating voltage of straws, fiber coupling, fiber readout, ribbon manufacture – appear to be soluble with modest R&D effort. Also, most must be dealt with for other parts of the detector and so the tracking application does not constitute an additional technology development burden.

The SFTS proposes incorporating both straws and fibers from the beginning and optimizing the mix to the evolving requirements. This approach maximizes technical feasibility, since the actual mix of straws and fibers can be adjusted to accommodate cost, occupancy, radiation hardness, and other considerations which may change with time.

1.4. Cost and schedule

We have performed a WBS costing exercise to at least level 5 for the first stage of the straw fiber tracker (superlayers 2-6 described in Table 1.1). We have used basically the same guidelines for the mechanical and fiber costing as those described in the note written by Koltick and Vandergriff[1] for the baseline fiber tracker. Straw tube electronics costs were developed at ORNL and at the University of Pennsylvania. Some features of the SFTS which result in cost savings are:

- The same mechanical engineering concept is used for both straw and fiber superlayers.
- All straws are axial, which allows simple and uniform construction.
- Rather than buying scintillating fiber from industry and manufacturing the fiber ribbons, we propose to purchase the ribbons ready-made. We include (see Appendix A) an informal BICRON bid showing the anticipated ribbon cost.
- Since we do not use fibers for precision momentum determination, we do not need to use very small diameter fibers. This reduces significantly the number of fiber channels and also reduces the demands on the fiber readout system.
- Similarly our fiber alignment demands are not so stringent and this reduces the cost of alignment.
- In the WBS we use the Rockwell/VLPC cost estimates to compute the fiber readout costs. The APD is expected to have similar per channel cost as the VLPC, but – since the APD is a room temperature device – all cryogenic costs are eliminated and the cost of the entire system would be significantly less.
- The proposed Shower Maximum Detector is also likely to use the APD for readout, so using the APD in the tracker involves no new technology development.

The cost of the base SFTS has been estimated to be $38.5 M, including both straw and fiber electronics and allowance for contingencies; exclusive of straw electronics, the cost is estimated as $28.8 M. R&D costs over the next few years would be modest for the mixed system because the optimized matching of the straw tube and fiber techniques means that neither technique would need to be stretched beyond our current knowledge of its performance limitations. Also, the SFTS lends itself naturally and efficiently to staging and upgrade that might be required as machine luminosity is increased.

The Straw Fiber Tracking System has undergone a full schedule evaluation. This evaluation was done in conjunction with the Hybrid Central Tracking chamber task and is used as the basis of the current schedule summary, which is discussed in Section 8.1. Examination of the schedule illustrates the flexibility of the SFTS approach.

The schedule that has been developed for the SFTS provides a critical path for the program. The production of support cylinders are the first elements to appear. This is beneficial, as the production of the cylinders does not violate the current technology, and may therefore begin on schedule. Additional items on the path are the tracking elements. These appear later in the schedule, which permits additional time for completion of critical R&D items.

Development of an updated schedule is continuing. This schedule will include all resources needed for production of the tracker, as well as duration and logic specifications. The design of the SFTS allows the project to be schedule in a manner which best utilizes the manpower and resources of the SDC project.

The current schedule for the SFTS was prepared on a system called Project Scheduler 4. This schedule will be converted to the Open Plan system in the near future for inclusion in the overall SDC schedule roll-up.

1.5. Report organization

This report is written in the same general format as the SDC Letter of Intent,[2] with the intention that it, or portions of it, can easily be incorporated in the SDC technical proposal. The remaining sections of this CDR provide a concise but comprehensive review of the straw-fiber tracking system and upgrade/staging options. We begin in Section 2 with a description of the SFTS design. Section 3 discusses aspects of the physics performance of the SFTS under various assumptions related to other detector systems. Section 4 discusses triggering capability, section 5 treats the integration of the SFTS with other SDC detector systems, and Section 6 considers the issues of upgrade and staging, maintenance and repairs, and radiation hardness. Sections 7 and 8 treat, respectively, cost and schedule considerations, including risk factors. Section 9 provides a concise summary of the SFTS, including an assessment of its major features in a tabular format; this is followed by a list of references and several appendices which provide detailed backup to points made in the main text.

2. Design of barrel tracker

This section discusses in detail the construction of the superlayers, the mechanical support frames, assembly procedures and the required electronics and utilities. Issues dealing with the interface of the barrel tracker with other components of the Solenoidal Detector are presented in Section 5.

2.1. Optimized superlayer structure

The efficient use of straw tube tracking elements and plastic scintillating fibers in the SFTS provides a cost solution to the outer tracker design. It is recognized that both straw tubes and fibers have significant but opposing strengths for particle tracking. Straw tube superlayers are better than fibers for precision single track measurements. Fiber superlayers, on the other hand, are better and probably easier to construct than straw tube superlayers for stereo measurement. A fiber stereo layer can be positioned arbitrarily close to either straw or fiber axial layers. Fibers offer better occupancy characteristics and two track resolution than straw tubes. These strengths have been accented in the SFTS by judicious placement within the tracker.

Straw tubes are naturally used for axial tracking applications; their inherent ability to provide precise track measurement makes them ideal for high resolution momentum determination, especially at large radius when the track density provides an acceptably small occupancy even at high luminosity. Placing them in an axial arrangement on superlayers is simple whether in individual straws or straw modules. The use of 4 mm diameter straw tubes reduces the total channel count and dictates their use in the majority of the superlayers. This approach has been followed in the SFTS design.

Plastic scintillating fibers are easily used for stereo measurements. The optimized SFTS places the stereo fibers on the outer superlayer. This location provides several benefits. By placing the fibers at the largest radius, occupancy levels are reduced to less than a percent (at design luminosity), even for 1.5 mm diameter fibers. The use of larger fibers reduces the channel count and increases light output. This permits the use of current technology room temperature readout devices such as avalanche photodiodes (APD's). These points reduce both the cost of the tracker and the risk associated with the use of plastic scintillating fibers. In addition, this

outer stereo superlayer significantly reduces track angle uncertainties and provides a precision z -ϕ measurement of each particle track before entry into the calorimeter.

Staging of the SFTS has been included in the superlayer optimization. The inner radius region of the outer tracker has been reserved for additional scintillating fiber tracking elements. This is a natural staging scenario owing to the high luminosity capabilities of the fibers. The fiber diameter will be less in the staged portion than in the outer superlayers, providing increased track accuracy and reduced occupancy. The small superlayer diameter also limits the channel count to an acceptable level. Final considerations given to this scheme are the mechanical interface of the staged superlayer. By placing it at the inner superlayer, the structural modification and disassembly requirements are significantly reduced. Staging becomes a built-in upgrade path for the detector with the straw-fiber barrel tracker design.

An overview of the barrel tracker is shown in Fig. 2.1. The following sections describe the construction and assembly procedure.

2.2. Straw tube superlayers

The straw-fiber tracker contains four superlayers composed of 4 mm diameter straw tubes positioned parallel to the axis of the carbon fiber support cylinder. The basic parameters of these superlayers are given in Table 2.1

The radiation length of the superlayers assumes straw tube drift cells with 25 micron gold plated tungsten sense wires, 38 micron mylar cell walls and 0.15 micron copper cathodes. The contribution from the support cylinder to the radiation length of each superlayer is estimated to be 0.36% X_0.

TABLE 2.1

Straw tube superlayer structure

Superlayer	Radius (cm)	Length (m)	Structure (4 mm straws)	Readout channels	Radiation length at $\eta = 0$ (% X_0)
2	85	5	6z	15.3k	0.7
3	110	6	6z	19.9k	0.7
4	135	7	8z	32.5k	0.8
5	160	8	8z	38.5k	0.8

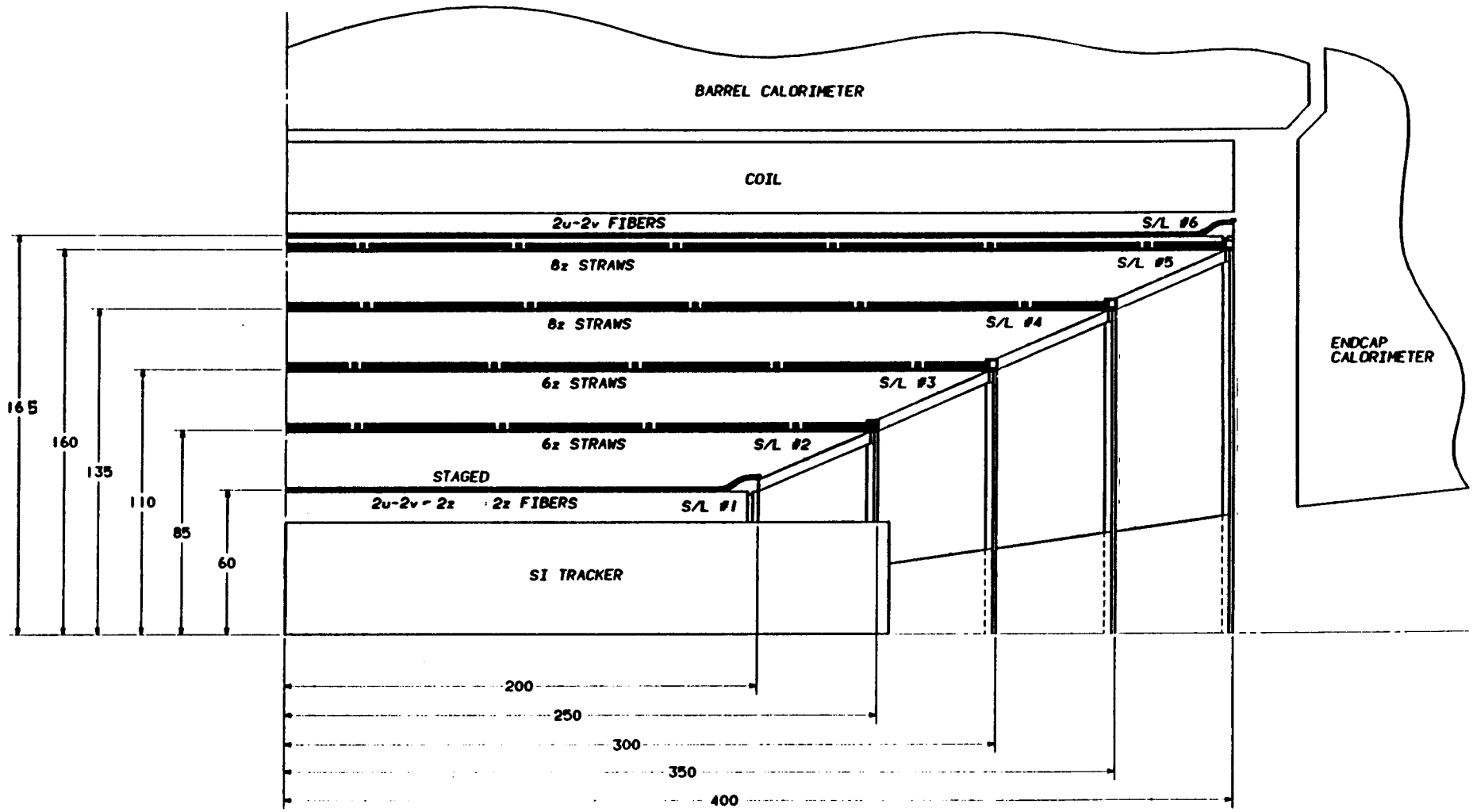

FIG. 2.1. SIRAW-FIBER TRACKING SYSTEM (SFTS)

ALL DIMENSIONS IN CENTIMETERS

omi

11/04/91

The straw tube superlayers contain only axial straws which pack hermetically and can be simply supported by the stable base support cylinder. One construction technique applies to all superlayers, resulting in the potential for mass production cost savings. Several options for straw tube superlayer construction are under active consideration within the SDC and a final decision will not be made until the required R&D is completed in early 1992. The straws could be prebundled in full modular composite shells[3] or in shell-less modules which use thin carbon fiber bands to form independent straw tube bundles[4]. Another superlayer construction technique would lay the straws directly on the stable-base support cylinder[4]. The detailed trade offs between these options were discussed in a recent SDC report[5] and will not be reviewed here.

The straw-fiber barrel tracker can use any of the straw tube superlayer techniques under active consideration. The one chosen will be a compromise between low cost and high placement precision.

In this CDR we have chosen a superlayer construction design in which the individual straws are applied directly to the surface of the support cylinder or the preceding layer of attached straws. Such a straw placement design provides the simplest cell geometry with the least amount of material and minimum detector dead space. In addition, this superlayer construction technique appreciably simplifies the drift gas and electronics cooling connections. These are all contained in the superlayer end ring along with detachable, modular electronics cards (see Section 2.5 for details).

There are two basic steps to this particular straw tube superlayer construction procedure.

<u>Testing of individual straw tube drift cells</u>

In our assembly technique for a straw tube superlayer the first step is to construct individual straws containing intermediate wire supports and straw tube end plugs. Figure 2.2 illustrates the steps in the tube assembly. The sense wire is guided through the tube with air flow. The sense wire and the mid-tube wire supports are designed to provide isolation and signal termination for the two halves of the tube. Reading out each half of a straw tube reduces the occupancy of each track sensitive element by a factor of two. Figure 2.3 shows the mid-tube isolation/termination

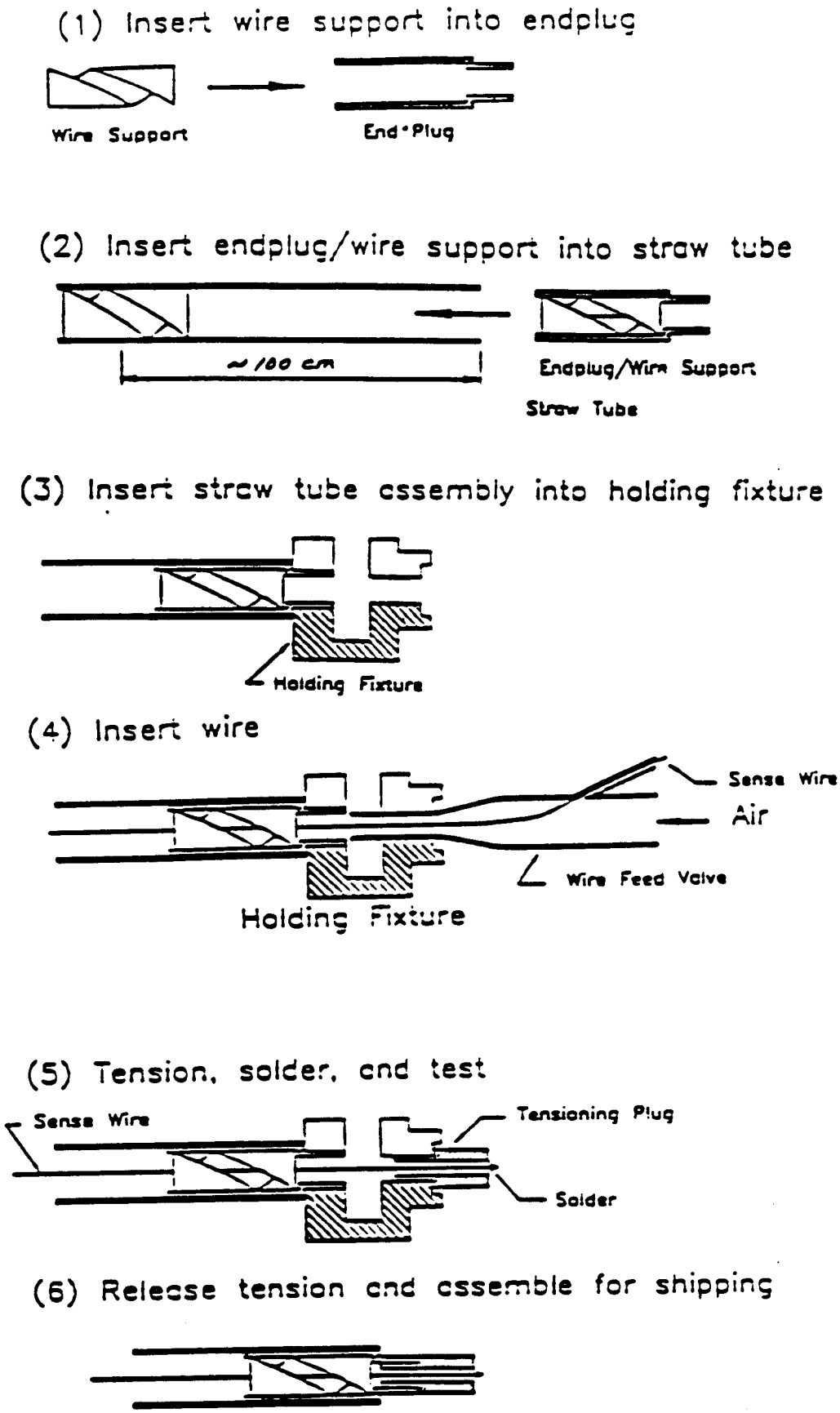

FIG. 2.2. Assembly and testing of individual straw tube drift cells.

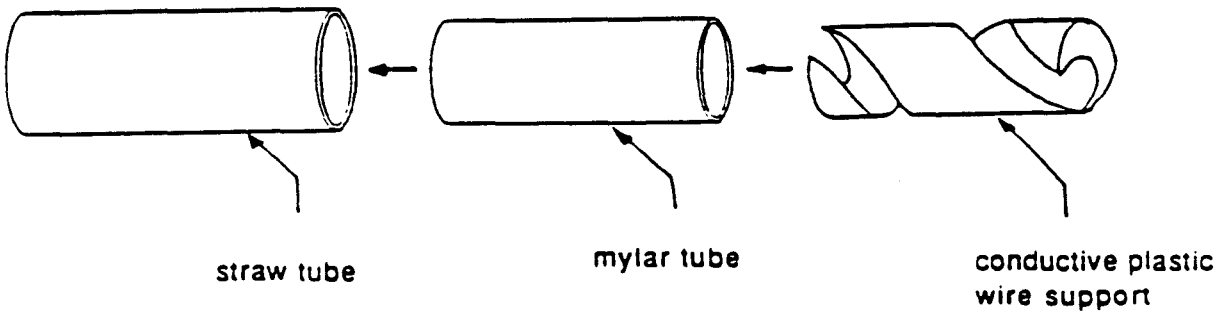

Mid-tube terminator design.

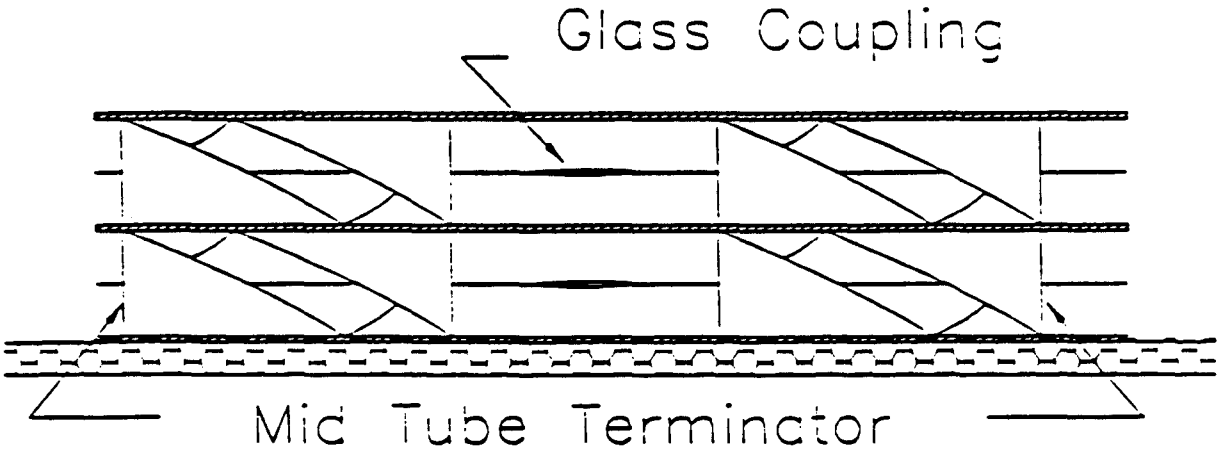

FIG. 2.3. Inner-tube termination.

method. The sense wire is actually two individual wires joined in the middle by a very thin glass tube with a ~100 μm hole. The capillary tube is fused to the wires, providing a strong, light-weight insulating joint. Termination is achieved by placing a wire support on either side of the midpoint of the sense wire which is constructed of a conductive plastic (~300 Ω resistance) and a 50 μm mylar tube (forming a capacitor with about 50 pF capacitance).

A tension plug is placed on the sense wire protruding from the straw tube. The sense wire is tensioned and soldered/crimped to the tension plug. The straw tube is held straight in a form and tested for gas leak, high voltage stability and calibration source gain. Tubes which pass these tests have their tension released and are placed in the tube laying assembly which positions and fastens the straw tubes on the structural support cylinder.

Straw tube placement in superlayers

A prototype straw tube placement mechanism is currently under assembly and will be briefly described here. It will have computer automated straw placement and position measurement functions. Figure 2.4 illustrates the design of a prototype straw tube placement machine; an end view of the prototype is shown. The straw tube guide is formed from two 3 m long precision ground beams, flat to 25 μm (total runout over 3 m). Precision spacers are used to separate the guides, leaving a slat with width approximately 4 mm and length 3 m. The straws are picked up into and dispersed from the 10 foot long slot by means of computer controlled vacuum pickup and over pressure ejection. The goal is to construct superlayers with a straw placement precision of 50 to 100 μm. For more details, see Ref. 4.

The flat stage which will be used to test the prototype mechanism will be replaced by the cylindrical structural support surface in the actual method. Instead of moving a flat stage with micropositioning stages the cylinder will be rotated through the appropriate angle under computer control to get the proper spatial positioning for the straw tubes. The straw tube registration will also be monitored at assembly time by means of measurement of the intensity of light from a collimated laser/photodetector that is reflected off the straw tube surface back into the photodetector. Preliminary tests with such a device have been very encouraging.

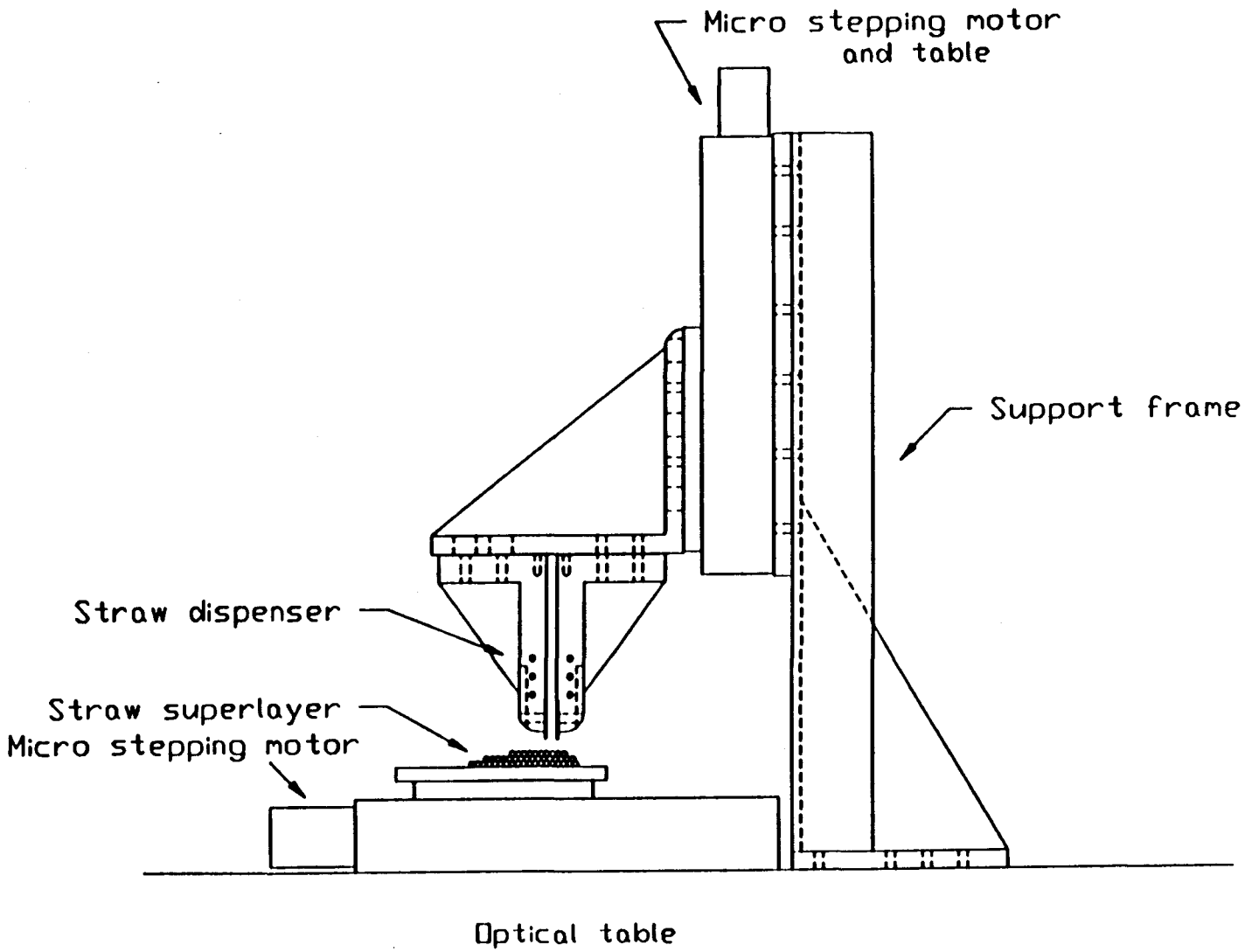

FIG. 2.4. Semiautomatic straw placement machine.

2.3. Scintillating fiber superlayers

The straw-fiber barrel tracker contains two scintillating fiber superlayers as described in Table 1.1 (p. 3). Both layers use helically wound fibers for ± 5° stereo and the inner layer takes advantage of the high luminosity potential of 1 mm diameter fibers. Superlayer 6 at a radius of 165 cm provides stereo information only and is used as part of the initial barrel tracker configuration. Superlayer 1 at a radius of 60 cm is included in the mechanical design but will be added as a high luminosity upgrade if budget constraints prohibit its installation at machine turn-on. The construction of each of these superlayers is described below.

The outer stereo scintillating fiber superlayer will be located at R = 165 cm, the outermost radius of the tracking volume. This configuration will allow a straightforward matching of track positions to the calorimeter system. We plan to use 1.5 mm diameter fibers in this location in order to reduce the number of channels and to increase the margin of the number of photoelectrons detected by the fiber readout device. We assume a fiber length of 4 m. For each stereo angle we use a double layer of fibers staggered naturally by half a fiber diameter. Each double layer is made up of manufactured fiber ribbons of 2x512 fibers per ribbon, and the total number of channels in the superlayer is 54.2k (53 ribbons). The ribbons will be positioned on a carbon fiber support structure which is independent of the support structures of the straw tubes. The scintillating fibers will be spliced to ~4 m long clear wave guide fibers connected to arrays of readout devices (*e.g.*, APD's or VLPC's).

As the luminosity is increased from the design value, it will become necessary to upgrade the tracking system at the inner radius, with a detector which has a finer segmentation. We therefore intend to add, at that time, a superlayer of plastic scintillating fiber with vector measurement capability at R = 60 cm. Using 1.0 mm diameter fibers in double layers staggered by half a fiber diameter, the superlayer will consist of a double layer parallel to the beam axis ($2z$), two double layers in ± 5° stereo ($2u$, $2v$), and another $2z$ layer. The total number of channels in this superlayer is 62.1 k (61 ribbons).

<u>Technical Feasibility</u>

We now review briefly the R&D status of scintillating fiber tracking and the results that have convinced us that the current design of the scintillating fiber

superlayers is technically feasible. These results come from work that has concentrated on the study of Geiger-mode APD operation.

The reasons we have concentrated on the APD as readout device for scintillating fiber are the following: (1) the device has high quantum efficiency, (2) the device has been available commercially for 15 years, (3) the device can be operated at or near room temperature, (4) if the device is operated in the Geiger mode, then the operation is very simple, meaning no amplifier is needed, and (5) per-channel costs ought to be less than other readout alternatives.

We have tested APD's tailored for our needs by the manufacturer, EG&G Canada. Modifications have been to the optical coupling between the diode and the fiber and not to the diode itself which, for all our tests, has been a standard 500 μm diameter EG&G device. The first device we tested had a 500 μm diameter cylindrical light guide which utilized the entire surface of the diode. We used this device to measure the photon yield and the attenuation length of 875 μm Bicron G2 fiber. The result is shown in Fig. 2.5(a). Because of the geometrical mismatch between the diameters of the fiber and the APD, a correction factor has to be used to obtain the total number of photoelectrons. The number of photoelectrons from the far end of the fiber is approximately 7. Our next attempt to improve the optical coupling between the fiber and the APD without changing the properties of the APD itself was to use a ball lens as a light collector. The diagram of the APD with a ball lens is shown in Fig. 2.6. Figure 2.5(b) shows the light curve for the same fiber mentioned above with the ball lens APD. This ball-lens scheme did not work as expected, because of the width of the photon angular distribution. A future step will be to introduce a nonimaging light collector (such as a solid-state micro Winston cone, for example). Another approach will be to use an APD with 1.5 mm diameter sensitive surface. This is also commercially available from EG&G. The room temperature dark count rate is ~10 times higher than that of the 500 μm device, but in the kHz range and still low by our standards. Both of these approaches offer the significant advantage that the same device can be used for all fiber diameters up to and including 1.5 mm diameter.

With the ball-lens APD we also have measured the photon yield and attenuation length of a 2 mm diameter G2 fiber to study the dependence of the attenuation on the fiber diameter. Figure 2.5(c) shows the result. The attenuation length of this

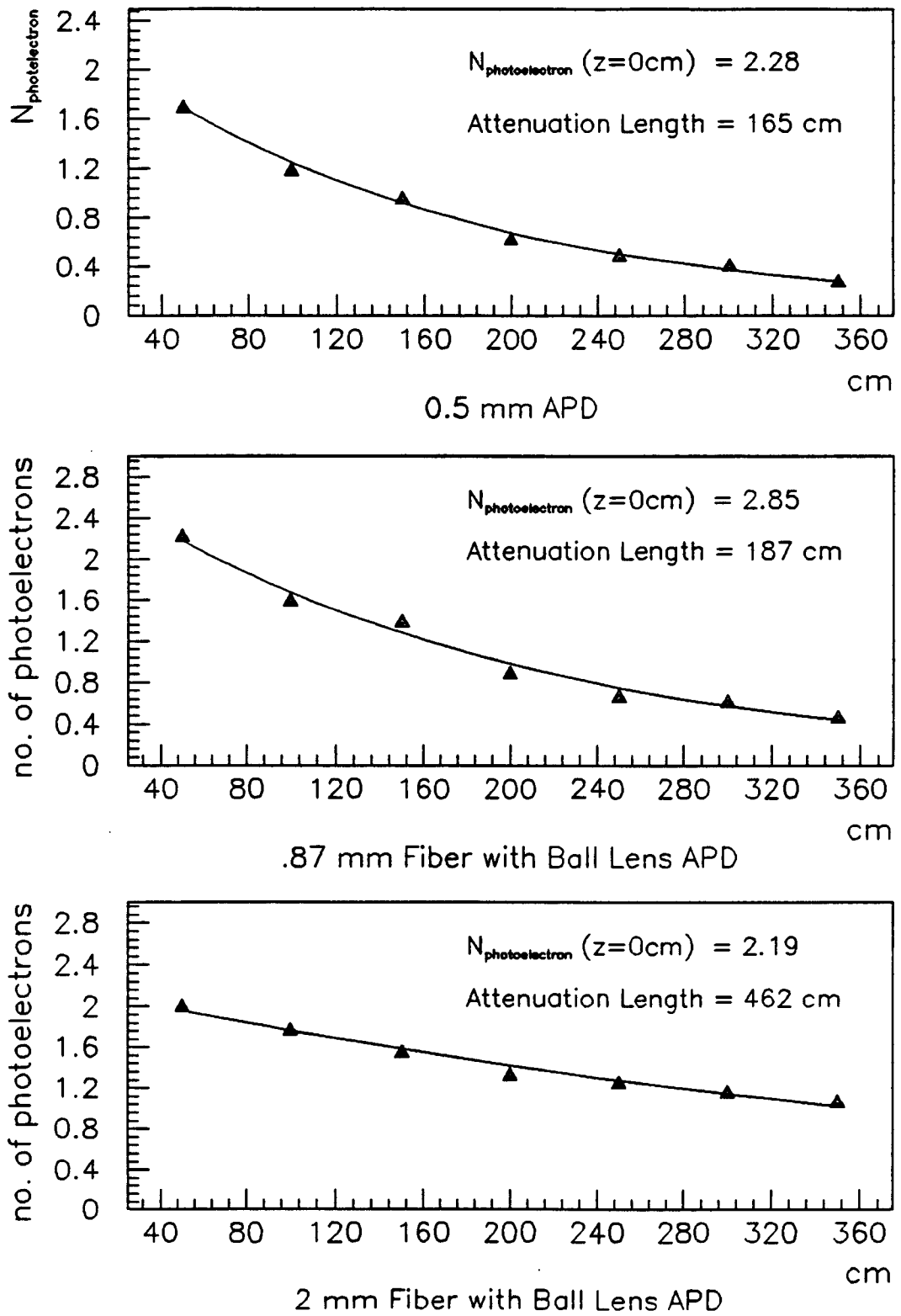

FIG. 2.5. Light curve produced using 4 m long Bicron G2 fiber with Geiger-mode avalanche photodiode. a) 875 μm diameter fiber, 500 μm APD with cylindrical light guide; b) 875 μm diameter fiber, 500 μm APD with ball-lens; c) 2 mm diameter fiber, 500 μm APD with ball-lens.

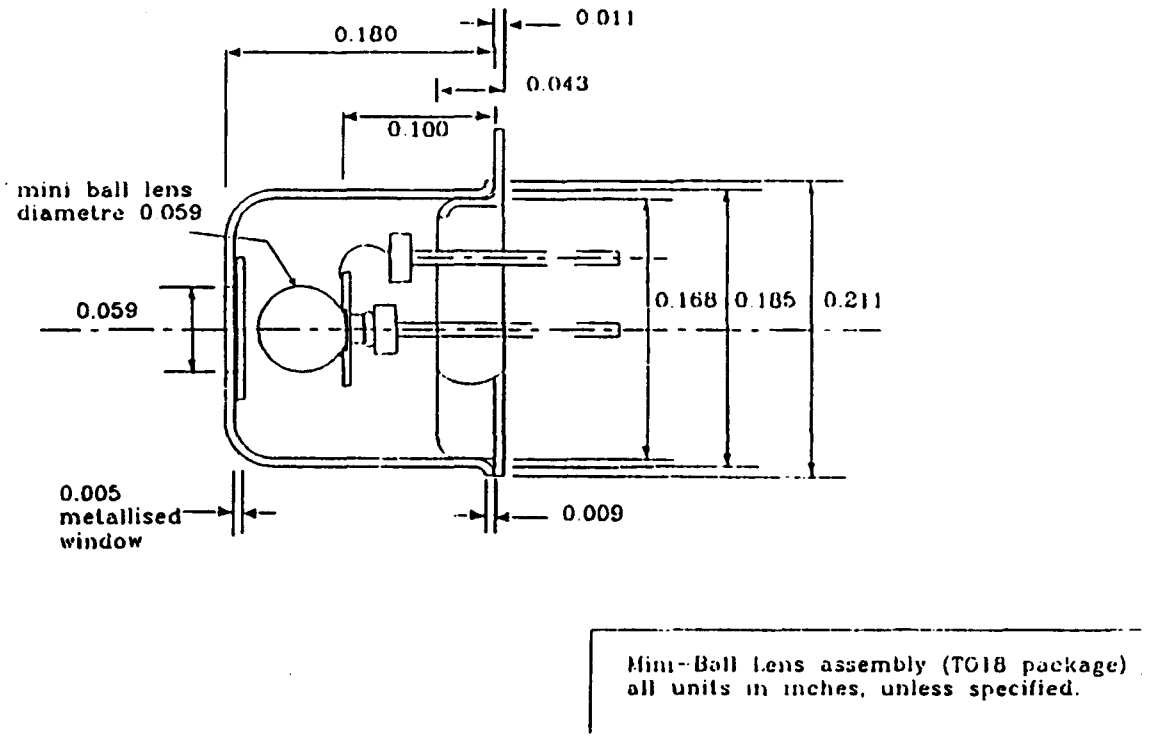

FIG. 2.6. Schematic of EG&G 500 μm diameter avalanche photodiode with 1.5 mm diameter high refractive index ball-lens.

fiber is measured to be 462 cm. The ratio of the attenuation lengths between the 875 μm fiber and 2 mm fiber is close to the ratio of diameters of the two fibers. This result demonstrates the obvious advantage of using fibers with a larger diameter; there are both more photons generated and a longer fiber attenuation length. The estimated detection efficiency of a 1.5 mm diameter fiber is based on these results. The expected detection efficiency is shown in Fig. 2.7. This is the plot that has convinced us that the proposed scintillating fiber superlayer is technically feasible. There is still room for improvement; however, the current characteristics of a 1.5 mm fiber with Geiger-mode APD yield a tracking element of high enough efficiency.

The one disadvantage of Geiger-mode APD operation is the long recovery-time needed after the device times. We have been unable to reduce this beyond ~150 ns. Work is continuing to investigate this problem and to identify possible fast-quench techniques. Another approach is to operate the device in sub-Geiger mode (where dead-times of <15 ns have been reported).

The occupancy characteristics of the outer superlayer (Section 3.1) are such that the Geiger-mode dead-time is probably already acceptable. For the inner superlayer, however, such a long dead-time would yield an unacceptable limitation.

2.4. Mechanical support structures

The mechanical support structure of the SFTS is responsible for mounting and supporting the straw tube and/or plastic scintillating fiber tracking elements. The structure must provide an extremely stable platform onto which these elements are mounted. This platform must meet the requirements of precision alignment and location for the tracking elements. Each tracking element is located and physically supported in superlayers. The superlayers are then attached to one another and the remainder of the SDC detector. The mechanical structure chosen for this task is a series of nested cylindrical shells, attached to one another by segmented shrouds (see Fig. 2.8). These are assembled into a completed SFTS, which is ultimately attached to the calorimeter support ring. The SFTS contains provisions for attachment of the intermediate and silicon trackers, which comprises the tracking portion of the SDC detector.

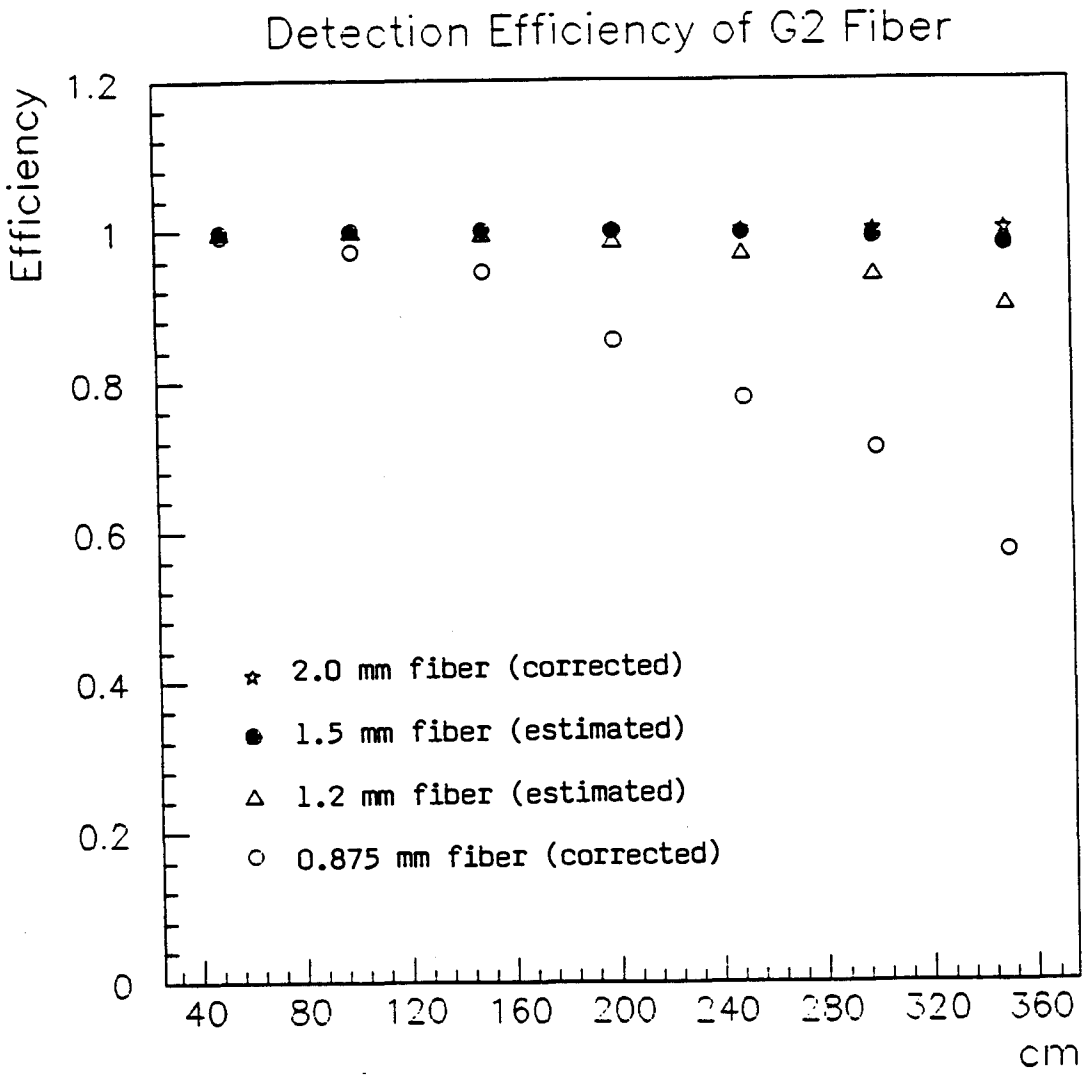

FIG. 2.7. Detection efficiency for a minimum ionizing particle traversing a circular cross-section scintillating fiber as a function of distance from the (readout) end of the fiber. The readout device is the EG&G 500 μm avalanche photodiode with ball-lens optical coupling to the fiber. The caption "corrected" refers to the geometrical correction discussed in the text. The 1.2 mm and 1.5 mm data are interpolated using the 2.0 mm and 0.875 mm data.

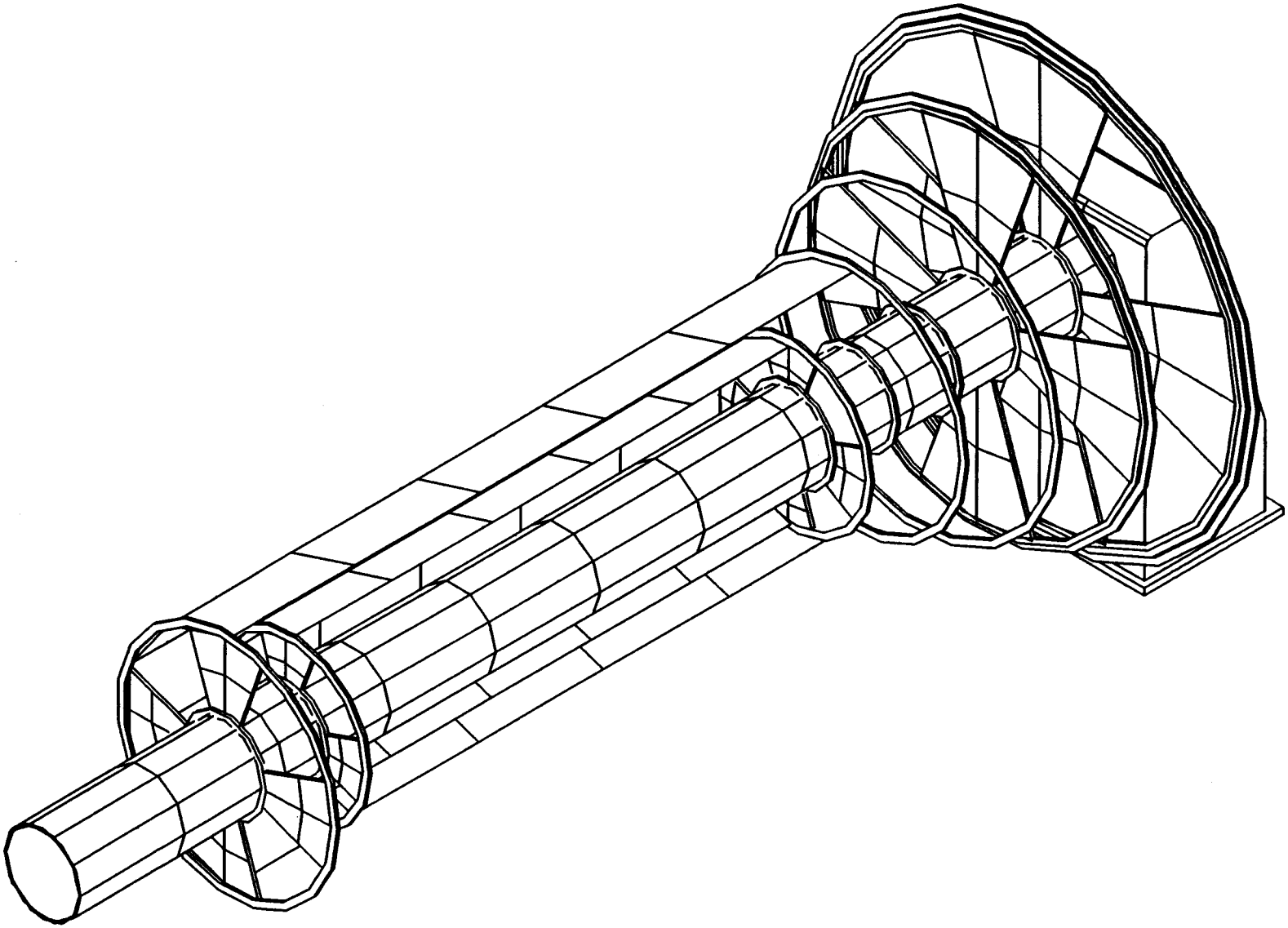

FIG. 2.8. *ISOMETRIC VIEW OF CANTILEVERED SHAFT & RETAINING CLAMPS*

Stable-base support cylinder

The method chosen by the SFTS group for supporting the tracking elements is a carbon-based composite cylinder. The support cylinder provides a lightweight, low radiation length structure that is radiation hardened and is stable under thermal variations. Analysis has revealed that the location of the tracking elements must be known to 30 μm, 400 μm and 300 μm for circumferential, radial and longitudinal location, respectively. The SFTS design utilizes a precision cylinder with tracking elements placed directly on the cylinder's surface to achieve the alignment goals. This method of support utilizes the inherent strength and simplicity of a cylindrical structure. By laying tracking elements directly on the support structure surface (see Fig. 2.9), a minimum of material is used, directly reducing the radiation length and fabrication cost of the detector.

The cylinder will be constructed using a face sheet-core-face-sheet layup. This fabrication method provides a lightweight, low radiation length structure that is radiation hardened, and provides excellent thermal stability. The current design will utilize face sheet thickness' of approximately 250 μm and a core thickness of approximately 1 cm. The face sheets will be graphite fiber reinforced epoxy composites sandwiched around a core of low density foam such as Rohacell. This combination has a thickness of 0.36% of a radiation length in a thermally stable package. This type of structure has been constructed in the past, and has been shown to be simple and economical to fabricate and assemble.

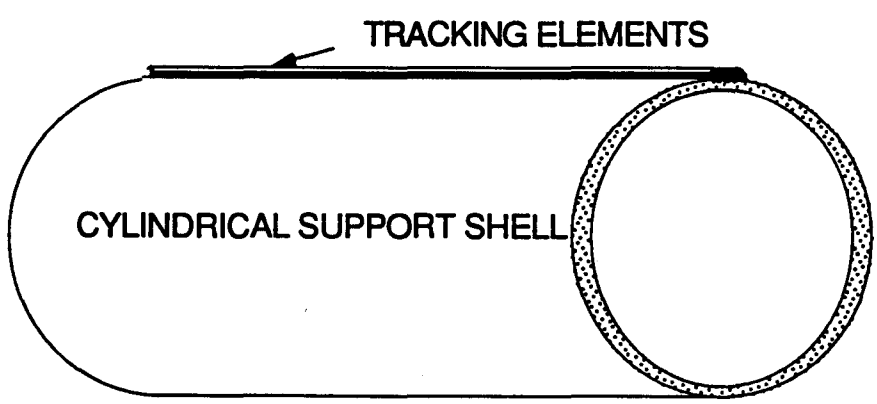

FIG. 2.9. Cylindrical support shell tracking element arrangement

The support cylinder has been analyzed for numerous loading conditions and configurations. Its structural integrity and stability has been evaluated and proven to be adequate to meet the SDC system requirements. Preliminary analysis reveals that the maximum deflection of the support cylinder is approximately 50 μm. In order to fully appreciate the behavior of the cylinders/support system, a full analysis of the tracker is currently being formulated and will be available during FY92.

The support cylinders are but one of the important factors in the completion of the support system for the SFTS. The support structure is the other component necessary for the success of the tracker. The support structure will provide the overall support to the central tracking system, including the silicon tracker. This support system will be the major item in controlling the location of the tracking components.

The support structure has been developed in conjunction with an assembly scheme for the SFTS. This is an essential step, due to the complexity of overall fabrication of the central tracker. The assembly sequence that has been developed allows the tracker to be fabricated, assembled, aligned, inspected, and shipped in a single, unified manner. This is required to control the the tolerance of the tracker.

Assembly of the tracker begins with production of the various sub-assemblies. This includes the straw and fiber superlayers, the support structure shrouds, the assembly fixtures and the inspection equipment. These are shown in Figs. 2.10 to 2.13. These components are all fabricated in parallel and readied for final assembly in a moderate clean room environment, and given their final inspection.

Tracker Assembly Sequence

After all components have been fabricated and compiled, the tracker is ready for assembly. The current plan calls for horizontal assembly, to more accurately duplicate the operating environment of the tracker. Figure 2.14 depicts the proposed assembly area layout for the SFTS. This assembly sequence can be done in a vertical position if subsequent evaluations reveal it to be more advantageous. Assembly begins with placement of the inner superlayer onto the assembly fixture.

S/L NO.	DIA "A"	DIM "B"
2	170	500
3	220	600
4	270	700
5	320	800

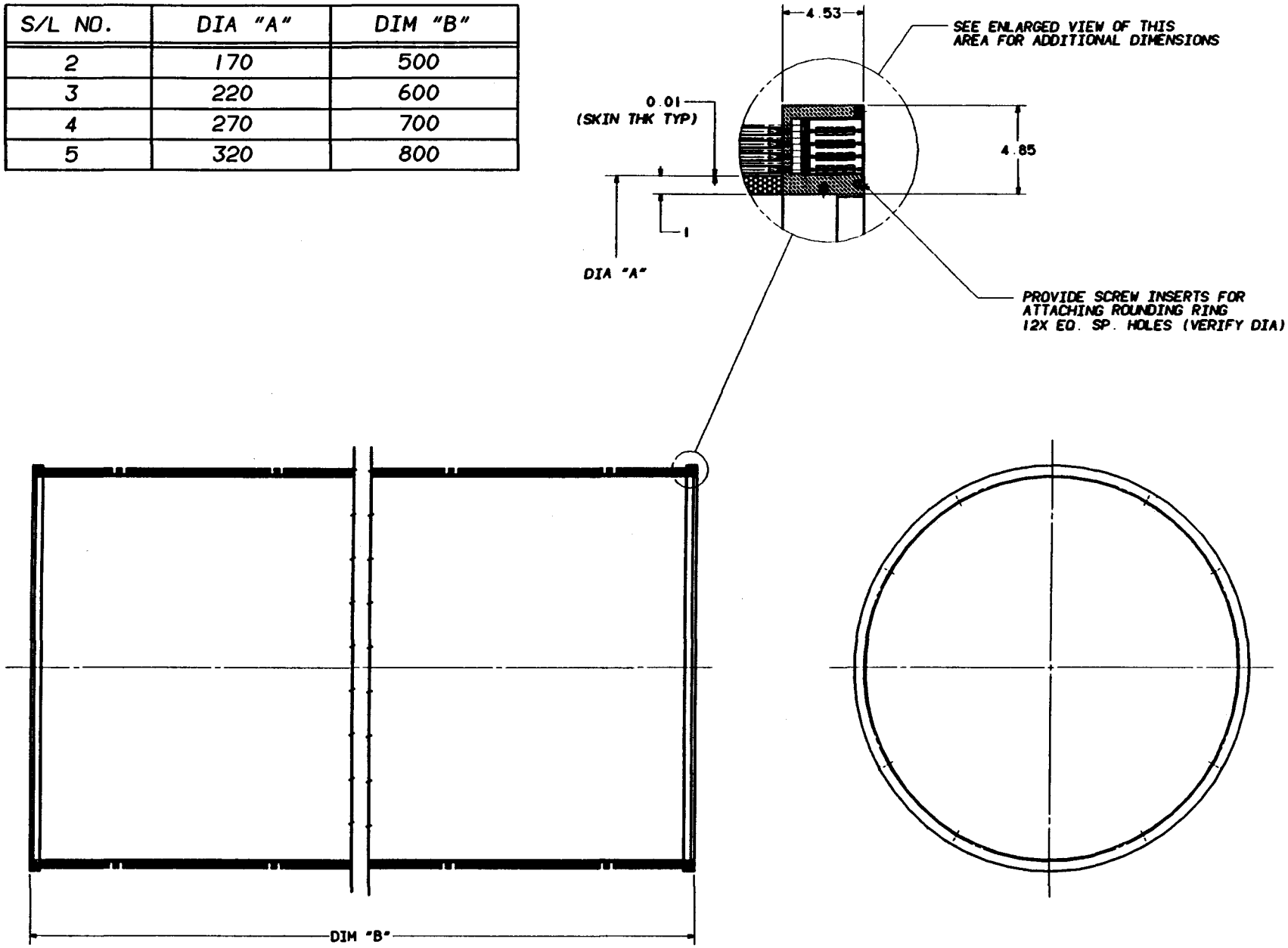

FIG. 2.10. SUPERLAYER CONFIGURATION (STRAWS)

ALL DIMENSIONS IN CENTIMETERS

S/L NO.	DIA "A"	DIM "B"
1	120	400
6	330	800

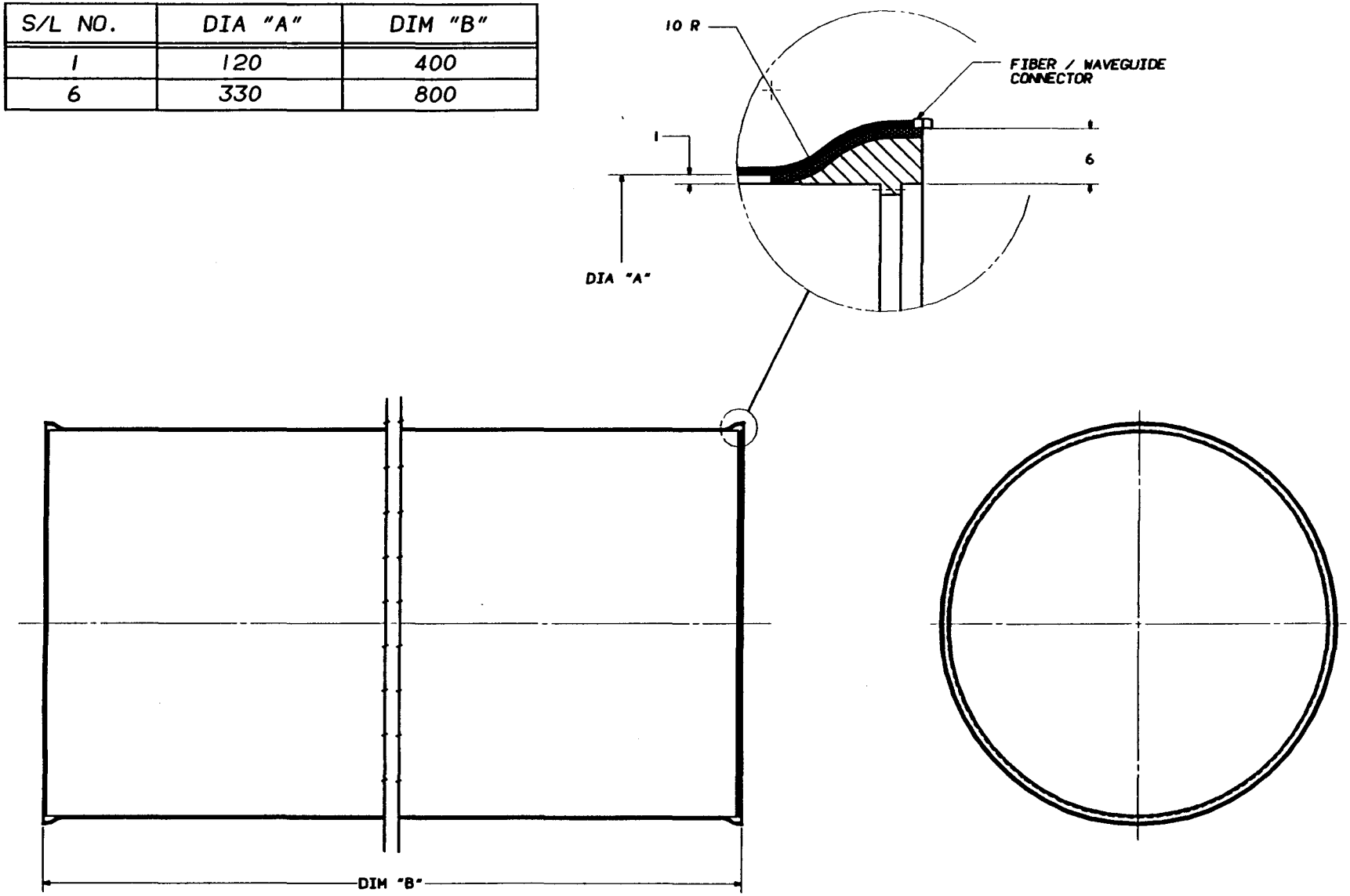

FIG. 2.11. SUPERLAYER CONFIGURATION (FIBER)

DIMENSIONS IN CENTIMETERS

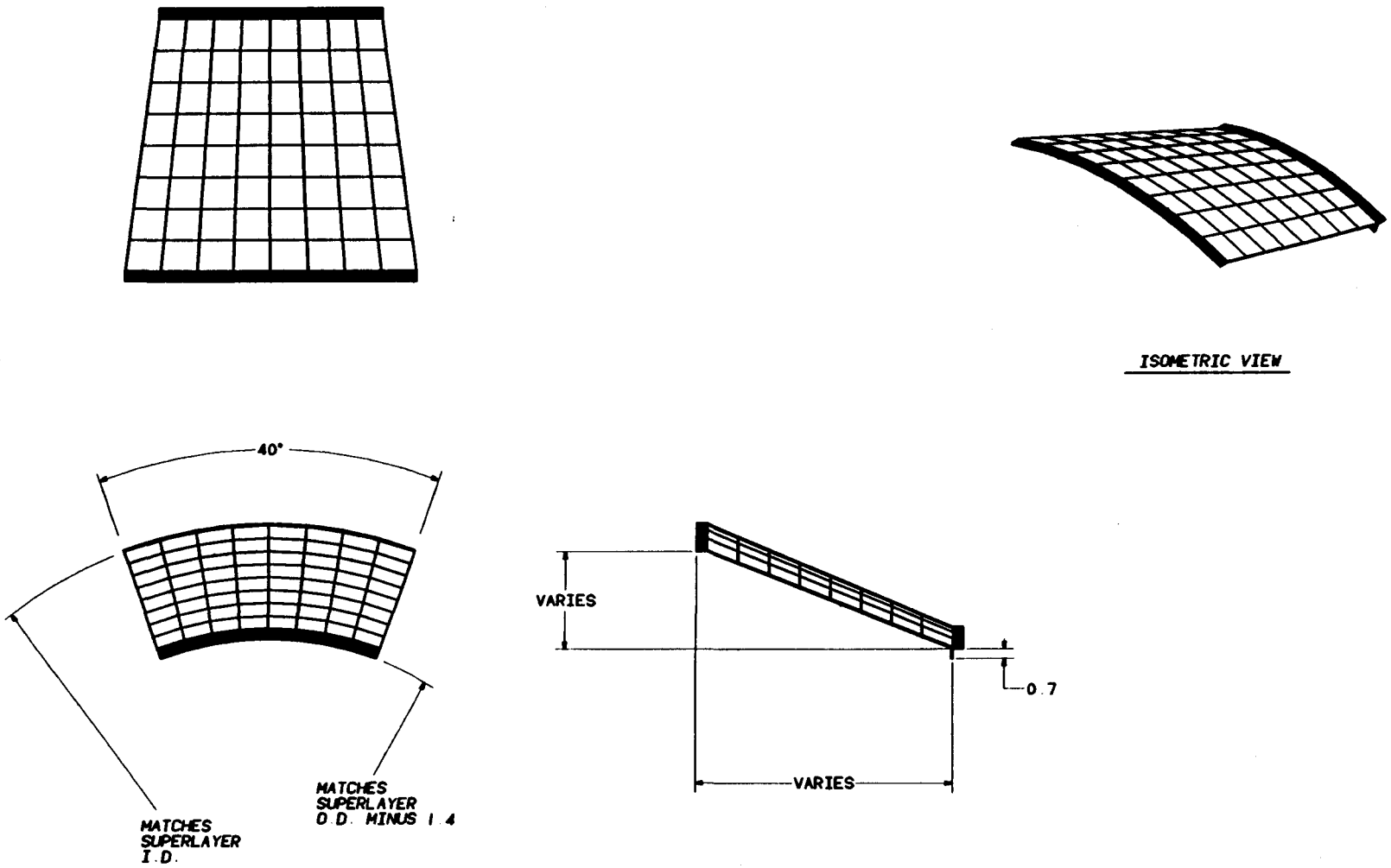

FIG. 2.12. SEGMENTED SHROUD DIMENSIONS

ALL DIMENSIONS ARE IN CENTIMETERS

CLEARANCE HOLES FOR ATTACHING TO SUPERLAYERS ARE NOT SHOWN

The assembly sequence is illustrated in Figs. 2.15 to 2.19. The inner superlayer is moved into position on the fixture. The rounding ring, attached to the superlayer, is located on the support spider and adjusted to be concentric with the centerline of the overall system. This superlayer is locked into position with the tooling. The second superlayer is then readied for assembly.The second superlayer is brought into position similar to the first (Fig. 2.17). It is aligned with the centerline of the system and also locked into position. The segmented support shrouds are then attached between the two superlayers (Fig. 2.18). The position of these components will be adjustable to allow perfect, stress-free alignment with the locked in superlayers. Once attached, the third superlayer is moved into position.

Superlayers three and four will be assembled identically to the first two. They will be located, aligned, inspected and then secured. This will complete the straw portion of the tracker. At this point, the final superlayer of fibers will be attached. Due to its closeness to the outer wire superlayer, it will be assembled in a slightly different manner.

The outer superlayer will be moved into position over the other superlayers. The cylinder end ring of the outer superlayer will attach directly to the end ring of the previous superlayer. Once again, adjustments will be made to center this superlayer prior to final attachment. This will complete the SFTS assembly (Fig. 2.19).

The SFTS may be assembled at a site remote from the SSC. The scenario that has been developed for the SFTS accommodates this and the shipping requirements. Upon completion of the SFTS superlayer assembly, an outer shell will be moved into position over the assembly. End plates will be attached to the shell and the entire unit sealed. The SFTS is ready for shipment, complete with tooling assembly fixtures which provide support during shipping. The unit is loaded onto a transporter and readied for final delivery.

The assembly sequence specified for the Straw-Fiber Tracker accommodates all requirements for the tracker. The support structure has been designed in conjunction with the assembly tooling, which is designed to interface with the shipping components. This systems engineering approach to the tracker design and fabrication reduces cost and complexity by integrating all requirements on the front end of the design.

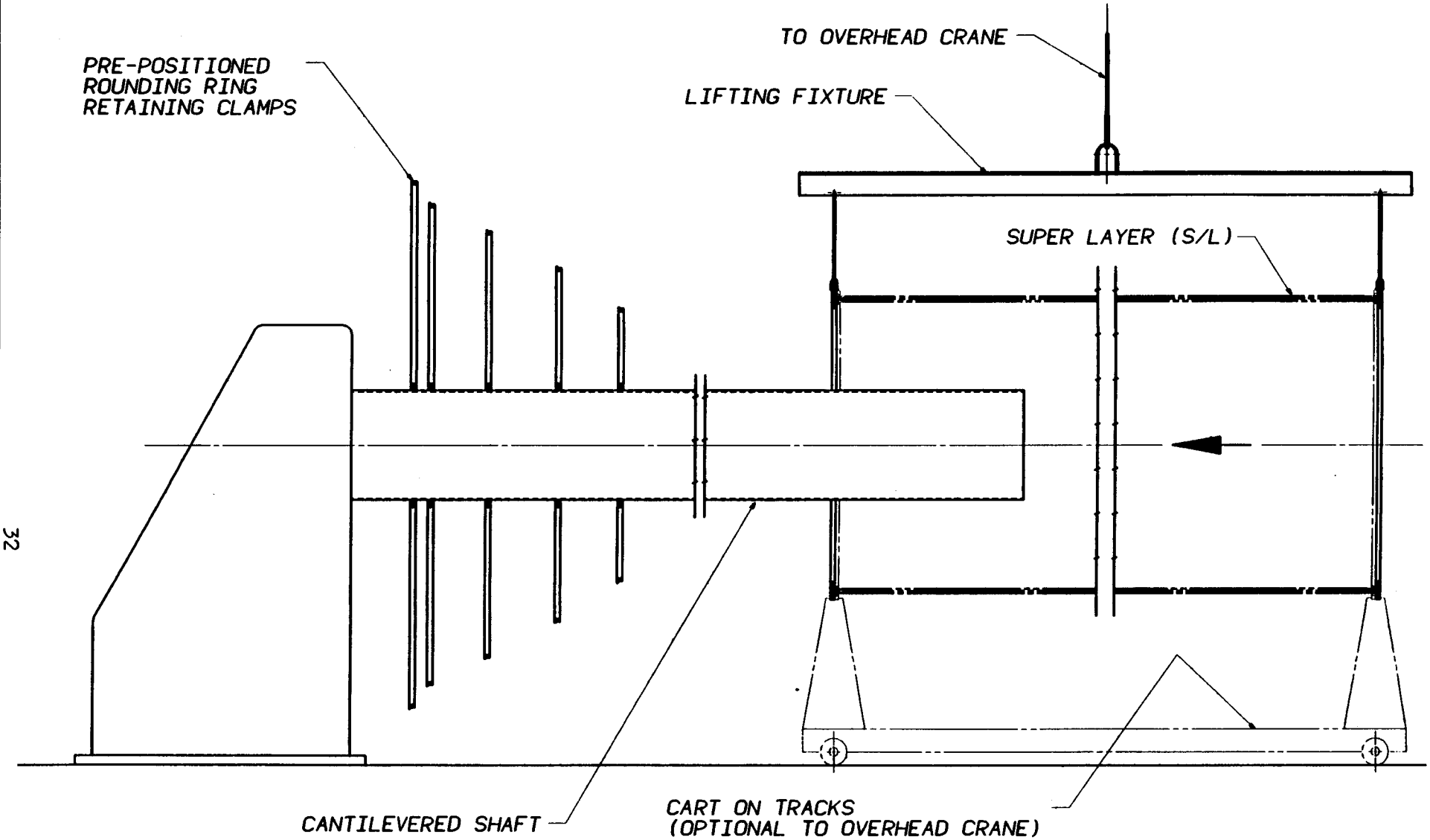

FIG. 2.15. INNER / OUTER CTC ASSEMBLY PROPOSAL

OVERALL CONCEPT

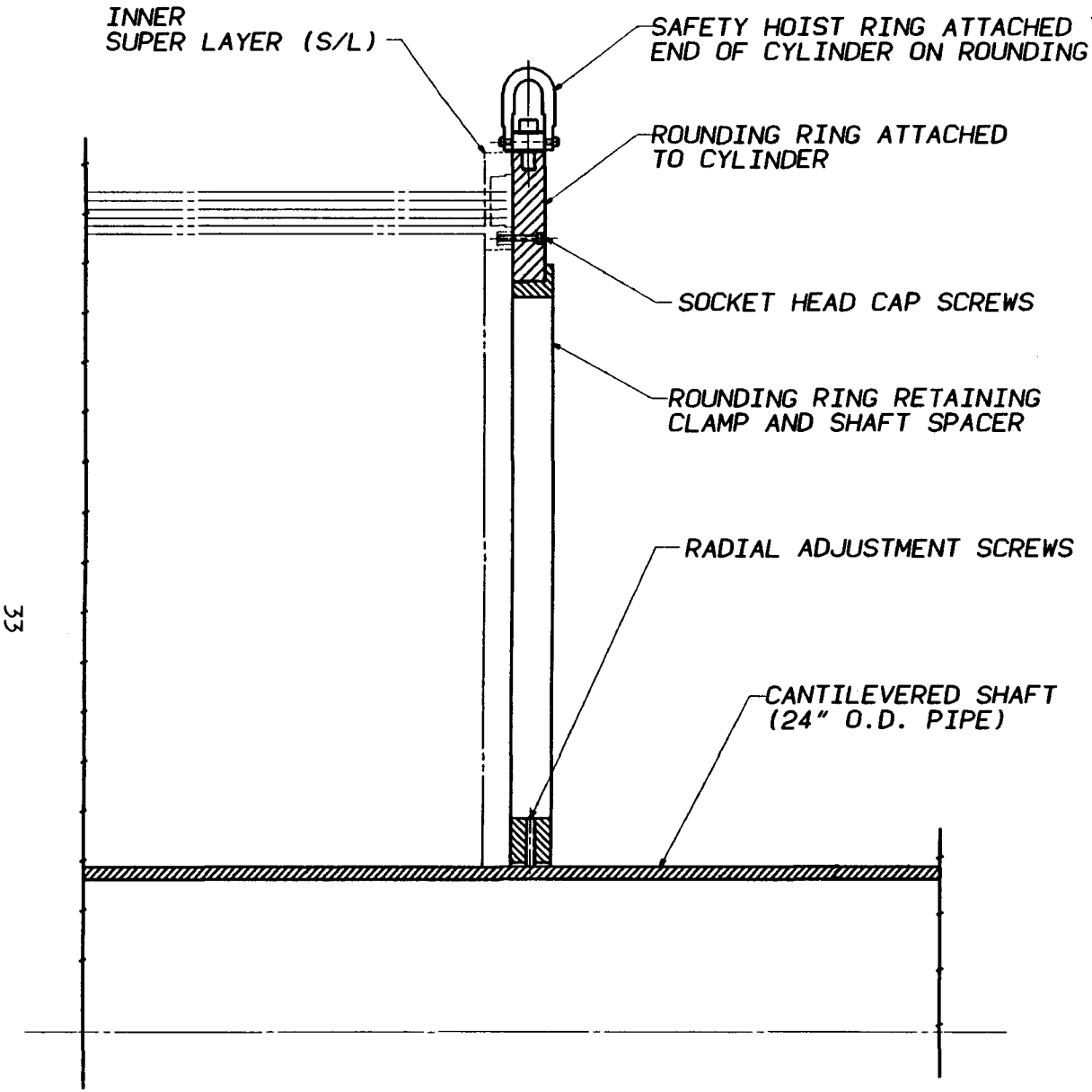

FIG. 2.16. INNER / OUTER CTC ASSEMBLY PROPOSAL

SEQUENCE A

STEPS FOR SEQUENCE A:

1. INSTALL ROUNDING RINGS TO EACH END OF SUPER LAYER (S/L) WITH SOC HEAD CAP SCREWS
2. INSTALL SAFETY HOIST RINGS TO EACH END OF S/L ON ROUNDING RINGS AS SHOWN.
3. ATTACH HOIST AND MANIPULATE OVER CANTILEVERED SHAFT TO APPROXIMATE POSITION WHICH WILL BE INDICATED ON SHAFT
4. ATTACH ROUNDING RING RETAINING CLAMP BY SLIDING OVER SHAFT TO A POSITION MARKED OR NOTCHED ON SHAFT. (THIS RING MAY BE REQUIRED TO ADJUST RADIALLY)
5. REMOVE SAFETY HOIST RINGS FROM BOTH ENDS.
6. POSITION AND ALIGN S/L

PROCEDE TO SEQUENCE B

ornl

STEPS FOR SEQUENCE B:

1. REPEAT STEPS 1 THRU 6 OF SEQUENCE A FOR SECOND SUPER LAYER S/L
2. PROCEDE TO SEQUENCE C

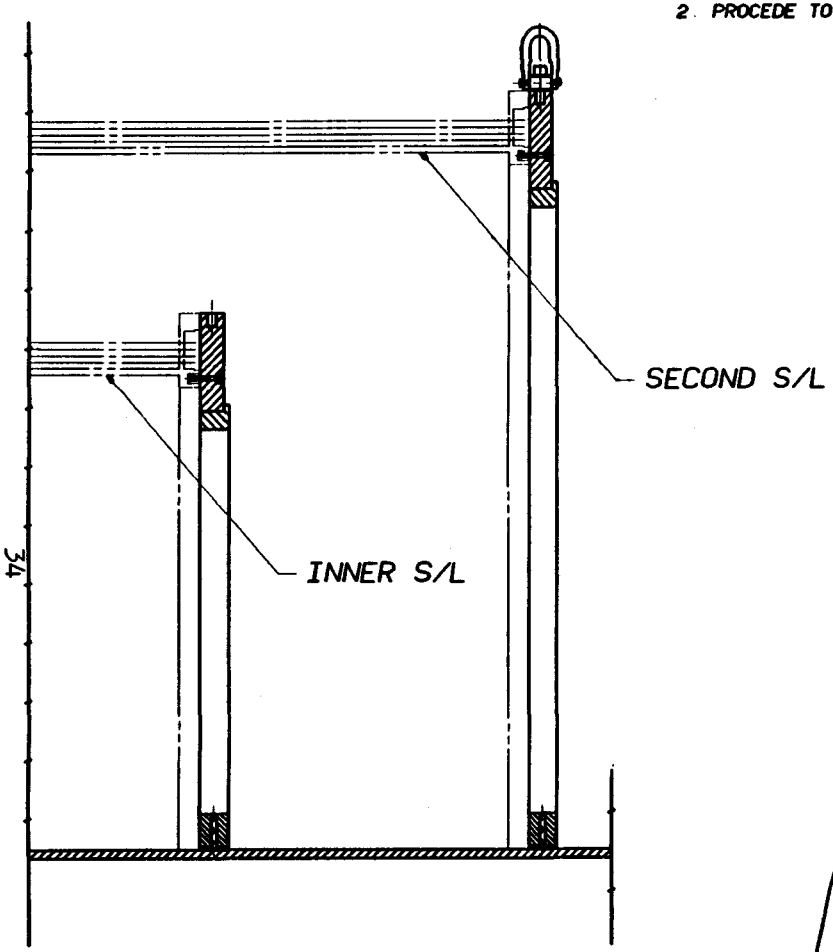

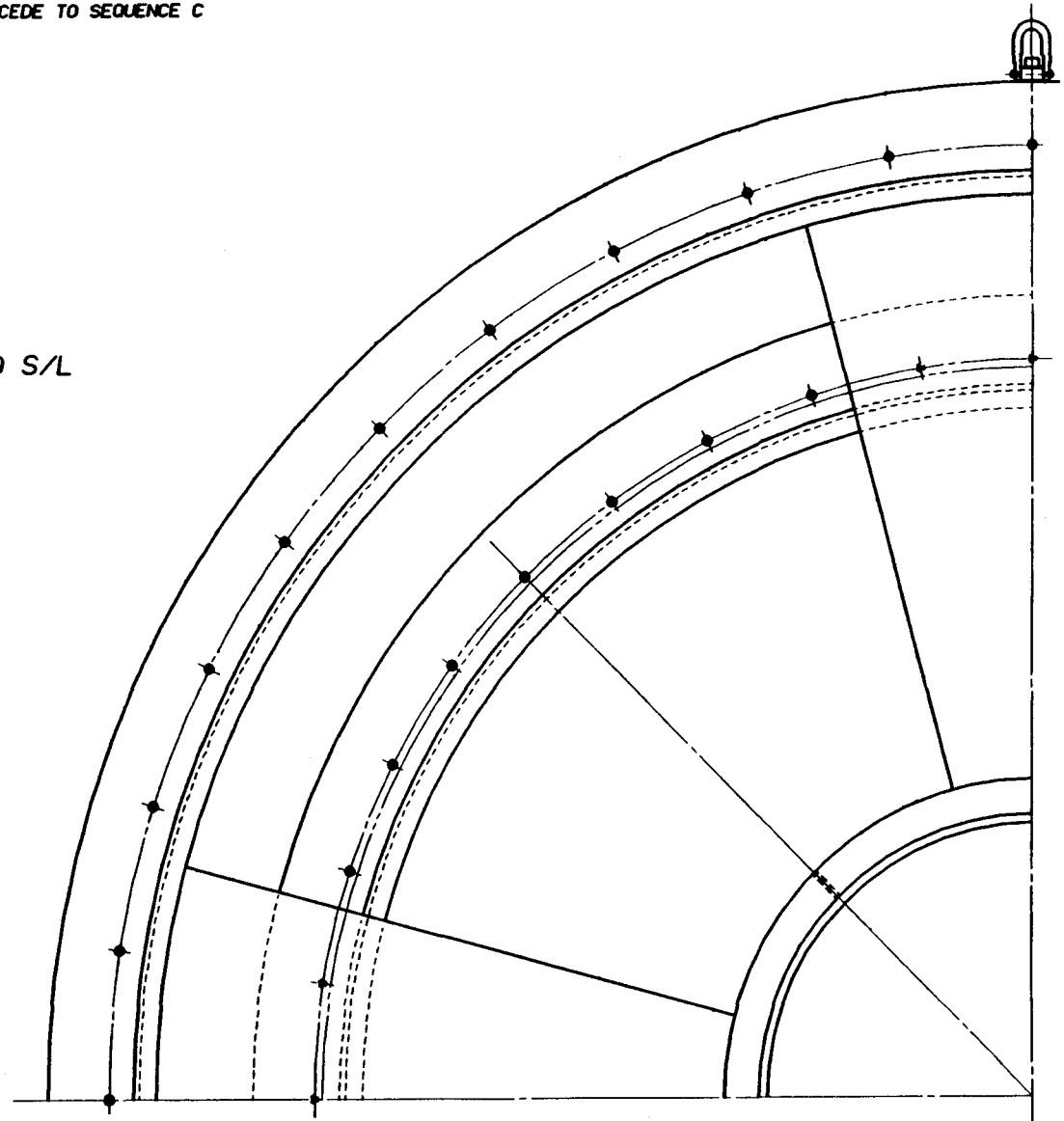

FIG. 2.17. INNER / OUTER CTC ASSEMBLY PROPOSAL

SEQUENCE B

STEPS FOR SEQUENCE C:

1. AFTER INNER AND SECOND S/L'S ARE POSITIONED AND ALIGNED, ATTACH SEGMENTED SHROUDS (FOUR EACH END) WITH SOCKET HEAD CAP SCREWS.

2. PROCEDE TO SEQUENCE D

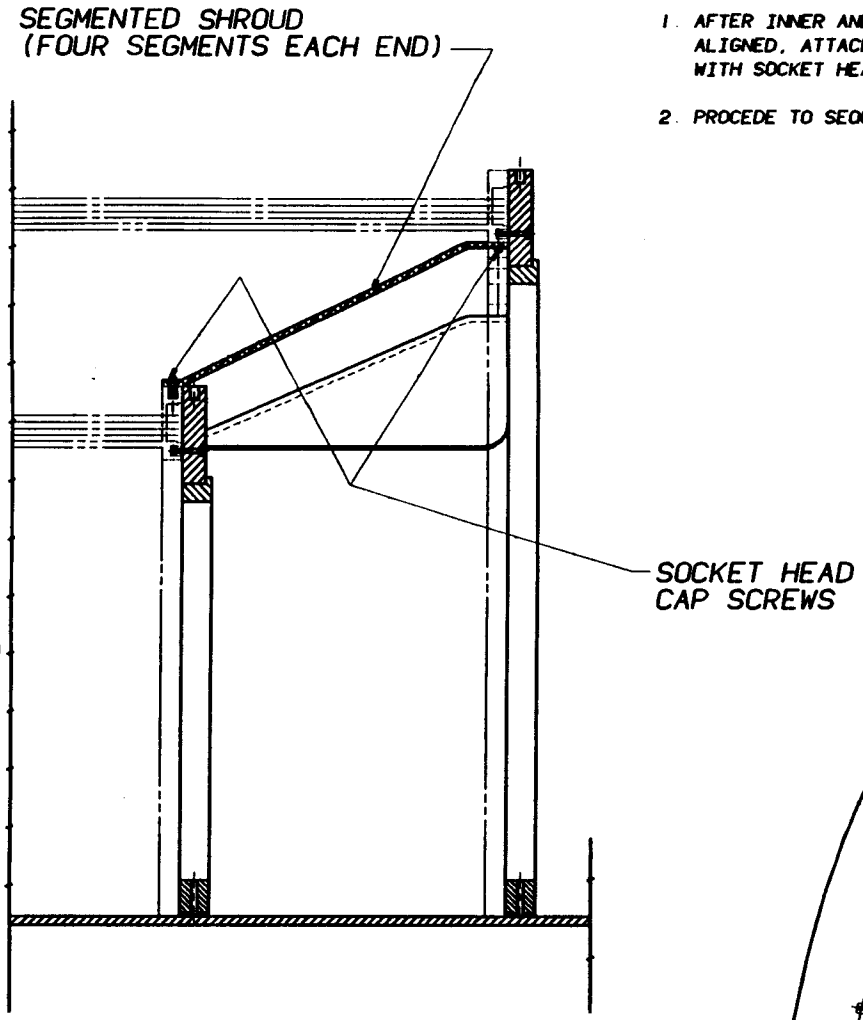

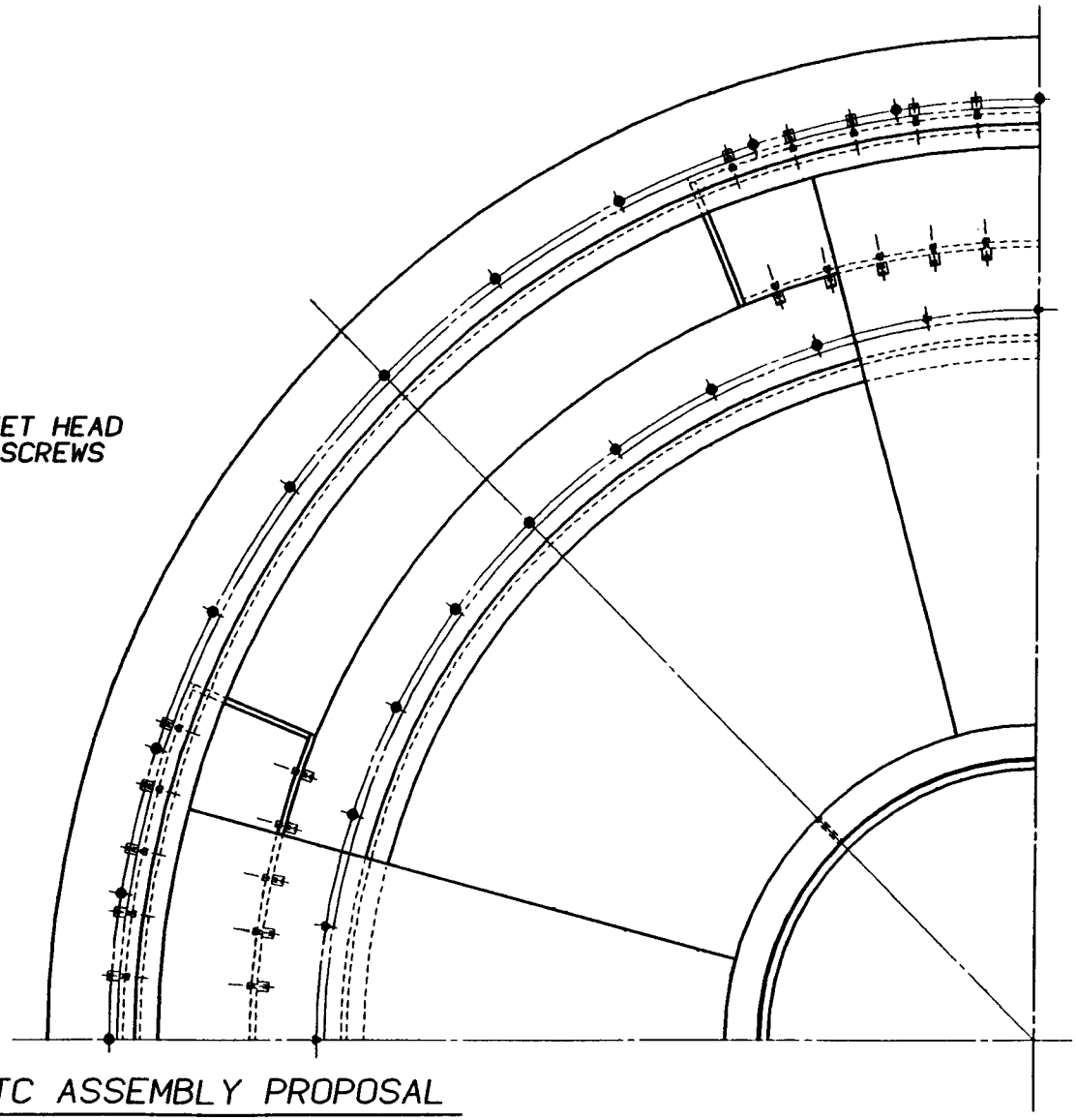

FIG. 2.18. INNER / OUTER CTC ASSEMBLY PROPOSAL

SEQUENCE C

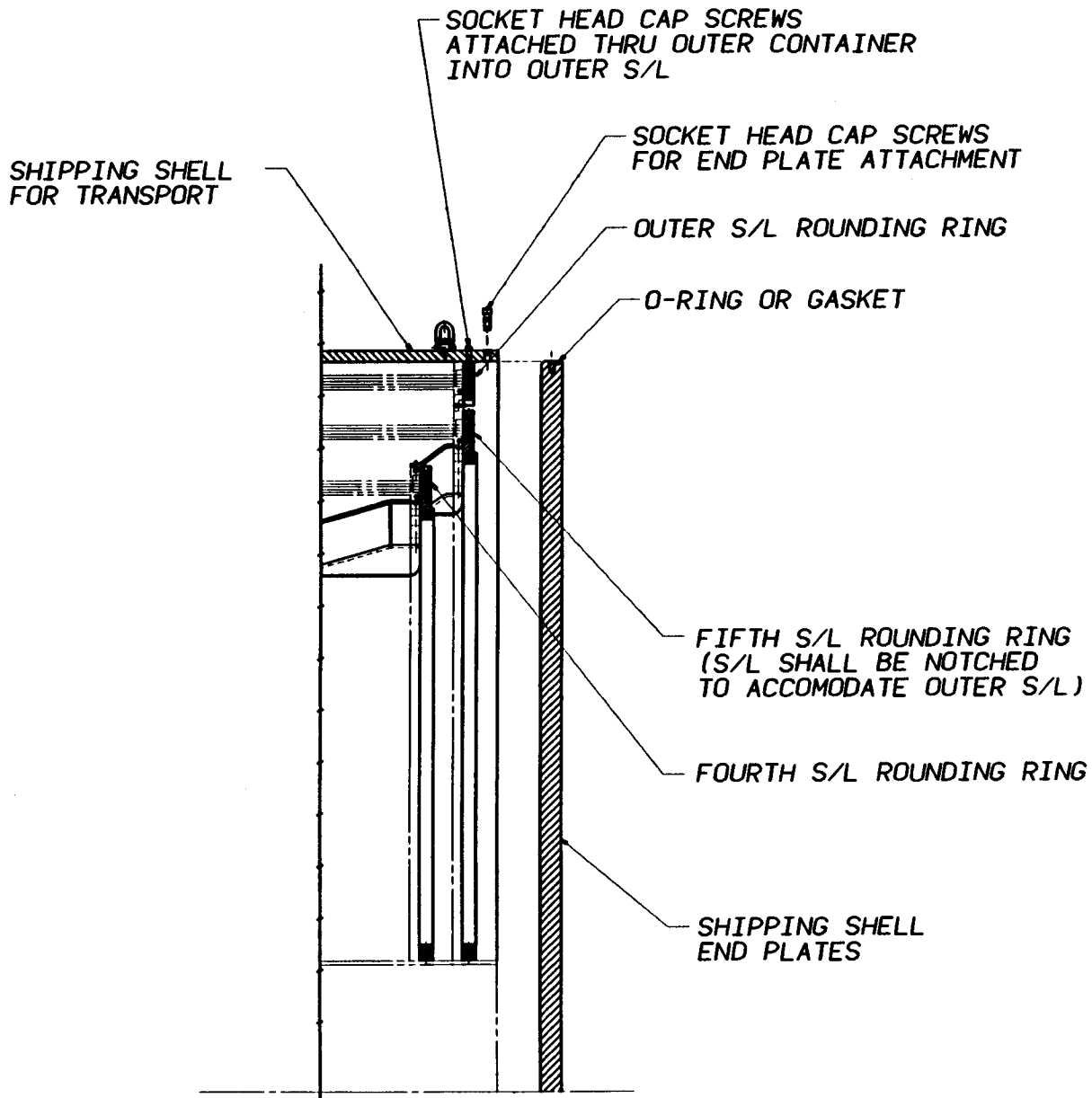

STEPS FOR SEQUENCE D

1. CONTINUE WORKING OUTWARD THRU FIFTH S/L REPEATING SEQUENCE A, B AND C.
2. ATTACH SAFETY HOIST RING TO OUTER S/L AND MANIPULATE INTO POSITION SLIDING ONTO NOTCHES WHICH ARE CUT CIRCUMFERENTIALLY AROUND FIFTH AND OUTER S/L'S AND ATTACH THESE S/L'S TOGETHER.
3. MANIPULATE SHIPPING SHELL INTO POSITION AND SECURE TO OUTER S/L ROUNDING RING USING SOCKET HEAD CAP SCREWS.
4. WHILE HOIST IS ATTACHED TO SHIPPING SHELL REMOVE COMPLETE UNIT FROM CANTILEVERED SHAFT BY LOOSTENING RADIAL ADJUSTMENT SCREWS ON ROUNDING RING RETAINING CLAMPS.
5. INSTALL SHIPPING SHELL END PLATES USING SOCKET HEAD CAP SCREWS.
6. EVACUATE SHIPPING SHELL AND FILL WITH NITROGEN.
7. LOAD SHIPPING SHELL ONTO TRANSPORTER.
8. SHIP TO SSCL SITE.

FIG. 2.19. INNER / OUTER CTC ASSEMBLY PROPOSAL

SEQUENCE D

2.5. Electronics and utilities

The readout electronics for both straw tube drift cells and scintillating fibers are under active study in on-going R&D programs (see, for example, Ref. 6). Although great progress has been made over the past few years, as of the date of this report, the high density readout electronics required for straw tube and fiber superlayers has not been fabricated and tested. The straw tube readout and trigger electronics have fairly specific chip-level designs although circuit board layout is less advanced. The fiber readout has options which look promising (APD's and VLPC's) but require system level development and reliable cost estimates. This section presents some design concepts which would satisfy the needs of the straw-fiber barrel tracker, and will be tested during FY92.

Straw tube readout electronics

The straw readout electronics can be divided into several functional blocks. From a systems-level perspective these blocks are (1) front-end electronics, (2) time measurement, (3) trigger generation, and (4) data readout. The front-end electronics consist of a preamplifier, shaper, and discriminator. These electronics are being implemented as a custom integrated circuit (ASD chip) by the University of Pennsylvania.[6] A single ASD chip will contain 8 channels. The readout electronics will be modular in nature allowing relatively easy assembly and maintenance. Therefore, for a group of ~200 straws, 25 ASD chips will be needed. The high-voltage (~2 kV) distribution to the straws will be part of the ASD chip assembly. The discriminator pulses from the ASD chips will be routed to both local time measurement and trigger generation circuits. In the case of time measurement, both the TVC chip from Penn and the TMC chip from KEK have been proposed. At this point, since the TMC chip development is further along, we plan to use it as the time measurement block. Approximately 4 disc channels can be routed into each TMC chip. Therefore, 50 TMC chips will be required for a group of 200 straws. For the trigger generation, a "trigger chip" that accepts ~16 inputs from the discriminators will be used. Again, for a group of 200 straws, ~12 of these chips will be required. See Section 4 for a detailed description of the trigger electronics.

Outputs from these local trigger generation chips will be sent on to the Global Trigger System. Time information from the TMC chips will be collected by local data collection chips (DCC). Each DCC will accept inputs from between 4 and 8 TMC

chips. The plan now for a group of 200 straws is to have 4 DDC's at the first level and a fifth DCC to concentrate information from these four. This fifth DCC would then transmit all information to the global DAQ system.

Due to the very dense spacing of components on circuit boards connecting to the straw tubes, and the high voltages that are present, there must be a protective conformal coating over the boards and components. Without a coating, a short circuit in a single straw could pull the input node to ground potential, inducing a flashover arc from neighboring channels, and cascade on until an entire layer is damaged. The conformal coating would greatly increase the breakdown voltage, allowing a single straw failure to be tolerated harmlessly.

One end of the straw tubes must be properly terminated with the straws characteristic impedance of 305 Ω + 59 pF[7] in order to reduce reflected signals arriving much later and causing poor signal to noise ratios or erroneous signal interpretations.

Connections between the straw tube wires and the front end electronics (or the termination on the opposite end) is achieved by using an elastomeric sheet with embedded wires on a 0.2 mm pitch, available from Shin-Etsu Polymer America, Inc. The elastomeric sheet is placed between the wire termination plate and a circuit board with a matching footprint. The pliantness of the sheet allows for variations in the flatness of the plate and board. Gas flow for the straw tubes is provided by the space between the wire termination plate and the end plate. The general arrangement is shown in Fig. 2.20.

Since only about 21 mW power is dissipated by the front end electronics (per channel),[8] heat removal will not be difficult. For 110,000 straw tube channels, total power dissipation is 2.3 kW. The worst case for a single superlayer, *i.e.*, the largest radius superlayer, is about 844 W. A forced air scheme such as the sketch shown in Fig. 2.21 would be adequate. Filtered air would blow into the electronics space at two entry ports, flow over the circuit boards, and exit through two exhaust ports. These estimates do not include first level trigger electronics. If the trigger electronics are included in the front end ASD modules, which is likely, power consumption will increase about 10 mW per channel. This will push the total power dissipation to 3.41 kW, or 1.25 kW for the largest superlayer. This amount of heat removal is still not a problem for a forced air scheme such as this.

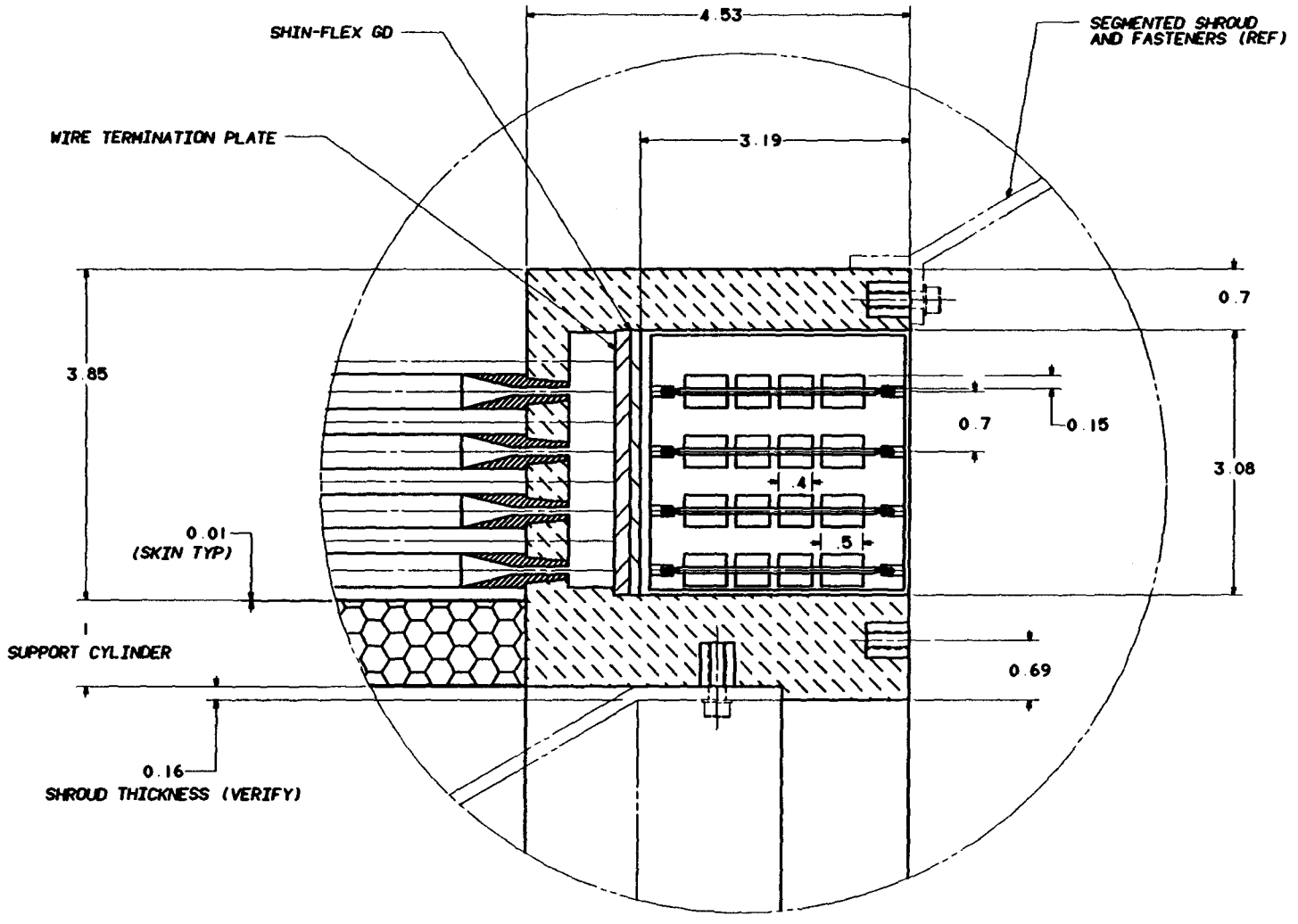

FIG. 2.20. SUPER / LAYER ENLARGED VIEW CYLINDER ENDS

DIMENSIONS ARE IN CENTIMETERS

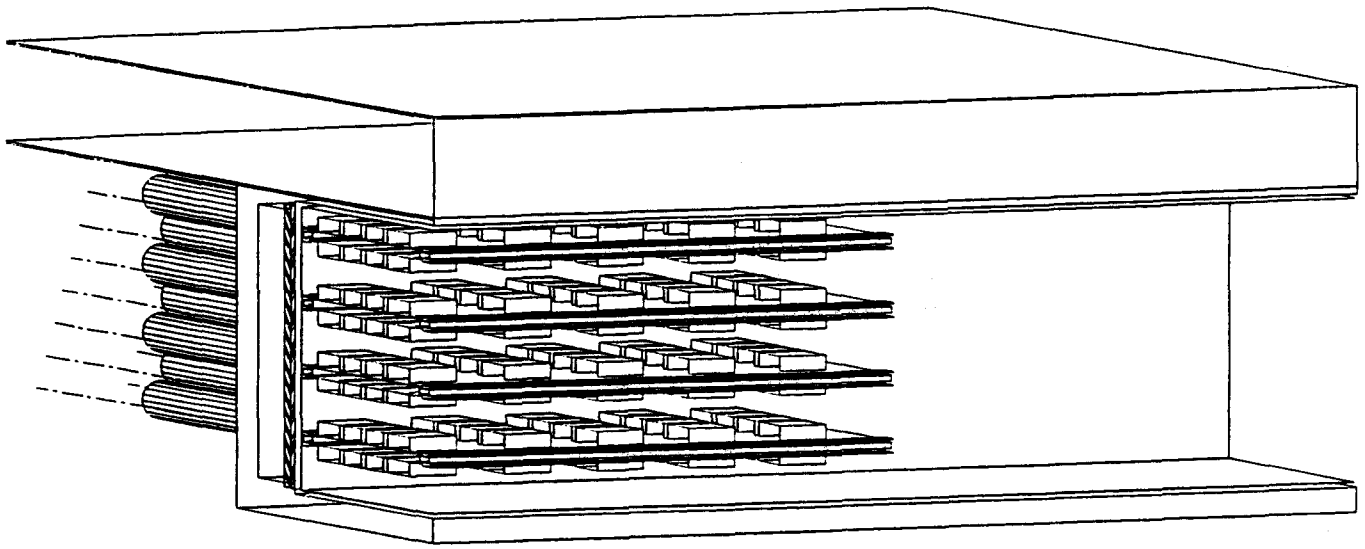

FIG. 2.21. Schematic of forced air cooling for straw tube electronics. View is looking toward end of barrel.

Fiber readout electronics

The outermost superlayer at R = 165 cm is composed of 1.5 mm diameter circular cross-section scintillating fibers. The length of each fiber is no more than 4 m. Both Bicron and Kurary produce fibers (either green or blue emitting) with adequate light yield and long enough attenuation length to give us several acceptable readout alternatives. Experience with the EG&G avalanche photodiode operating in Geiger mode shows that even Bicron G2 fiber produces enough light to give an efficient tracking element (see Fig. 2.7 in Section 2.3). Bicron G2 is definitely not the best fiber currently available. The only APD Geiger-mode disadvantage is the long post shot dead-time (~150 ns). With an occupancy of design luminosity of 0.5% (see Section 3) a ten crossing dead-time is surely a moot problem.

According to its design characteristics, the Rockwell VLPC is a better photon detector than the APD. It is certainly operationally more complicated and probably more expensive than the APD. All current indications are that the APD is good enough for this application; the VLPC is probably too good.

It is conceivable that a standard (small) photomultiplier tube, with bi-alkali or multi-alkali photo-cathode coupled with 1.5 mm fiber would give high enough efficiency.

Whichever readout device is chosen for these fibers, it is highly probable that the Shower Max Detector (SMC) will use the same technology. The avalanche photodiode is a particularly attractive option. It has three distinct modes of operation. In proportional mode it can be used with the SMD and in Geiger mode for the SFTS outer fiber layer. The inner fiber superlayer, with its higher occupancy, could not accept the Geiger mode dead-time of ~150 ns but would be able to use the APD in sub-Geiger mode.

Some R&D is still needed before a final decision can be made. In this CDR we tend towards the most conservative approach. We assume the VLPC with its high cost and complexity as the device of choice. The VLPC device promises several advantages such as low voltage operation of about 7 volts, very high quantum efficiency, very fast recovery time, and a high signal to noise ratio. A disadvantage to the VLPC, however, is that it must be operated at a temperature of approximately 7 K. Front end electronics will be contained in an intermediate temperature cryostat (liquid nitrogen).[9]

2.6 Material in SFTS

The support structure for the SFTS tracker will consist of low density, low Z materials in an effort to minimize the effect of radiation losses The stable base cylinders will be made of graphite epoxy which sandwiches a very low density foam. These cylinders will be supported by four panels at each end of the cylinders which will also be made of graphite epoxy and foam. The cylinders and panels are assumed to be fabricated of two 0.305 mm thick graphite epoxy face sheets and a 1 cm thick foam core. The CDR design contains five support cylinders in the tracker. The scintillating fibers themselves are made of polystyrene which has a relatively high radiation length. Table 2.2 shows which materials are used in the fabrication of the fiber tracker and their respective radiation lengths and densities.

TABLE 2.2

Straw-fiber tracker materials

	Radiation Length (cm)	Density (g/cc)	Comments
Aluminum[1]	8.9	2.7	Based on mass weighted average of Aluminum (2) and Oxygen (3)
Alumina Oxide	6.2	3.9	
Copper[1]	1.43	8.96	
G-10[1]	19.4	1.7	
Glass[1] (Borosilicate)	12.7	2.23	Used as a passivator in electronics
Graphite Epoxy[2]	25.0	1.68	
Lucite[1]	34.4	1.18	Used as connector for fiber optics
Straws[3]	24.0		Combination of Mylar, epoxy, and polycarbonate
Polystyrene[1]	42.4	1.032	
Rohacell	875.0	0.048	Scaled by density from Graphite Epoxy
Silicon[1]	9.36	2.33	
Tungsten[1]	0.35	19.3	

1 *Reviews in Modern Physics* 56(2):S53, Part II, April 1984.

2 Straw Tube Superlayer Design Concepts, Prepared for SDC Tracker Review, May 20, 1991, University of Colorado, Duke University, Indiana University, ORNL, and WSTC, Section 4.5: Materials in the Particle Path, pp. 30-32.

3 Superconducting Super Collider, Silicon Tracking Subsystem, Research and Development, LA-12029, Table 3-2, P. 17, Los Alamos National Laboratory.

In calculating the radiation lengths through the various materials, some assumptions were made. First of all, the outermost fiber superlayer was not included in the calculations since it is so near to the coil. The length through a fiber was averaged as $\pi d/4$, where d is the fiber diameter. The thin support panel which supports the outer and intermediate trackers is averaged over the circumference as $4s/2\pi r$ where s is the arc length subtended by a single panel and r is the radius of the panel. The factor of four in the numerator is because there are four panels.

The straw portion of the SFTS consist of 28 layers of straw tubes. The straw tubes are constructed of Mylar and have a wall thickness of 38 μm. The cathode is 0.15 μm thick copper. The anode portion of the straw tube is a 25 μm gold plated tungsten wire. These components are averaged over the 4 mm diameter of the straw tube, and then increased by 10% to include other factors such as epoxy and gas. The average radiation lengths of the straw tubes are shown in Table 2.2.

The results of these calculations for the outer tracker are shown in Fig. 2.22 as a function of η. Figure 2.22 shows that at $\eta = 0$ the material is approximately 3.0% of a radiation length.

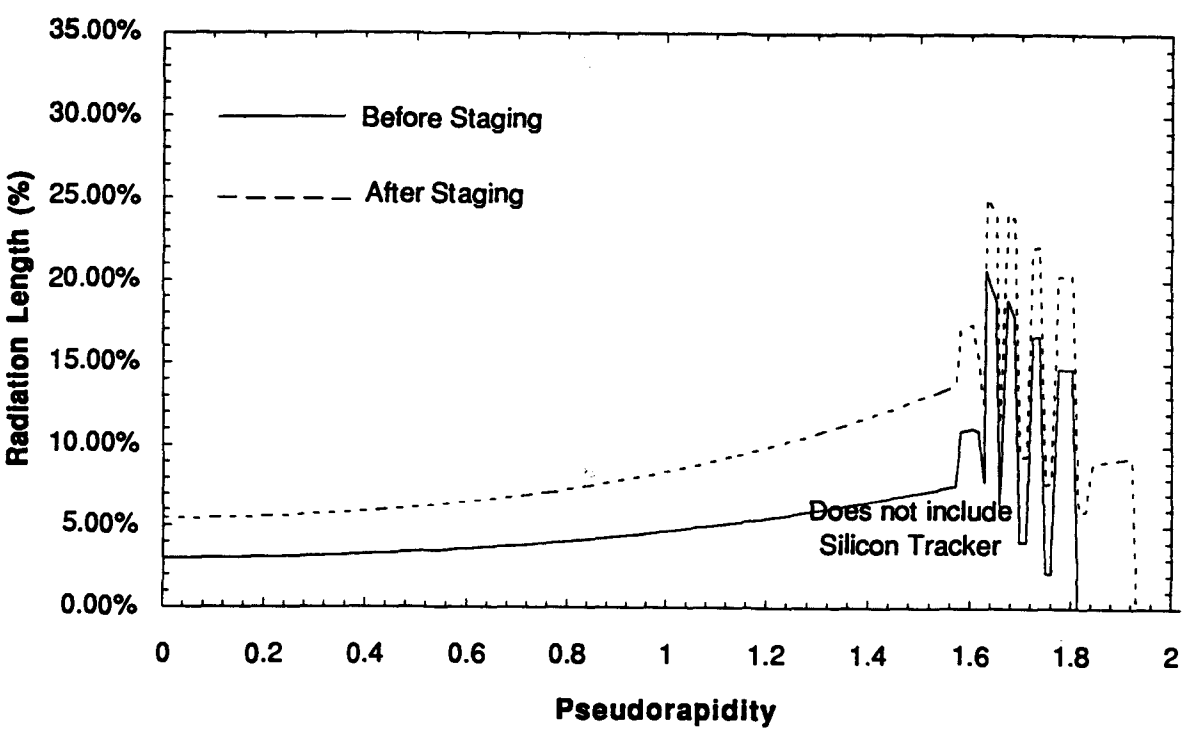

FIG. 2.22. Material radiation length of the SFTS.

3. Physics performance

3.1. Simulation procedure

The detector simulation is based on the GEANT program in the context of the SDC Shell. All interactions of energetic charged and neutral particles with the material of the detector are simulated. The beam pipe consists of 3 mm of Beryllium. The inner tracking detector simulated here corresponds to the LoI design, and consists of 8 double-sided barrel layers of silicon between radii of 18 and 39 cm, of pitch 50 μm and 5 mrad stereo angle, and 22 forward layers. (Subsequent descoping of the silicon detector has concentrated on the forward layers, leaving the number of barrel layers intact, except for moving the inner layers closer to the beam.) Some additional studies are described in Section 3.7, where the number of silicon barrel layers was reduced to 4, between radii of 9 and 36 cm. The outer barrel design is that described in Sections 1 and 2. Briefly, it consists of 4 superlayers of 4 mm axial straw tubes, followed by a single scintillating fiber stereo superlayer comprising two crossed double layers of 1.5 mm fibers at stereo angles of ± 5°.

The simulation takes account of drift time and dispersion (for straws only), propagation time along the wire or fiber, particle time-of-flight, electronic dead time, and background from both in- and out-of-time events. The 4 previous and 2 subsequent beam crossings to the crossing containing the triggering event are fully simulated. An effective drift velocity of 67 μm/nsec in a uniform 2 Tesla magnetic field is assumed. Sensitive times are taken to be 40 ns for straws and 15 ns for fibers. For the geometric calculation of hits, both fibers and straws are assumed to have circular cross sections and to be close-packed. Geometric inefficiencies result from straw tube walls, fiber cladding, and the gaps between straws or fibers. For the calculation of particle interactions, the straw material is assumed to be collapsed into concentric cylinders of the correct density near the rear of each individual straw layer.

A typical drift time spectrum is shown in Figure 3.1. Straw tube occupancies as a function of radius are shown in Figure 3.2. At the design luminosity, they vary from 8% to 3% from inside to outside for an average beam crossing, and are approximately twice as great for a Higgs → 4 lepton trigger. The occupancy of the outer fiber superlayer for an average beam crossing at design luminosity is

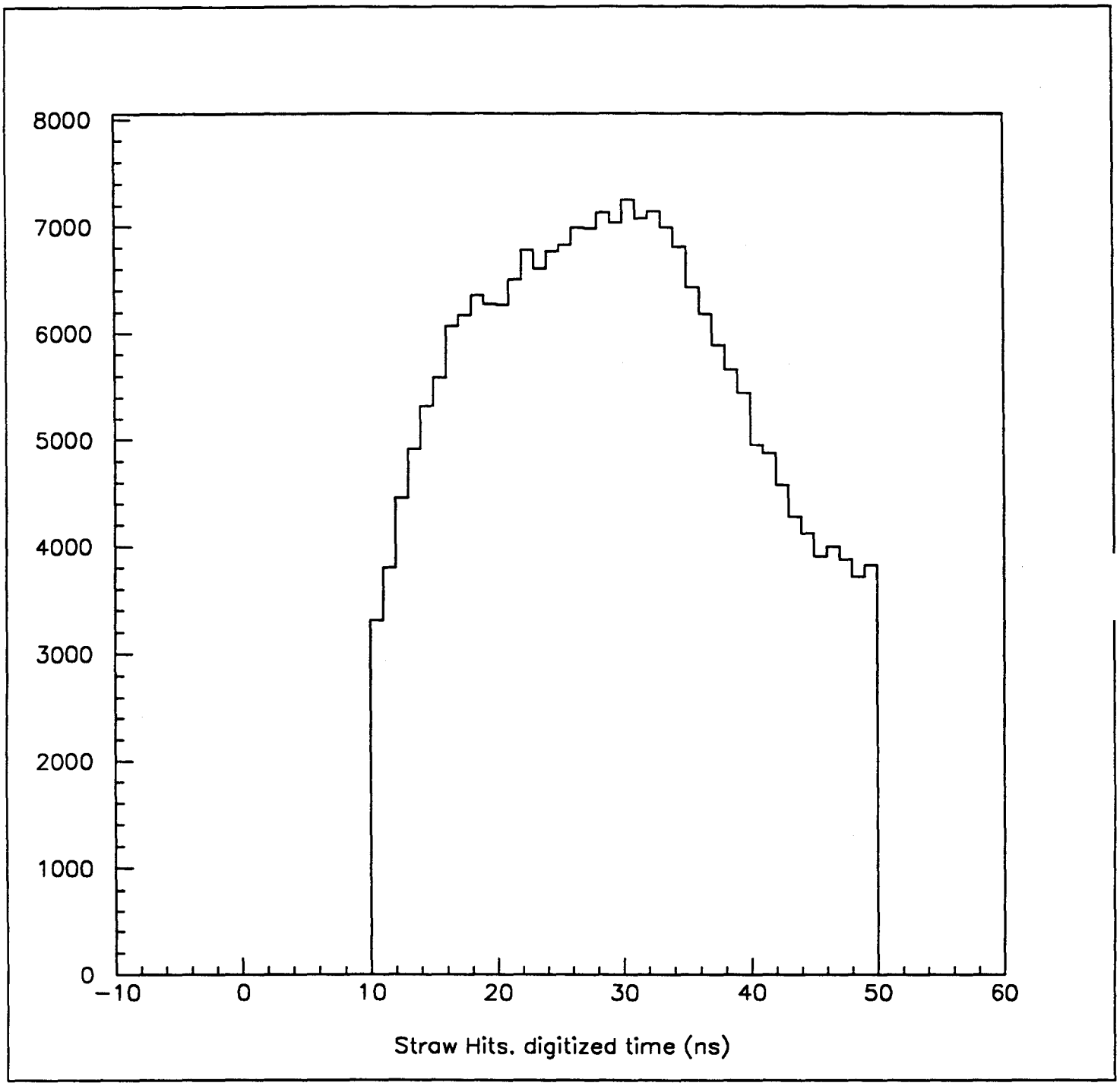

FIG. 3.1. Typical straw tube drift time spectrum, for 40 ns gate width.

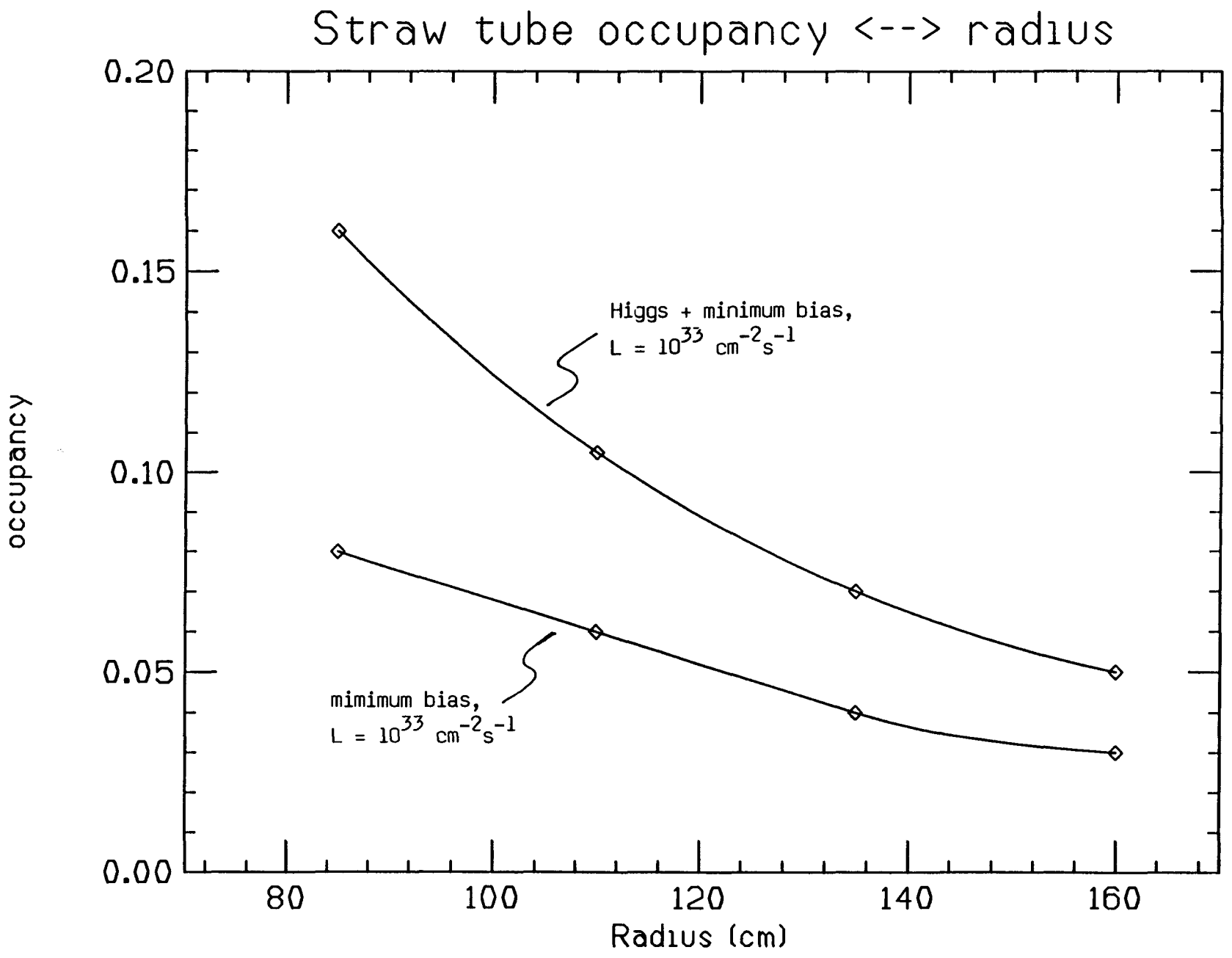

FIG. 3.2. Straw tube occupancy as a function of superlayer radius.

approximately 0.5%. Tests have been made of including the material of the magnet coil in the simulation. No significant change in the occupancy of the outer superlayers was observed.

Minimum bias events have been generated using the program Pythia. They have a mean charged multiplicity of approximately the charged track per unit rapidity per radian. Higgs events decaying into 4 charged leptons were generated using ISAJET and a Higgs mass of 300 GeV/c^2. Single, isolated muons were generated with P_t = 200 GeV/c, isotropically distributed in phi, and also in rapidity between the limits of ± 0.88, corresponding to the limit of the silicon barrel tracker.

3.2. Pattern recognition

Local track finding methods are used, which depend on the spatial proximity of points on the same track. Such methods do not depend on assumptions about the event vertex, and are relatively insensitive to non-uniformities in the magnetic field.

An independent search is made in each straw superlayer for track segments which are approximately radial, to within about 20°. This is based initially on the pattern of hit tubes only, and requires 4 (5) hit layers out of a 6- (8-) layer superlayer, respectively, with an inner gap of not more than one layer. Then a first fit is made to the drift time, which permits a preliminary resolution of the left-right ambiguity, and from the degree of stagger determines the t_0 correction needed for the propagation time along the wire. A final fit gives the segment position and direction for use in segment linking. At this stage, axial information only is used.

Track segments in the outer straw superlayer are extrapolated the short distance to the stereo fiber superlayer, and matched to pairs of u and v scintillating fiber clusters. The close proximity of the u and v stereo plane fiber layers to an axial straw tube layer greatly reduces the matching ambiguities. These could be further reduced once the entire axial track is found, by using the stereo silicon information.

The segments are then linked into chains, starting from the outside of the detector, where the track density is lowest. Again, no assumption is made about tracks originating from the origin or primary vertex. All nearby pairs of segments are tested to see if they are consistent with a circle: this is possible, since each segment has both a position and a direction measurement. Once a chain of 4

segments or more has been found, it is re-extrapolated to look for any segments which might have been missed on the first pass.

Finally, the chain (or chains) are fit to determine the track parameters, using a circle fit, followed by a separate s-z fit (where s is the track arc length). Where a beam constraint was used, the uncertainties were ± 10 μm in the transverse directions, and ± 1 mm in the longitudinal direction.

The average time per event for simulation and reconstruction is approximately 1 hour at 4 Mips for a Higgs candidate at design luminosity.

Track finding efficiencies in the barrel region ($45° < \theta < 135°$) have been estimated, both for isolated, $P_t = 200$ GeV/c muons, and for muons from the decay of a Higgs boson. At the design luminosity, the tracks are found with an efficiency of approximately 99% in each case.

3.3. Single isolated track resolution

The ideal resolution of the proposed tracking system has been studied using isolated, $P_t = 200$ GeV/c muon tracks with no background. Typical track fit residuals at the vertex and in the inner and outer tracker are shown in Figures 3.3 (a-f) for r-ϕ and s-z projections, respectively. The track fit imposes a vertex constraint of 10 μm in each transverse direction, and 1 mm longitudinally. The r,ϕ residuals in the silicon are smaller than the expected 10 μm resolution, since the track segments are not all independent, but contain shared hits. The straw superlayer resolution shows the expected value of about 60 μm expected in the absence of systematic alignment errors.

All tracks were successfully reconstructed. A momentum resolution of 2.5% is obtained, which does not change when a minimum bias background corresponding to the design luminosity is added.

Figure 3.4 shows the distribution in the reconstructed tangent of the dip angle for single tracks at a rapidity of -0.88 and a random, isotropic distribution in azimuthal angle. This corresponds to a resolution in dip angle of approximately 2 mrad. For tracks without a stereo measurement in the outer tracker, this would be ~4 mrad with or ~10 mrad without a 1 mm vertex constraint in z.

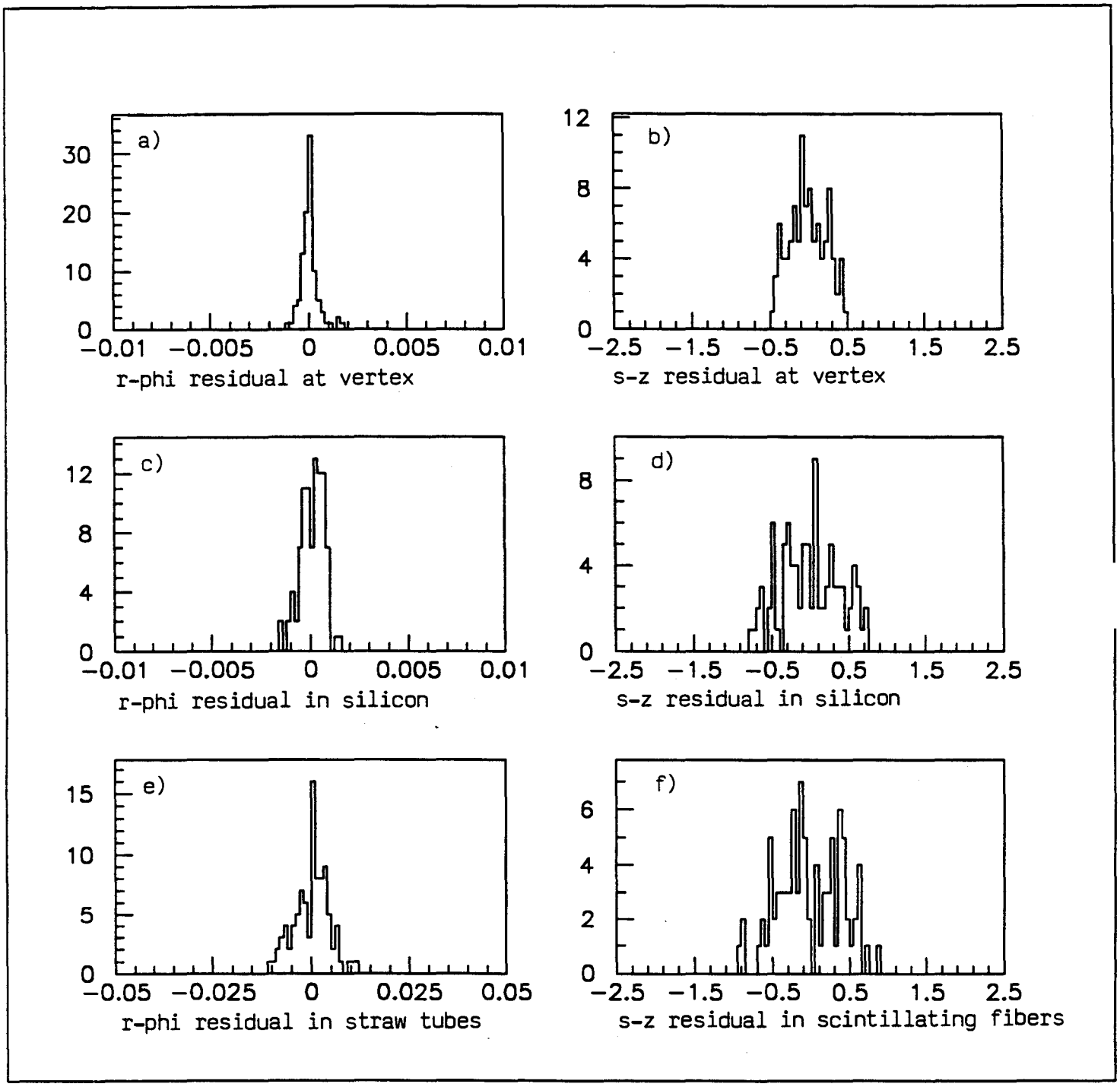

FIG. 3.3. Track fit residuals for high P_t tracks.

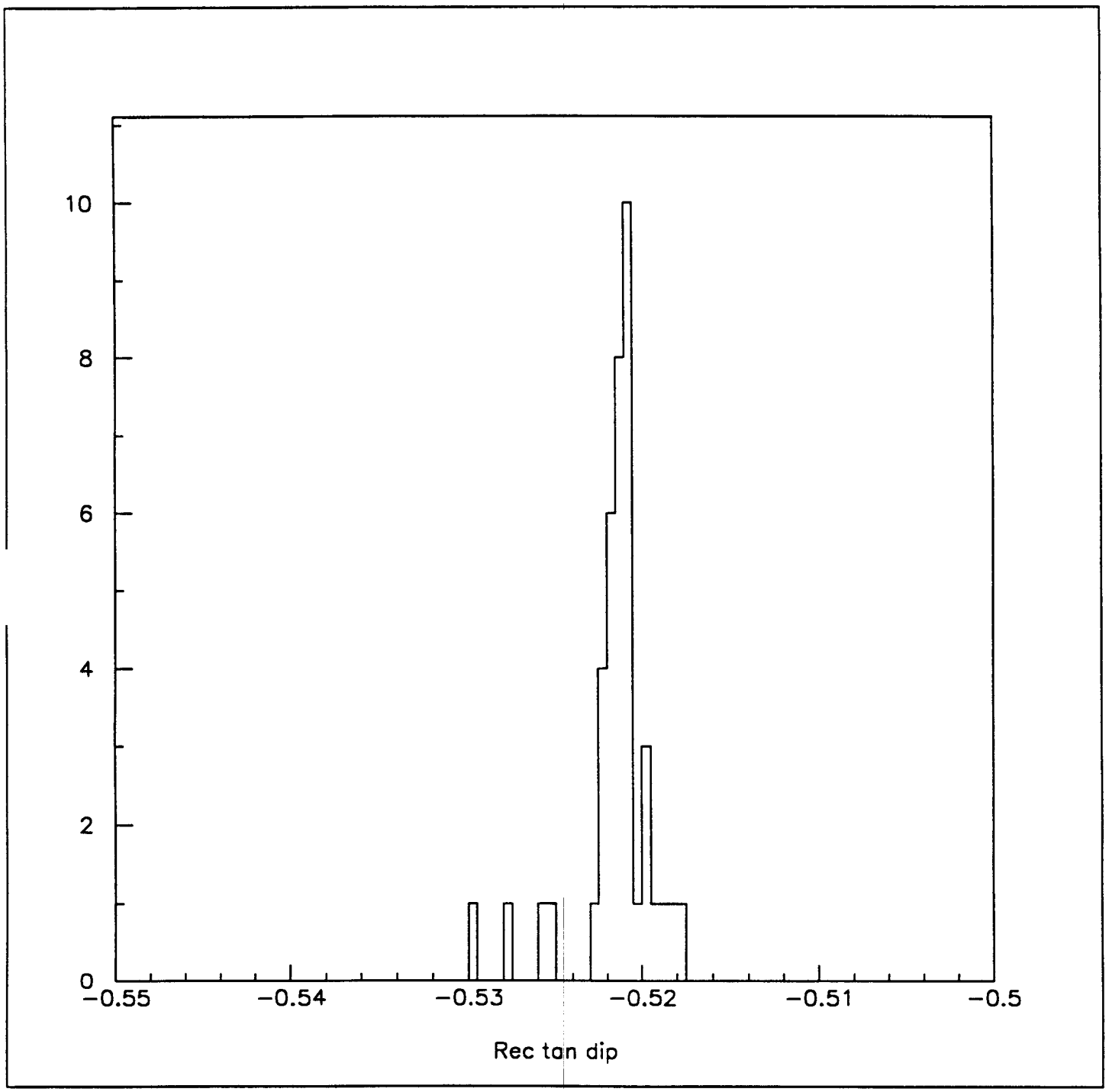

FIG. 3.4. Reconstructed tangent of dip angle for single high P_t tracks.

(The effect of a non-uniform magnetic field on momentum resolution has been investigated. For tracks confined to the silicon barrel region, it is small. Studies combining the forward silicon tracker with the ends of the outer barrel, where the non-uniformities are much greater, are still needed.)

3.4. Higgs $\rightarrow Z^0Z^0 \rightarrow$ 4 leptons performance

A sample of Higgs events where all four decay leptons lie within the silicon barrel region, i.e., $\tan(\lambda) < 1$, has been generated. All reconstructed tracks with $P_t > 10$ GeV/c are assumed to be leptons. The reconstructed dilepton mass distribution is shown in Figure 3.5, where the Z^0 mass resolution is approximately 3%. Figure 3.6 shows the four lepton mass distribution; the Higgs mass resolution is approximately 5-6%. The reconstruction efficiency for this (small) sample of simulated Higgs events is 100%.

3.5. Tracks in jets

Work on the reconstruction of tracks which are part of a jet is on-going. Results will be reported in the 3 January 1992 final version of this CDR.

3.6. Matching to other detectors

The bending plane for a muon in the iron toroids is perpendicular to that in the central tracking region. Good matching between the central tracker and muon chambers helps both the second momentum measurement and especially the rejection of decay muons and hadronic punch through. Good accuracy at the outside of the tracking chamber is also valuable for matching to calorimeter showers. The proposed tracking detector would give resolutions of approximately 2 mrad in dip and 3 mm in z at the outside of the tracking volume without a z vertex constraint. The inner silicon detector alone would give resolutions of approximately 10 mrad and 14 mm in z.

3.7. High luminosity

Figure 3.7 shows the straw and fiber occupancies as a function of luminosity. For the straws, the contribution to occupancy from a single in-time Higgs event is comparable to that coming from the $L = 10^{33}$ cm^{-2}-s^{-1} minimum bias background in

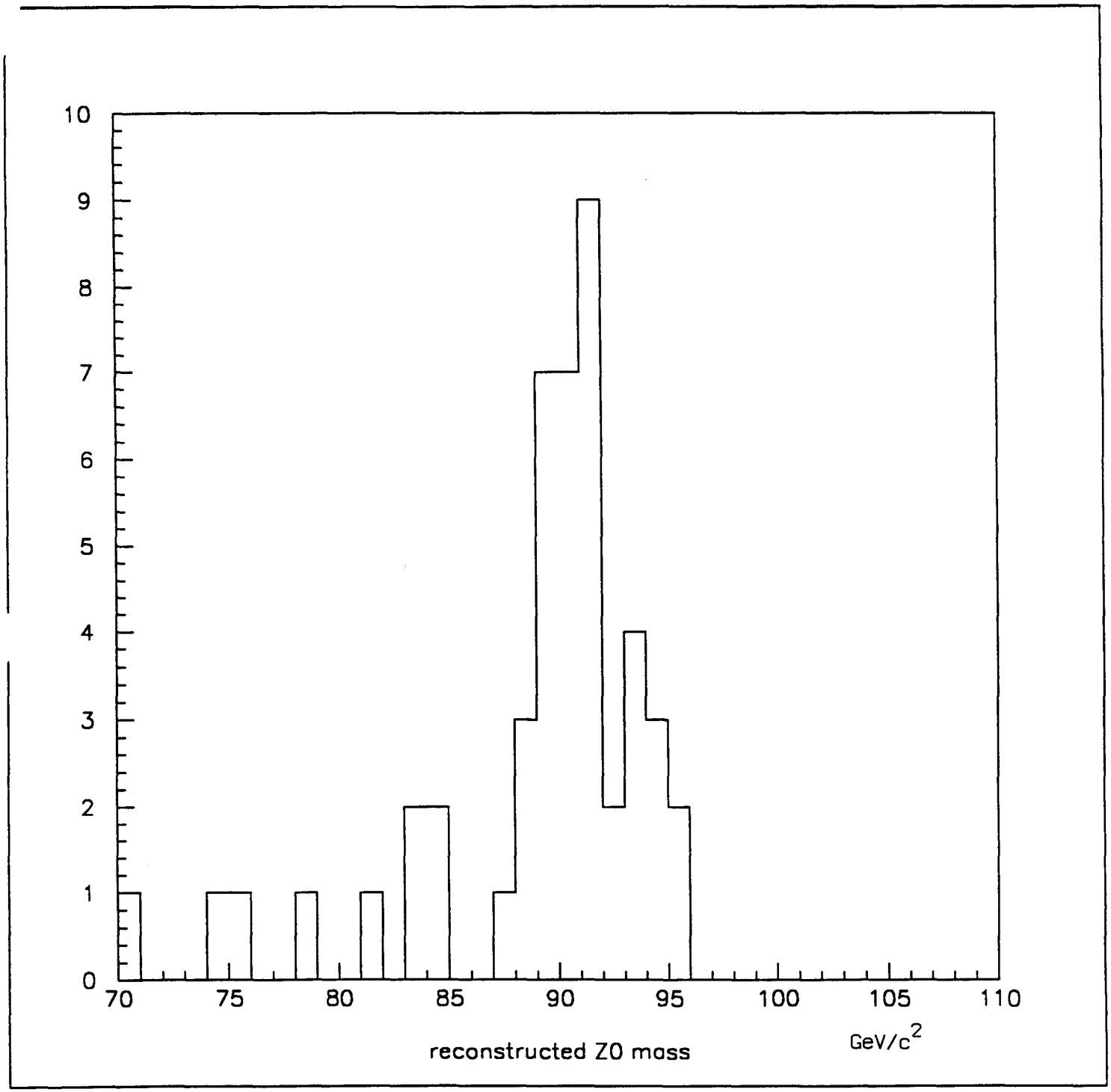

FIG. 3.5. Dilepton mass distribution for simulated Higgs → 4 lepton events.

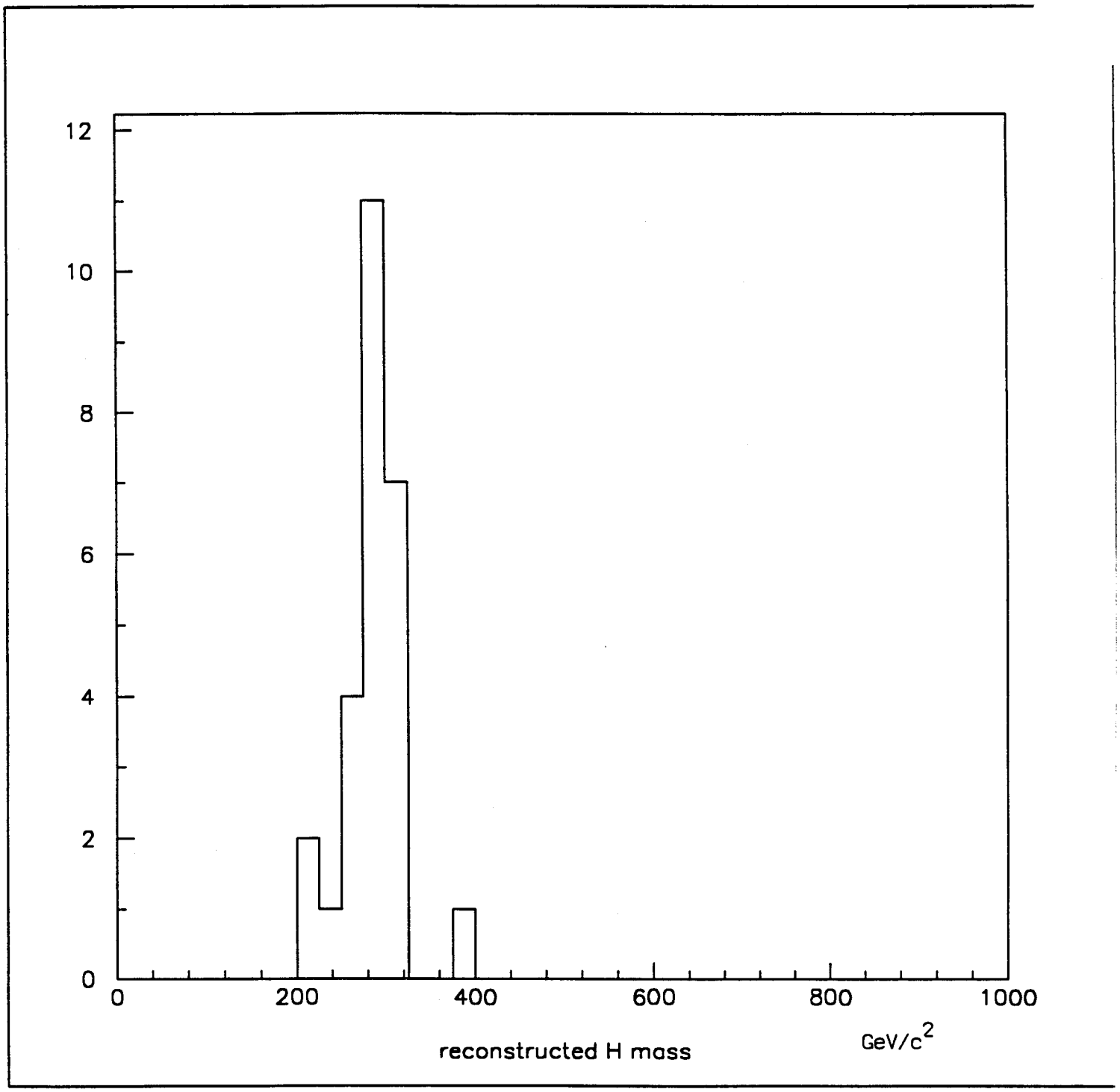

FIG. 3.6. Four lepton mass distribution for simulated Higgs → 4 lepton events.

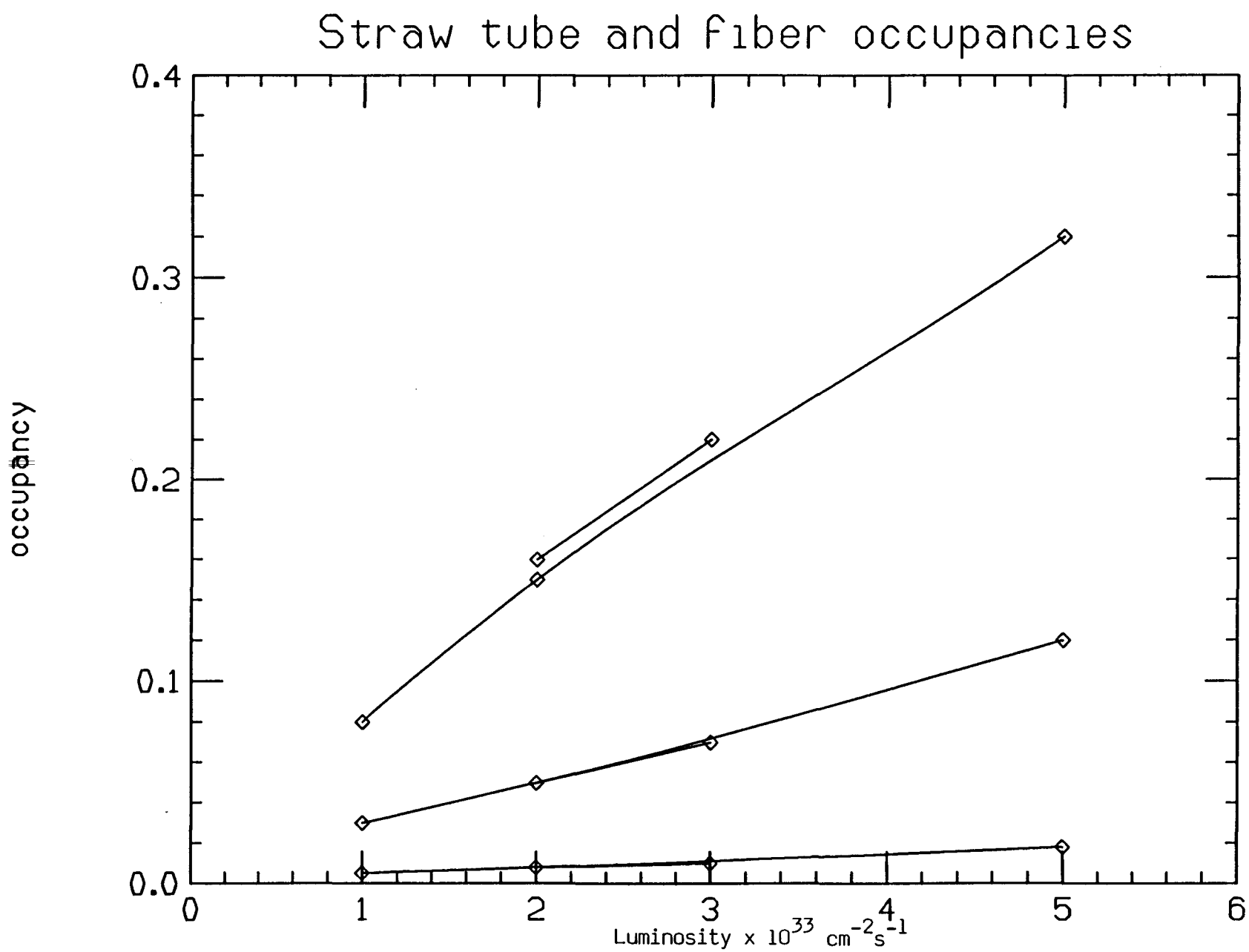

FIG. 3.7. Straw and fiber occupancies as a function of luminosity.

the 40 ns time gate. As the luminosity increases towards 10^{34} cm^{-2}-s^{-1}, the occupancy of the inner layers rises less than linearly due to the loss of multiple hits on a single straw.

The track finding efficiency is shown as a function of luminosity in Figure 3.8. Note that a Higgs event at $L = 10^{33}$ cm^{-2}-s^{-1} has a similar occupancy to a single muon on a $L = 2x10^{33}$ cm^{-2}-s^{-1} minimum bias background. The efficiency remains high even beyond the design luminosity, though the statistics are poor at very high luminosities. Figure 3.9 shows that the momentum resolution starts to become non-Gaussian at very high luminosities, with tails resulting from poorly reconstructed tracks.

3.8. Implications of further descoping

A configuration has been studied where the inner silicon barrel has been reduced from 8 to 4 double layers, with no modifications to the reconstruction software. The reconstruction efficiency for isolated, P_t = 200 GeV/c muons is shown in Figure 3.10. Contrary to Figure 3.8 for 8 silicon layers, a significant loss of tracks is seen already for a minimum bias background corresponding to $L = 2x10^{33}$ cm^{-2}-s^{-1}. However, provided the tracks are found, the momentum resolution remains good at a little over 3%.

(We have started to study a configuration with 8 inner silicon layers and only two outer tracking layers. For such a configuration, the tracks should first be found in the silicon detector alone. The important questions are the efficiency with which they can be linked to hits or segments in the outer layers, and also the trigger efficiency.)

3.9 Interdependence of inner and outer trackers

We have attempted to look at the tracking efficiency and momentum resolution of the inner and outer tracker separately. With the inner tracker alone, the momentum resolution is substantially degraded to 15% for P_t = 200 GeV/c tracks with a tight (10 μm) vertex constraint, or >30% without a vertex constraint. As noted above, the combination of inner tracker plus outer tracker being proposed here yields a momentum resolution of ~2.5% at 200 GeV/c. The resolution in dip

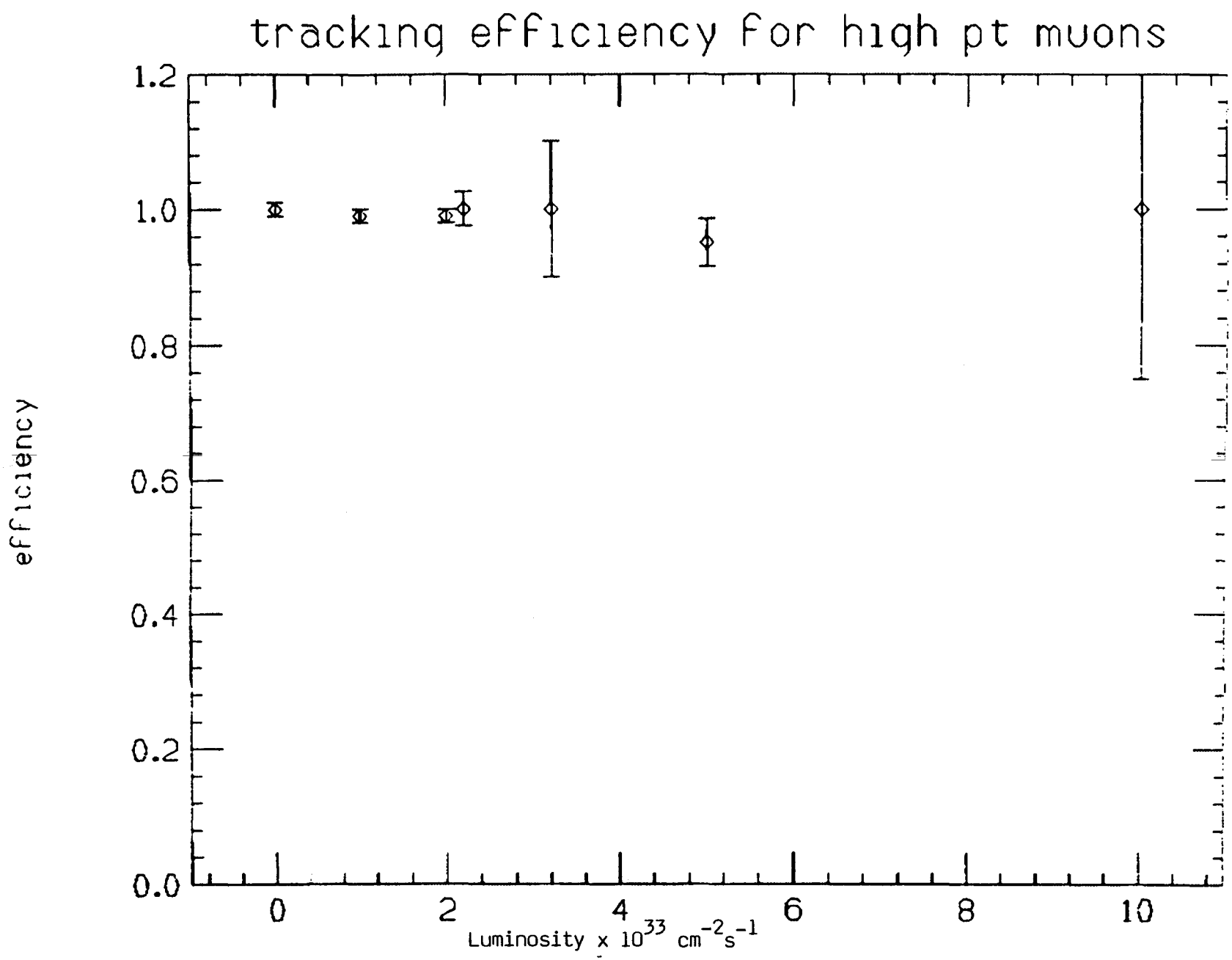

FIG. 3.8. High P_t track finding efficiency as a function of luminosity.

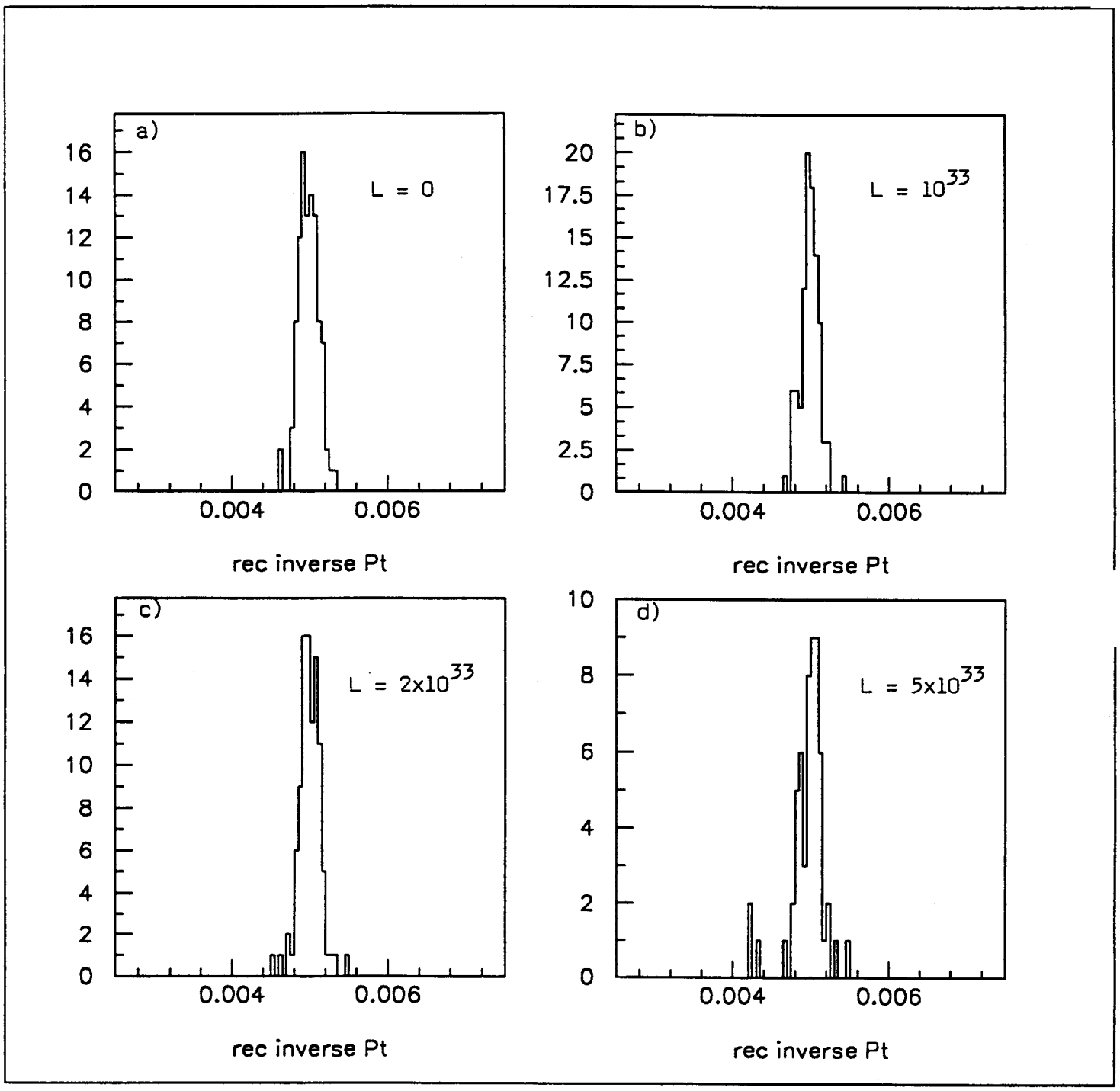

FIG. 3.9. Reconstructed transverse momentum distribution at luminosities of a) 0, b) 10^{33}, c) 2×10^{33} and d) 5×10^{33}

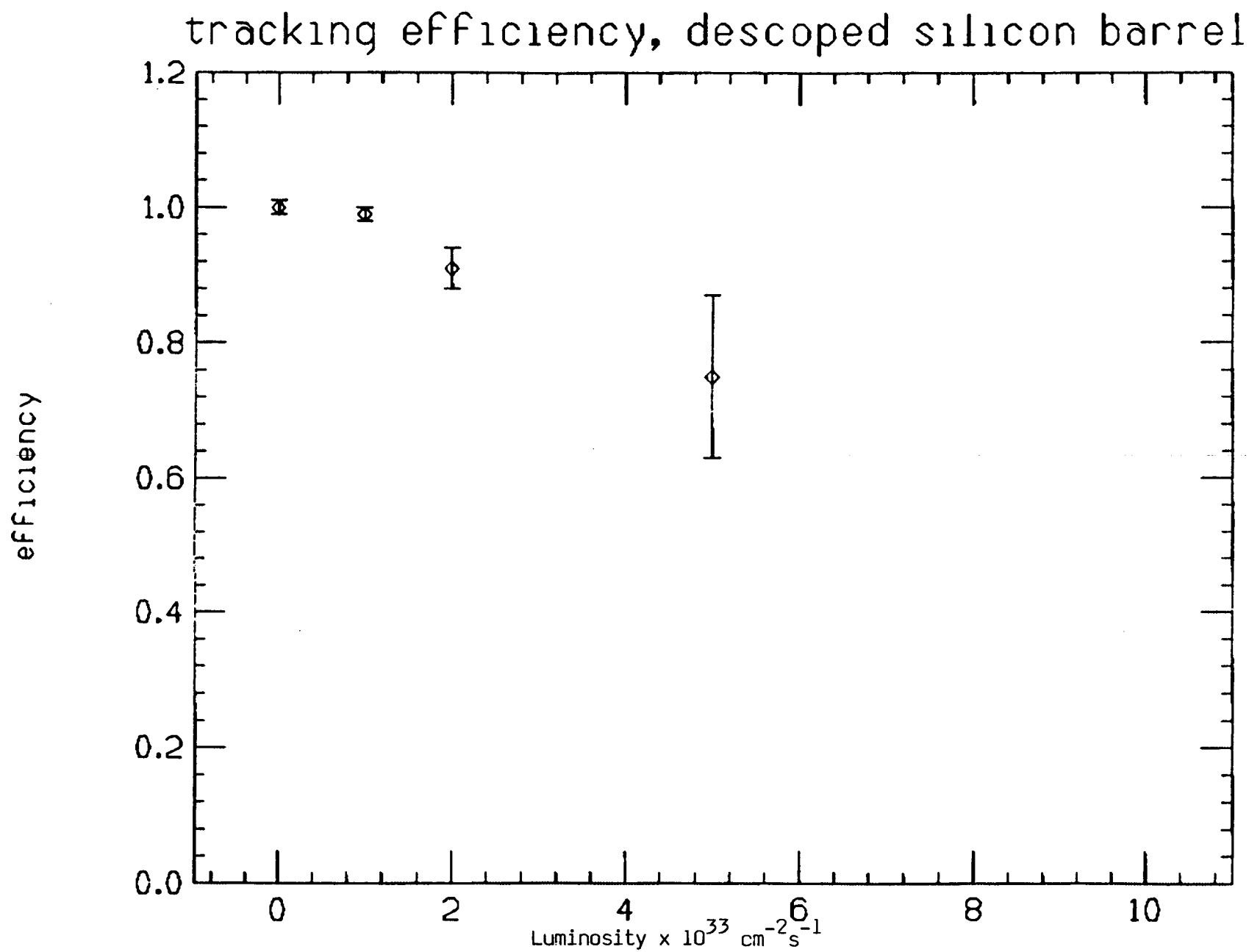

FIG. 3.10. High P_t track finding efficiency as a function of luminosity for a descoped inner silicon tracker.

angle, and consequently two-body effective mass, are similarly degraded. For the outer tracker alone, the track finding efficiency is poor, as there are no longer sufficient track segments, at least for the reconstruction algorithm used here.

We conclude that, for the hybrid design presented here, the inner and outer trackers are interdependent, and that neither can function adequately in the complete absence of the other.

4. Trigger capability

The proposed trigger design is based on superlayers of 8 straws. The processing of signals from these straws for triggering will be integrated into the front-end cards with the trigger signals extracted from the discriminator outputs as they pass between the bipolar preamplifier/discriminator chips and the CMOS level 1 storage chips. The trigger will be formed in chips specifically designed for trigger processing. Output from the trigger chips, stiff track signals, will pass to the global trigger logic through an information path independent of the data acquisition path.[10,11] If one chooses to process 4 trigger groups in each trigger chip, then each trigger chip inputs 20 straw signals. Of these signals, 4 are copies of the cells input to the adjacent trigger chip so that the number of unique inputs to each trigger chip is 16. This is to be compared to the 4 channels/chip of the preamplifier/discriminator and of the level 1 storage. In chip count the trigger is 1 of 8 (1 trigger circuit for every 4 preamplifier/discriminator circuits plus 4 level 1 storage circuits). This 12.5% increase in the electronic component count will be reflected as a cost increment for the trigger. A better estimate might be 15% since there will clearly be additional development costs. Higher channel count is possible in the trigger chips but connection complications work against their use.

The robustness of the trigger depends on the level of redundancy of the trigger information. A single 8 deep superlayer of straws provides triggering with an efficiency and false triggering rate that is quite sufficient at low luminosities and backgrounds. Multiple trigger layers offer increased efficiency and greater rejection of false triggers. Since the trigger chips are completely integrated within the chamber electronics, it is prudent to include these trigger chips on more than one superlayer of straws. The optimal choice of trigger layers is 3. These trigger layers must be axial and function most efficiently if placed at large radii. This choice permits a level 1 trigger composed of 2 of 3 coincidences of wedges in ϕ. The overall trigger design assumes that the trigger primitives used in the level 2 trigger decision are generated and issued as part of the level 1 information flow. The choice of 3 trigger superlayers provides for significantly enhanced processing and momentum resolution in triggers formed at level 2. This offers precise strip, calorimeter, and muon matching at level 2 if and when such processing is found to be necessary or desirable.

4.1. The single superlayer trigger

Stiff tracks are sensed in the superlayer of straws by demanding that the arrival times of hits from the wires be consistent with the patterns possible for high momentum tracks. The drift times in radially aligned tubes change linearly as the track diverges or converges from the radial line connecting the wires. The amount of this change is a measure of the transverse momentum of the track. These times can be quickly processed to select tracks that are sufficiently radial to be higher than a preselected cutoff in momentum. In addition, the time variations in signal arrivals can be eliminated so that a unique crossing number can be assigned to each stiff track sensed. With the correct choice of signal handling, the residual time jitter can be reduced to that from variations in the arrival times from the distribution of track z positions. The 8 ns jitter is well within the 16 ns crossing time and should not lead to any incorrect crossing tags. A simulation of this distribution of output times is displayed in Fig. 4.1. The simulation includes minimum bias events from several previous crossings. As a result, the outputs for times other than the desired peak are also seen.

The circuit that provides both momentum selection and crossing number is a digital mean timer.[12] The characteristics of a digital mean timer are that it accepts two digital pulse inputs and outputs a single pulse at the average time of the two inputs offset by a fixed delay if and only if the time difference of the two inputs is less than a preset number. Figure 4.2 displays one of 8 proposed connections of these mean timer circuits to an 8 deep superlayer. Two pairs of radially aligned wires, one from each side of the 1/2 cell staggered pattern, are separately averaged to a common radial position. These two averages are again averaged in a third mean timer that makes use of the fact that the sum of the distances from the track to the left and right staggered patterns is a constant. This second mean timer eliminates the variation in pulse times due to differing drift distances. Several patterns meeting these conditions are processed in parallel in separate circuits. This parallel processing is possible since mean timer circuits are very small as measured in silicon area. A single mean timer is much less than 1% of the area of a modest CMOS chip. The outputs from the 8 individual pattern circuits are combined as 2 of 8 coincidences into a single output that flags a stiff track. A programmable transverse momentum threshold is provided.

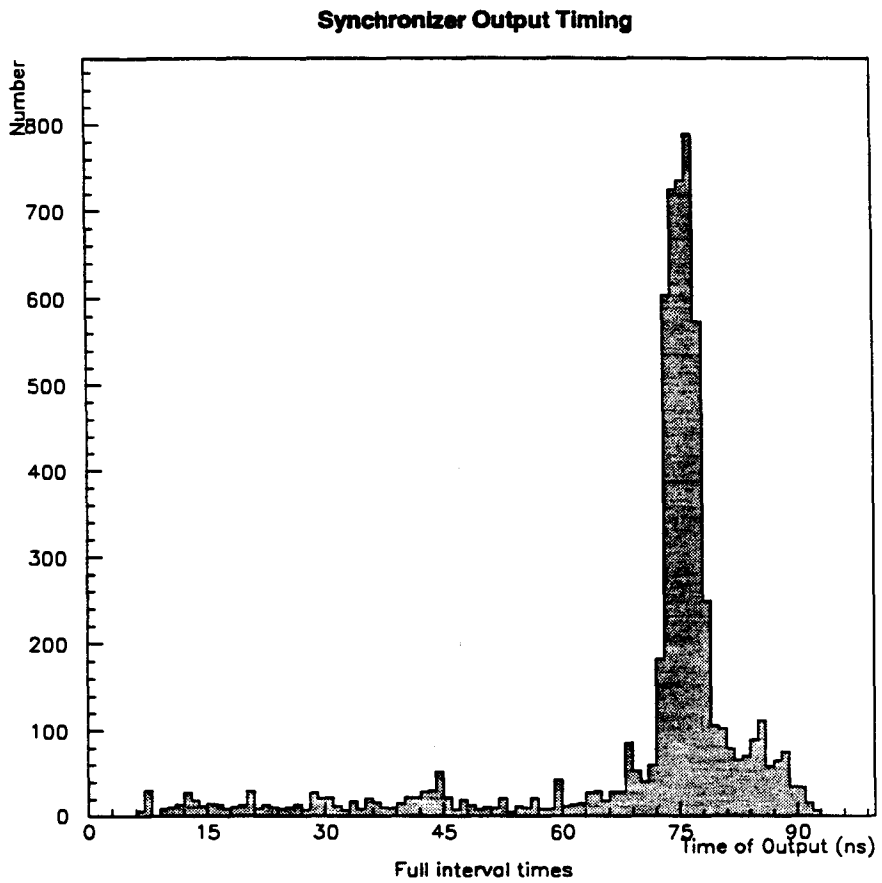

FIG. 4.1. Pulse timing for the GEANT simulation of tracks in the outer layer of the SDC detector instrumented with mean timer circuits that produce an output time displaced from the particle passing time by a fixed value, ≈45 ns. An additional 30 ns delay is seen in the plot due to the particle flight time to the superlayer and the propagation time of the signal to the end of the straw. This particle and signal flight time varies over a range of about 8 ns and is therefore the major contributor to the spread in the arrival times.

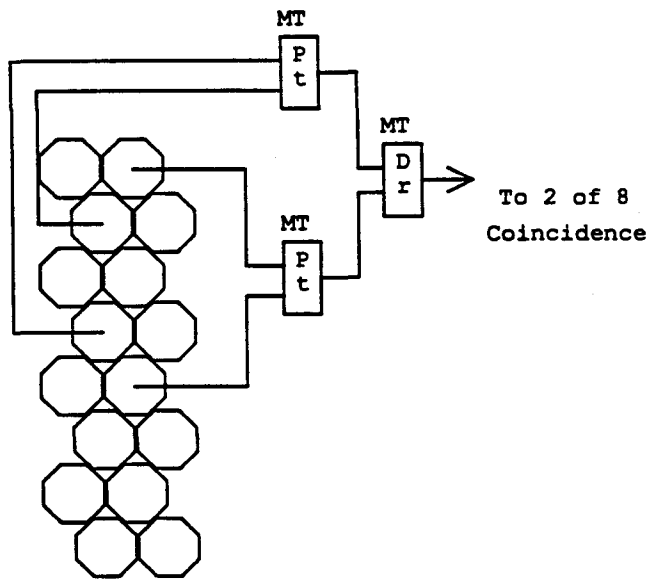

FIG. 4.2. A representative mean timer connection for an 8 tube superlayer. The connection shows two mean timers each requiring hits to be consistent with a present momentum lower limit and output pulses averaged in time to a common radial position. The third mean timer averages these output pulses to arrive at a final pulse whose timing is fixed relative to the particle passage time plus the signal propagation time from its z position to the end of the straws. The pattern shown is one of 8 used in a two fold coincidence to produce a stiff track trigger.

4.2. Simulation of the superlayer trigger

Extensive simulation of this triggering algorithm has been performed. This simulation was carried out for the outermost superlayer of the proposed straw tube tracker at the design luminosity of 10^{33} $cm^{-2}s^{-1}$. The results of these simulations are summarized in Fig. 4.3. In this figure the turnon behavior of the trigger is shown for a 10 GeV setting of the threshold. The sufficiency of this threshold behavior has been demonstrated recently for electrons by Sullivan.[10] Table 4.1 gives the triggering efficiency as a function of transverse momentum from the turnon curve of Fig. 4.3. The table also gives the false triggering rate of the design as a function of the hit occupancy within the trigger group. False triggers are defined as triggers not accompanied by a track greater than 3 GeV. According to the work of Sullivan,[10] this false rate has little effect on the quality or rate of the electron triggers. The results displayed in Fig. 4.3 indicate that the trigger efficiency rises steeply from

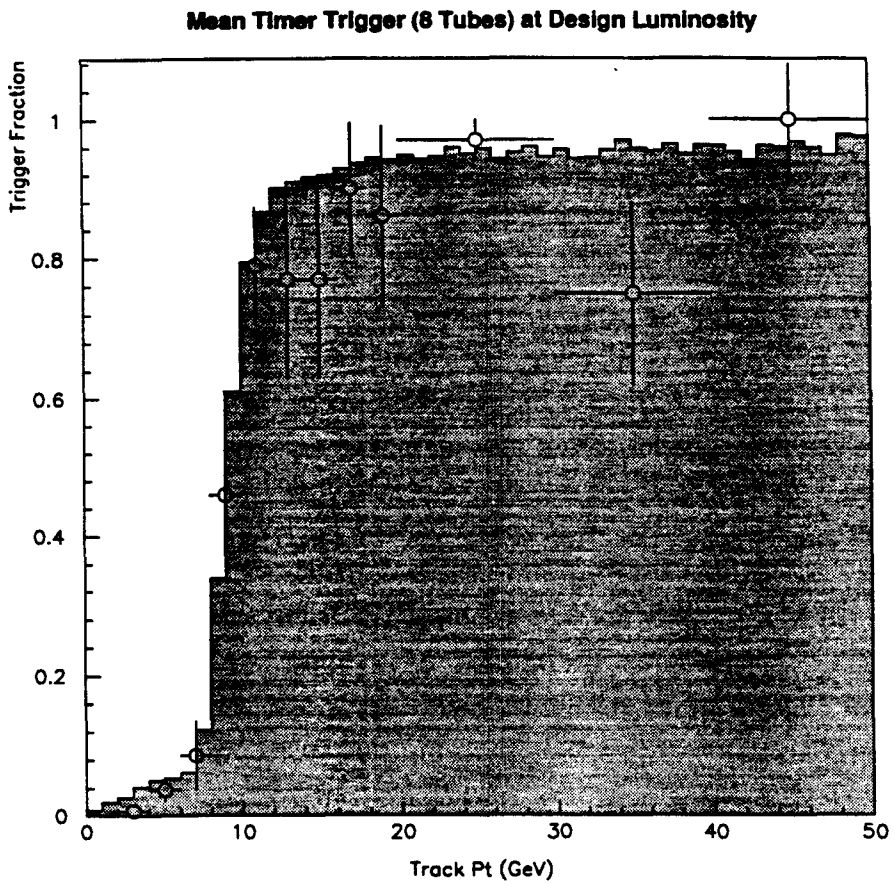

FIG. 4.3. The efficiency as a function of P_t for a digital mean timer based trigger operating on signals from an 8 tube deep superlayer of packed straw cells. The points are from a GEANT simulation of Higgs $\rightarrow$ ZZ events at 10^{33} $cm^{-2}s^{-1}$ luminosity and the shaded histogram is for a fast parameterized simulation tuned to match the GEANT points.

TABLE 4.1.

Trigger Threshold	
P_t	Fraction Accepted
1.0	0.0080
2.0	0.0192
3.0	0.0272
4.0	0.0420
5.0	0.0516
6.0	0.0541
7.0	0.0621
8.0	0.1232
9.0	0.3396
10.0	0.6109
11.0	0.7940
12.0	0.8656
13.0	0.9005
14.0	0.9093
15.0	0.9162
16.0	0.9194
17.0	0.9284
18.0	0.9366
19.0	0.9441
20.0	0.9409
21.0	0.9486
22.0	0.9425
23.0	0.9467
24.0	0.9597
25.0	0.9600

False Rate	
Occupancy	Fraction Accepted
0.30	0.0000
0.35	0.0005
0.40	0.0011
0.50	0.0044
0.60	0.0247
0.70	0.0535
0.80	0.1111
0.90	0.2206
1.00	0.2447
1.10	0.3125
1.20	0.4495
1.30	0.4763
1.40	0.6209
1.50	0.6756
1.60	0.6984
1.70	0.8086
1.80	0.8333
1.90	0.8429
2.00	0.9735

threshold to around 94% and that the false triggering rate due to occupancy of overlapping soft tracks is well under one per crossing at SSC design luminosity. IN addition, the effect of a nonuniform B field at the 6% level[13] as expected in the central tracker softens the turnon threshold slightly. Changing E × B effects in the end regions of the central tracker are of the same order and contribute a similar softening to the threshold. The trigger momentum resolution of 10% at 10 GeV is not expected to degrade beyond 15% due to these B field related variations.

4.3. Chip performance

Trigger chip development for SSC gas tracking detectors began[14] with the fabrication of an analog implementation of a circuit called a synchoronizer. This circuit is essentially a dual analog mean timer. It has been superseded by the digital implementation already introduced above. The digital circuit requires no calibration and no special effort to avoid cross coupling of analog and digital sections of the chip. All future work will be with the digital chip.

The digital circuit is based on 2 ns digital delay elements. It contains 15 delay elements in the momentum (angle) selection portion of the circuit and 30 delay elements in the total drift time section. This gives it a range of up to 30 ns in the timing difference of radial wires and up to 60 ns of maximum drift time. Values less than these extremes are programmable within the chip. The circuitry for locking of the delay element timing to an external clock is provided within the chip as are numerous diagnostic points. We have tested the delay cell and locking circuits and have found them to function over the range of 1.3 ns to 4.0 ns, consistent with the CAD simulations. The mean timers have been observed to function including the drift time and momentum restriction circuitry. No design errors have so far been found.

Figure 4.4 illustrates the overall performance of the chip. In this plot the relationship of the aligned wire inputs is demonstrated. Since the LV511 IC tester used in this work samples outputs rather than measures times, the relationship between the input timer is evaluated and displayed for a predetermined fixed output time. This is equivalent to measuring the relationship that exists between two numbers that have a constant average. The correct relationship is linear with a falling 45° slope. In addition, the IC imposes a maximum allowed time difference

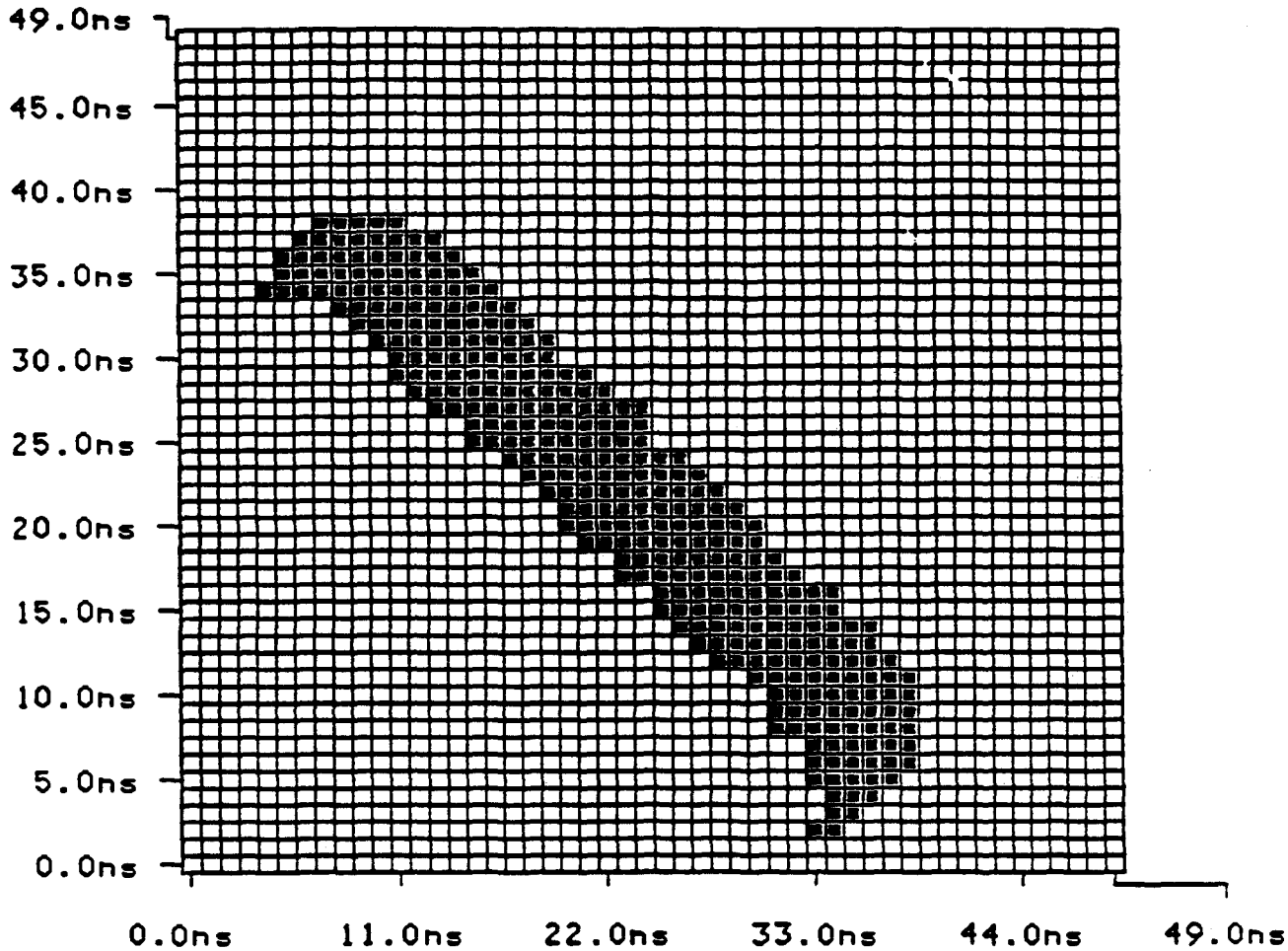

FIG. 4.4. A test plot of the P_t cut port of the mean timer IC. The axes are the times of the aligned wire inputs and the plotted points are those values of the axis coordinates for which an output was generated at a predetermined value. A falling 45° is expected for correct averaging of the input times. The cutoff of the line at large coordinate differences is due to the time difference restriction (momentum cut).

between its inputs. The region of signal output seen if Fig. 4.4 illustrates both of these characteristics. A falling 45° line with a cutoff at large coordinate differences is evident. Plots have been generated (not shown) for more restrictive time differences and observed to behave as designed.

4.4. Trigger modularity and data flow

The stiff track signals from the individual superlayers are designed to flow to a global trigger processor located at ground level. The exact modularity of this data collection is still being debated. The trigger data multiplexing depends on whether the choice is made to send the trigger primitives (stiff tracks with trigger group locations) synchronously or asynchronously. This also remains under debate. The modularity and information flow for the straw trigger outlined below must therefore be considered preliminary since the precise details of the information flow must await firm decisions about the general data flow of trigger information.

A natural choice for the trigger grouping is into 64 regions of ϕ. This leads to about 80 trigger units from 20 trigger chips distributed over 16 cm of circumference. If one wishes to accept only one stiff track signal from each of these 64 ϕ regions while restricting the bandwidth from each region to one GHz fiber channel, then the data from each stiff track must be compressed into 16 bits. IF three bits are allocated to momentum information, then the position information can be easily represented in the remaining bits. Even with this restricted choice of one stiff track for each of the 64 regions, the bandwidth of the data flow is seriously underutilized. With less than one in five of the crossings yielding a single stiff track signal, the 64 trigger data fibers contain data a small fraction of 1% of the time. A scheme where each region presents any second stiff track to both its neighbor regions for transmission should that region not contain a stiff track, is a possible way to use the distributed bandwidth to overcome the local congestion. Asynchronous transmission schemes take this shared bandwidth to its logical conclusion.

Whatever the transmission scheme the trigger data, the stiff track finder must issue its track primitives in the form of trigger unit ϕ location and track momentum. In synchronous transmission the arrival time designates the crossing. In asynchronous (buffered) transmission the crossing number must be included with the data so that resynchronization can be accomplished by the central trigger processor.

4.5. Summary

The preferred design for the trigger of the straw tube central tracker consist of integrated stiff track sensing on 3 superlayers of axial straws. The stiff tracks found, the trigger primitives, are to be collected for regions of ϕ and transmitted via fibers to the global trigger electronics on the surface. This trigger data can be sent synchronously each 16 ns or asynchronously with crossing number tags. The number of such trigger fibers if of the order of 128 or less with a rather low duty cycle. The trigger primitives will be stored in the global trigger crates for processing by the first and second trigger.

Both trigger levels are expected to make use of these trigger primitives in a manner that evolves as the luminosity of the collider increases. Initially, the first level trigger will likely use a simple coincidence of 2 out of 3 superlayers in crude ϕ bins. Sophisticated first level triggers might do combinatorial logic on the pattern of hits including the actual trigger unit ϕ location. This could provide improved momentum resolution up to the constraints imposed by the nonuniform field effects.

The second level trigger will likely process all the superlayer primitive information in conjunction with the calorimeter and muon data. Since these other systems offer z information, the matching to them includes the option to correct the momentum of the central tracker with z known. For this correction to improve the momentum, individual superlayer trigger ϕ locations will be needed.

The instrumentation of trigger chips on three superlayers of straws appears completely justified since it:

- Permits a natural enhancement of the trigger as the luminosity increases. Without this data few options will exist and changes in the on-chamber electronics will be very difficult.
- Eases the integration of the front end and trigger electronics by making all axial layers identical.
- Represents a modest (perhaps insignificant) cost since the innermost axial layer has the fewest channels.
- Provides handles to overcome unanticipated problems.

5. Integration with other systems

5.1. Overview

Since several options are being considered for some of the systems with which the SFTS must integrate, we have had to make some assumptions; for this purpose, we have assumed a silicon tracker as identified by the Seiden group and a gas microstrip intermediate tracker. We discuss here the major integration issues, which include consideration of support of the silicon tracker and supply of its utilities, physical accommodation of an intermediate tracker, support and utility requirements that must be provided by the calorimeter, and electronics access and the resulting physical requirements these place on the radius of the barrel toroid.

5.2. Silicon tracker

The outer tracker will provide structural support for the silicon tracker. The support points will be located on the inner cylinder of the outer tracker and the interface will consist of a bolt circle of drilled and tapped holes the number and size of which will be established in coordination with the silicon tracker design team. The outer tracker will be designed to allow installation and removal of the silicon tracker after installation of the outer tracker in the detector. Space will be provided for routing utilities for the silicon tracker between the outer tracker and the intermediate tracker (see Fig. 5.1) to a location where they can be routed between the barrel and endcap of the calorimeter.

The requirements for structural support of these utilities have not been established but it is assumed that some attach points on either the outer or intermediate tracker structure will be required for the silicon tracker utilities. A major issue is the routing of the butane cooling line for the silicon tracker due to the somewhat tortuous path which is dictated by physics requirements of the outer and intermediate trackers. After leaving the outer tracker, space must be provided in the calorimeter design to accommodate routing and support of the silicon tracker utilities.

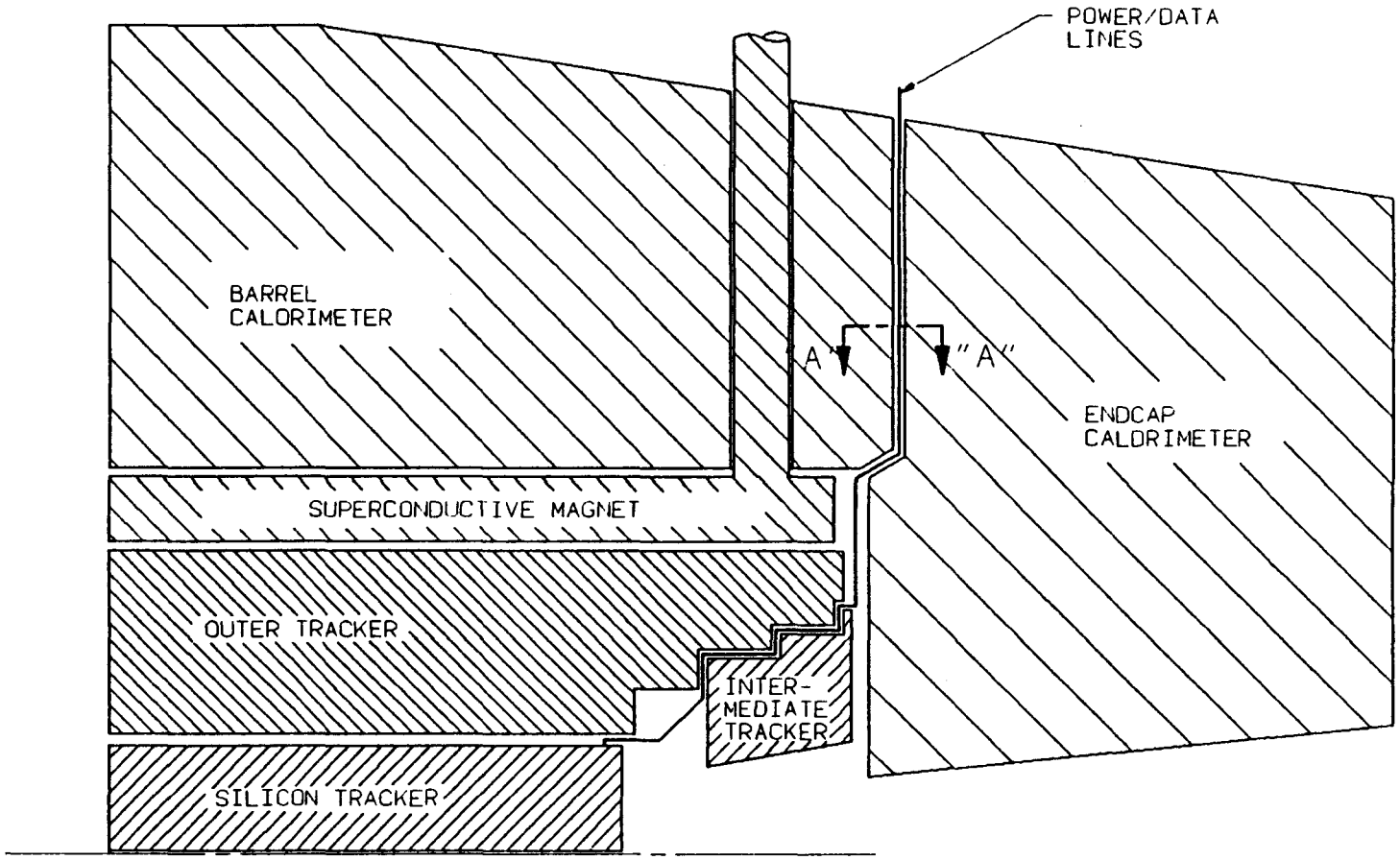

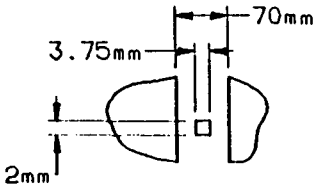

SECT. "A"-"A"

FIG 5.1 SILICON TRACKER POWER/DATA LINE ROUTING

5.3. Intermediate tracker

The gas microstrip version of the intermediate tracker has several alternative designs. The number of disks at each end of the tracker varies from three (z = 3 to 4 m) to five (z = 2 to 4 m). The current SFTS design asumes three annular disks for the intermediate tracker located at z = 3.0, 3.5 and 4.0 m (see Fig. 1.1 on p. 2). The most important interaction between the barrel and intermediate tracker is associated with mechanical support and alignment. The SFTS design assumes that the barrel tracker will be supported by the barrel calorimeter and that the intermediate tracker will be supported in a manner which allows its removal to provide a 1 m access space at the end of the barrel. No work has been done to date on the question of relative alignment. Once the intermediate tracker geometry has been fixed, the questions of mechanical interface and relative alignment will be examined.

5.4 Calorimeter

The SFTS is a self-contained unit. It contains all components necessary for its internal support. External support for the SFTS is required for overall mounting within the SDC detector. This system must be stable and sufficiently rigid to support the mass of the central tracker. The calorimeter has been selected as the interface point for supporting the tracker. Additionally, the calorimeter interface must allow for routing and support of all central tracker utilities. The current design for this interface is shown in Fig. 5.2.

The central tracker, which includes the SFTS, the intermediate tracker and the silicon tracker, will have a mass of approximately 1,000 kg. The calorimeter support system must be capable of sustaining this load. The support system must also accommodate alignment of the tracking system relative to the I.P. of the detector. The current design utilizes a static alignment system which will be adjusted during final installation of the detector.

The calorimeter support system design has not been finalized, but the preferred approach is presented here. Supports will be attached to the calorimeter at several radial locations. The supports will be routed to a ring which is located at the end of the superconductive magnet. The ring will serve as a common mounting point for the outer tracker and the intermediate tracker. All adjustments to the alignment will be made relative to this ring. The ring will provide the overall stability for support of the tracker from the calorimeter.

6. Other factors

6.1. Staging and Upgrade

The full straw-tube tracking system described extensively in this report consists of six superlayers with 106.2k straw channels and 116.3k fiber channels. The innermost fiber superlayer (at R = 60 cm) is primarily intended to boost the performance characteristics of the system as the SSC luminosity increases beyond the design value of 10^{33} $cm^{-2}s^{-1}$. All physics performance simulation to date has used the system without this inner fiber superlayer. In addition, the primary cost estimate given in Section 6 is for a system without this inner superlayer.

As the SSC luminosity approaches 10^{34} $cm^{-2}s^{-1}$ this inner superlayer, with its excellent occupancy characteristics and independent stereo and vector information, should ensure an operational tracking system. In addition, at lower luminosity it should reduce the interdependence of the inner and outer portions of the tracker. Neither of these points has received any detailed simulation studies.

Practically speaking, staging is a financial exercise. There is little doubt that the innermost superlayer would improve the tracking performance. If it can be incorporated into the straw-fiber tracker from the beginning, so much the better. It must be there when the SSC luminosity is high. Exactly when it is installed depends on when the funding makes it realistic.

Another important issue related to this staged piece of the tracking system relates to technical feasibility. We could build today the outer stereo fiber superlayer. Both precision and readout requirements are sufficiently relaxed that today's expertise is adequate. The innermost superlayer is slightly more ambitious. The fiber alignment requirements are more stringent, the fiber diameter is narrower (so less light is produced in the fiber) and the average fiber occupancy is higher than for the fiber at large radius. Whereas today's fiber and today's readout devices (*e.g.*, avalanche photodiodes operating in Geiger mode, or even standard photomultiplier tubes) could be used for the outermost layer. Some R&D work is still needed before we have a convincing solution for the innermost layer.

6.2. Maintenance and repairs

The high reliability design and static nature of the outer tracker minimize the requirements for maintenance and repair. The straw electronics packages will be

designed in assemblies such that replacement can be accomplished within the one meter access space (see Section 4.5). The concept for maintenance of these electronics will be to remove a non-functioning card and replace it with a new one. All tests and check out can be accomplished externally to the detector and therefore no test equipment for electronics will need to be carried into the tracker area.

The remaining components requiring maintenance and repair consist of the ionization gas supply and return system and the electronics cooling gas supply and return system. These systems consist of non-metallic tubing and connections which will require leak checks and, if leaks are found, removal and replacement. The leak checks can be accomplished within the one meter space and it is anticipated that removal and replacement can also.

The frequency of these repair activities has not been determined, but in the case of the gas supply systems scheduled maintenance inspection checks should be performed anytime the detector is down for maintenance of the other systems. Also a visual inspection should be performed for the entire tracker including structure, electronics, and gas systems.

Scheduled maintenance is not anticipated for the fiber system but a connector between the scintillating fiber and the light waveguide fibers will allow their removal and replacement, if any must be replaced.

In the unlikely event that replacement of an entire superlayer is required, the detector must be disassembled to the point where an entire cylinder can be removed and replaced. This requires up to eight meters of clear space at the end of the tracker and will also require removal of the silicon tracker.

6.3. Radiation hardness

Annual doses at design luminosity within the central tracking volume occupied by the SDC detector have been estimated (*e.g.*, Groom[15]) not to exceed ~5 krad at 65 cm from the beam pipe, which scales to ~500 krad for ten years operation at 10^{34} $cm^{-2}s^{-1}$ luminosity. Corresponding neutron fluence estimates for a Pb-Sc calorimeter are about 10^{12} and 10^{14} cm^{-2}, respectively; these can be reduced by about an order of magnitude through the use of a polyethylene liner. Preliminary radiation damage assessments of straw-tube and scintillating fiber components irradiated to approximately ten times these levels have been generally encouraging. However, definitive low-rate tests of integrated systems are lacking. The importance of this

point is illustrated by the work of Majewski, Zorn, et al.,[16] which indicates that damage to scintillating fiber irradiated at low dose rates is higher than damage to similar fiber irradiated at high dose rates, but much worse in an argon (rather than an oxygen) environment..

Radiation hardness testing of straw components has been encouraging. Straws and glues appear to suffer no significant damage at neutron fluences of the order of 10^{15} cm^{-2}, fast, and 10^{16} cm^{-2}, thermal, and simultaneous gamma-ray doses of 100-500 krad, as reported by Dunn, et al.[17] Zhou, et al.[18] demonstrated the operation of straw tubes in a neutron environment to a total fluence of about 1.1×10^{13} cm^{-2}. Despite these encouraging initial results, more tests of straw systems that employ the actual gases, wires, electronics, etc., expected to be used in the SFTS are planned. These tests include low-rate, mixed-field irradiations in a special facility now under development at North Carolina State University which will allow electrical monitoring of the straw tubes during irradiation. It is necessary to show, for instance, that centering wire supports do not significantly expand or contract after exposure to high radiation levels, that the radiation environment does not materially affect the gas/anode/cathode interaction at operating voltages over extended time periods, and that the front-end electronics are sufficiently rad-hard.

The situation with respect to fiber technology is somewhat similar. Tests of fibers to date indicate that radiation resistance of scintillators is improving, and existing fibers (*e.g.*, 3HF) appear to be good a candidate for central tracking applications, showing no appreciable damage at radiation levels of 0.5 Mrad. At 0.5 Mrad and 3 m fiber, the loss of light is 10% for high rate of irradiation and 28% for low rate of irradiation with the fiber in argon. These are worst case values. The whole 3 m fiber will on the average be exposed to half this amount in 10 years at $L = 10^{34}$ $cm^{-2}s^{-1}$.

Dunn, et al.[17] have shown that APD's operated in the geiger mode begin to exhibit substantial increases in dark count rate after exposure to fast neutron fluences of less than 10^7 cm^{-2} (see Fig. 6.1). This indicates that APD's, even if used in sub-Geiger mode, will have to be located outside the calorimeter. This can easily be accomplished by optical-fiber coupling between the scintillating fibers and the APD's, if fiber light output is sufficient. Our future tests will thus concentrate on light output, scintillating-to-optical fiber coupling, and fiber coupling to APD's and/or VLPC's.

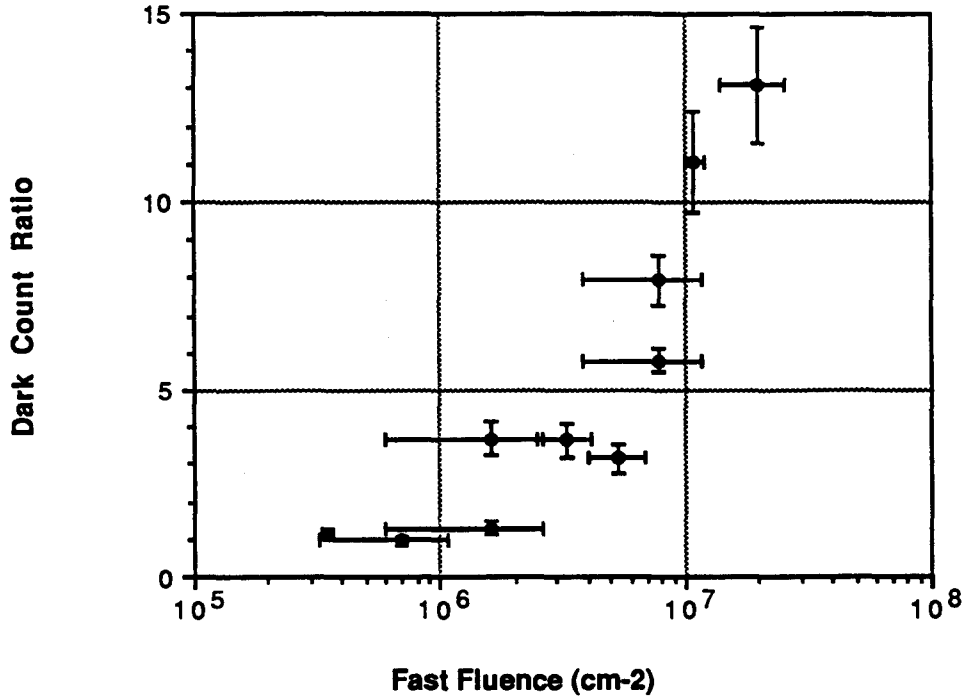

FIG. 6.1. Ratio of post- to pre-irradiation dark count rates *versus* fast neutron fluence for APD's.

7. Cost

7.1. Methodology

Costing and scheduling for the straw-fiber tracking system proposal is done in accordance with the guidelines set forth by the SDC management. Each component required for the fabrication and assembly of the SFTS is identified in the Work Breakdown Structure (WBS). The cost estimate is prepared by generating time and material estimates for each item identified in the WBS. The schedule is prepared in a similar manner. The WBS elements are assigned a duration and logic sequence in the program schedule. The cost and schedule currently reside in separate documents but will eventually be contained in the program schedule by assigning resources to each WBS item. Both the cost and schedule have been compiled in a final package detailing the requirements for producing the SFTS.

A WBS has been prepared for the SFTS which identifies each of the components necessary to produce a complete, functional tracker. The WBS is broken down into logical element groups. These groups define the major subassemblies in the SFTS. For the SFTS, there are 14 groups including the Straw Tube Components; the Scintillating Fiber Components; the Support Structure; Tracking Sub-Assembly; Equipment, Tooling and Fixtures; Cooling System Components; Utilities; Wire Electronics; Pre-Installation Test; Shipping Provisions; Installation; Facilities; and Program Management. Under each of these major headings are breakdowns of the components necessary to complete that portion of the SFTS. The complete WBS defines all items associated with the fabrication and assembly of the central tracker, and their cost.

The costing of the SFTS begins with the preparation of the WBS described above. Contained within the WBS form are several columns used for input of cost data. The major columns in the form are the Quantity, Engineering, Administrative, Technician and Major Procurement columns. The engineering, administrative and technician columns are filled with man-days data, while the major procurement columns is used for input of purchase dollars. Labor rates are applied to the man-days items and combined with the major procurement columns to provide a base WBS cost in dollars. A contingency column is then filled in and added to the base cost which is summed to provide the total WBS cost. Figure 7.1 gives a summary of the cost for the 14 groups.

STRAW-FIBER TRACKING SYSTEM
COST SUMMARY

USAGE	TRACKING ELEMENT	QTY	S/L'S		T.E. DIA	S/L RAD	LAYERS
INITIAL	PLASTIC SCINTILLATING FIBERS	54208	1		1.53	165	4
	PSF TOTAL	54208	1				
INITIAL	STRAW TUBE	38513	1		4.2	160	8
INITIAL	STRAW TUBE	32495	1		4.2	135	8
INITIAL	STRAW TUBE	19858	1		4.2	110	6
INITIAL	STRAW TUBE	15345	1		4.2	85	6
	STRAW TUBE TOTAL	106212	4				

WBS NUMBER	WBS OR ACTIVITY DESCRIPTION	QTY	EN M/D	AD M/D	TEM M/D	$MAJOR(K$)	WBS M/D	WBS MAT (K$	WBSBASE (K$)	CONTING %	CONTING(K$)	WBS TOTAL(K$)
1.2.1	STRAW TUBE COMPONENTS		1020	0	0	1035	1020	1035	1505	31	472	1978
1.2.2	SCINTILLATING FIBER COMPONENTS		1712	0	116	762	1828	762	1586	41	648	2233
1.2.2.6/7	FIBER ELECTRONICS		1170	0	217	2413	1387	2413	3018	46	1384	4402
1.2.3	SUPPORT STRUCTURE		705	0	1455	508	2160	508	1269	30	381	1650
1.2.4	SUPERLAYER ASSEMBLY		707	0	4698	253	5406	253	1989	36	714	2703
1.2.5	TRACKING SUB-ASSEMBLY		120	0	400	40	625	40	264	42	110	374
1.2.6	EQUIPMENT, TOOLING & FIXTURES		2775	0	335	3582	3110	3582	4961	21	1038	5999
1.2.7	COOLING SYSTEM COMPONENTS		215	0	0	23	215	23	122	30	37	159
1.2.8	UTILITIES		983	0	240	960	1223	960	1485	28	419	1904
1.2.9	WIRE ELECTRONICS		6490	0	0	4603	6490	4603	7593	29	2167	9761
1.2.10	PRE-INSTALLATION TEST		600	0	1000	0	1600	0	576	30	173	749
1.2.11	SHIPPING PROVISIONS		425	0	165	150	590	150	395	25	98	493
1.2.12	INSTALLATION		430	0	900	220	1330	220	688	23	158	846
1.2.13	FACILITIES		600	0	0	1000	600	1000	1276	15	197	1474
1.2.14	PROGRAM MANAGEMENT		5075	2030	0	361	7105	361	3171	18	564	3735
	TOTALS		23028	2030	9526	$15,910	34689	$15,910	$29,898	29	8560	$38,458

FIG. 7.1. Cost summary for the straw-fiber tracking system.

The procedure for costing the SFTS is consistent with that used by other group in SDC. All items have been assigned design, fabrication and purchase "costs" as well as contingencies. Each phase of the SFTS project is included, with costing based on a start date of October 1992. Summary descriptions and justifications of each major WBS category are included below.

7.2. Breakdown

The SFTS is broken down into 14 major WBS categories. These categories define the components, procurements, tooling, and assembly steps necessary to build the tracker, and the steps necessary to follow it through installation at the SSC. The categories are broken into logical element groups to facilitate analysis of the estimate. Each element is listed below, with a short description of the items included in that section.

WBS element 1.2.1, Straw Tube System, defines the components necessary to produce the straw tracking elements. The straw tracking elements are full length straw tube assemblies that are electronically broken at the midpoint. The channel count for the straw tube portion of the SFTS is shown in the WBS, with each element of the 1.2.1 WBS keyed to that number. 1.2.1 does not include the electronics portion of the straw system. This is included in WBS element 1.2.9.

The Scintillating Fiber System, WBS element 1.2.2, defines the scintillating fiber portion of the SFTS, including the electronics. Several assumptions have been made in the estimate in this section to demonstrate consistency with the other groups. The VLPC's have been costed here, along with all the components necessary for their function. The APD electronics system is still a viable option for the larger (1.5 mm) fibers used in the SFTS, but the VLPC's provide a more conservative and comparable estimate. There are two areas that differentiate the SFTS estimate from the all-fiber estimate. The first is the assumption made concerning the fiber ribbons. A vendor estimate (see Appendix A) has been received for fabricating the 1024 element fiber ribbons and has been used in the SFTS WBS. The option of building tooling for the ribbon fabrication has been rejected due to the low number of fibers involved and the high cost of tooling. The second area of differentiation is that we have used a per-channel cost of $42 instead of $28 for VLPC's, to account for a volume purchase of less than 100 k units. All other areas of the SFTS costing analysis are consistent with those of the Scintillating Fiber System.

The Support Structure for the SFTS has been defined in WBS element 1.2.3. Details of the support structure are given in Section 2.4 of this report. The basis for the design is the use of full length carbon-composite cylinders attached to one another with segmented shrouds. Costing for the composite pieces is based on estimates provided by industry and the composites division at ORNL. This section includes the cost for the components only. The tooling is included in WBS element 1.2.6.

1.2.4, Superlayer Assembly, defines the steps required to assemble the tracking elements and place them on the support cylinders. The costs of these elements are driven by technician labor. The straw tube assembly includes a cost for miscellaneous supplies necessary in the assembly process. Straw tubes are placed on cylinders one at a time to build up superlayers. Stereo scintillating fiber ribbons are placed on the cylinders in 1024 element arrays and then connected to the waveguide fiber ribbons. The waveguides routing cost is included in this section also.

The overall Tracking Sub-Assembly is included in WBS element 1.2.5. This section specifies the time required for attaching the superlayers to one another and then aligning them. It also includes some miscellaneous hardware costs.

Equipment, Tooling & Fixtures are included in section 1.2.6. This includes cylinder fabrication mandrels, tracking element locating fixtures, alignment systems, handling fixtures and other mechanical and electrical hardware. The costs for these items are based on experience with similar equipment in other applications as well as vendor estimates based on preliminary sketches. Tooling for the SFTS accounts for approximately $6 million of the total budget, which reflects the amount of automation necessary for assembly of a central tracker of the magnitude required for the SDC.

WBS elements 1.2.7 and 1.2.8 are Cooling System Components and Utilities. These items represent the systems necessary to cool the electronics, supply the drift gas, and supply liquid helium for cooling the VLPC's. Costs of the components are based on systems of similar capacities that have been used in other applications.

The Wire Electronics costs are included in section 1.2.9, and are shown in Fig. 7.2.

WBS NUMBER	WBS OR ACTIVITY DESCRIPTION	QTY	EN M/D	AD M/D	TEM M/D	$MAJOR(K$)	WBS M/D	WBS MAT (K$	WBSBASE (K$)	CONTING %	CONTING(K$)	WBS TOTAL(K$)
1.2.9	WIRE ELECTRONICS											
1.2.9.1	LV Supplies	30	66			15	66	15	45	25	11	57
1.2.9.2	LV Distribution to Detector		88			0	88	0	41	25	10	51
1.2.9.3	LV Distribution on Detector		66			0	66	0	30	25	8	38
1.2.9.4	HV Supplies	55	66			28	66	28	58	25	14	72
1.2.9.5	HV Distribution to Detector		88			0	88	0	41	25	10	51
1.2.9.6	HV Distribution on Detector					0	0	0	0	15	0	0
1.2.9.6.1	Resistors	106212	13			27	13	27	33	15	5	37
1.2.9.6.2	Channel Decoupling Capacitors	106212	15			106	15	106	113	15	17	130
1.2.9.6.3	HV Cables on End of Chamber	531	78			0	78	0	36	30	11	47
1.2.9.6.4	Connectors	1062	55			5	55	5	31	40	12	43
1.2.9.6.5	HV Filter Capacitors		15			0	15	0	7	10	1	8
1.2.9.7	Front-End Electronics					0	0	0	0		0	0
1.2.9.7.1	Preamp/Shaper/Disc. (8ch/chip)	13276	528			531	528	531	774	25	194	968
1.2.9.7.2	TVC/AMU or TMC (4ch/chip)	26553	1056			1991	1056	1991	2478	30	743	3221
1.2.9.7.3	Data Collection Chip (16 ch/channel)	6638	1056			664	1056	664	1150	30	345	1496
1.2.9.7.4	LV Decoupling Capacitors	2124				4	0	4	4	15	1	5
1.2.9.7.5	Receiver for Slow Signals					0	0	0	0	15	0	0
1.2.9.7.6	Driver for Readout Signals					0	0	0	0	15	0	0
1.2.9.7.7	Connector for Input Signals	531				106	0	106	106	15	16	122
1.2.9.7.8	Substrate for Electronics	531	528			478	528	478	721	30	216	938
1.2.9.7.9	Termination Resistors					0	0	0	0		0	0
1.2.9.8	Data Acquisition Interface					0	0	0	0		0	0
1.2.9.8.1	Synchronizer Chip		1056			0	1056	0	487	25	122	608
1.2.9.8.2	Trigger Signal Out Drivers					0	0	0	0	25	0	0
1.2.9.9	Trigger System Interface					0	0	0	0	25	0	0
1.2.9.9.1	Level 1 Interface	10621	396			531	396	531	714	30	214	928
1.2.9.9.2	Level 2 Interface		396			0	396	0	182	30	55	237
1.2.9.10	Calibration System					0	0	0	0		0	0
1.2.9.10.1	Pulsers (1/box)	33	396			116	396	116	299	30	90	388
1.2.9.10.2	Distribution for Calibration		528			0	528	0	243	30	73	316
	TOTALS		6490	0	0	$4,603	6490	$4,603	$7,593	29	$2,167	$9,761

FIG. 7.2. Cost analysis of straw electronics for the straw-fiber tracking system.

Upon completion of the SFTS fabrication, the tracker will undergo a Pre-Installation Test. This task is shown in element 1.2.10 and includes both a functional test and an alignment inspection. This test sequence will be performed at the SSC prior to final installation in the SDC detector.

The SFTS is currently being designed for remote site fabrication and assembly. To accommodate this process, Shipping Provisions must be made. WBS element 1.2.11 details costs for shipping, shipping containers and an atmospheric control system for the shipment of the tracker. While this is the current plan, the option remains for assembling the SFTS at the SSC.

Once the detector has been shipped to the SSC and undergone pre-installation testing, it is ready for installation. Section 1.2.12 list specific tooling and procedures necessary for completing the SFTS installation procedure.

WBS element 1.2.13 defines Facilities necessary for fabrication and assembly of the SFTS. These numbers are representative of upgrade and modification costs necessary to meet the size and cleanliness requirements of the tracker. Facility management costs are not included in this estimate, as they are included in the overhead of individual component purchase prices.

The final WBS element, and also a major contributor, is the Program Management of the SFTS project. This estimate assumes a seven year lifetime of the project and the manpower necessary to perform the managerial and control functions. This estimate also includes material cost estimates for operating the management office during the duration of the program.

7.3. Work breakdown structure

The final cost of the straw-fiber tracker, including wire electronics and contingencies, is $38.5M. This cost includes all components necessary to fabricate the tracker with 106,212 wire channels and 54,208 fiber channels. Figure 7.3 contains the complete WBS and cost for the tracker. The SFTS pays a small penalty in cost by requiring the development of both wire and fiber technologies. However, the dividends realized by making full use of the predominant strengths of the two systems significantly overshadows the development costs. The Straw-Fiber Tracker has been designed to provide the physics community with its tracking and triggering requirements, without demanding heroic feats from the engineering team. The

WBS NUMBER	WBS OR ACTIVITY DESCRIPTION	QTY	EN M/D	AD M/D	TEM M/D	$MAJOR(K$)	WBS M/D	WBS MAT (K$	WBSBASE (K$)	CONTING %	CONTING(K$)	WBS TOTAL(K$)
USAGE	TRACKING ELEMENT	QTY	S/L'S		T.E. DIA	S/L RAD	LAYERS					
INITIAL	PLASTIC SCINTILLATING FIBERS	54208	1		1.53	165	4					
STAGED	PLASTIC SCINTILLATING FIBERS	14784	1		1.02	60	2					
STAGED	PLASTIC SCINTILLATING FIBERS	47309	1		1.02	64	6					
	PSF TOTAL	54208	1									
INITIAL	STRAW TUBE	38513	1		4.2	160	8					
INITIAL	STRAW TUBE	32495	1		4.2	135	8					
INITIAL	STRAW TUBE	19858	1		4.2	110	6					
INITIAL	STRAW TUBE	15345	1		4.2	85	6					
	STRAW TUBE TOTAL	106212	4									
WBS NUMBER	WBS OR ACTIVITY DESCRIPTION	QTY	EN M/D	AD M/D	TEM M/D	$MAJOR(K$)	WBS M/D	WBS MAT (K$	WBSBASE (K$)	CONTING %	CONTING(K$)	WBS TOTAL(K$)
1.2	CENTRAL TRACKER											
1.2.1	STRAW TUBE COMPONENTS											
1.2.1.1	End Plate		0									
1.2.1.1.1	Wire Tension Plate	415	100			10	100	10	56	50	28	85
1.2.1.1.2	Grounding	32	60			16	60	16	44	50	22	65
1.2.1.2	Straw Tube Unit	0	0									
1.2.1.2.1	Straw Tube	106212	125			106	125	106	164	30	49	213
1.2.1.2.1.1	Wire Support	743481	125			372	125	372	429	20	86	515
1.2.1.2.1.2	Wire	106212	0			53	0	53	53	40	21	74
1.2.1.2.1.3	Center Termination	106212	200			212	200	212	305	40	122	426
1.2.1.2.1.4	End Plug	212423	80			106	80	106	143	20	29	172
1.2.1.2.1.5	Wire Termination	212423	250			106	250	106	221	40	89	310
1.2.1.2.1.6	Straw Tube Connector	106212	80			53	80	53	90	30	27	117
1.2.2	SCINTILLATING FIBER COMPONENTS											
1.2.2.1	Fibers	0	0									
1.2.2.1.1	PSF	54208	500			0	500	0	230	44	101	332
1.2.2.1.2	Waveguide	54208	350			0	350	0	161	16	26	187
1.2.2.2	Ribbon Fabrication	0	0			0	0	0	0		0	0
1.2.2.2.1	PSF Ribbons	53	265			360	265	360	482	60	289	771
1.2.2.2.2	Waveguide Ribbons	53	265			360	265	360	482	30	145	627
1.2.2.2.3	End Aluminization	53	83		106	5	189	5	75	25	19	94
1.2.2.3	Connectors	0	0									
1.2.2.3.1	Fiber To Fiber Connectors	53	85			11	85	11	50	56	28	78
1.2.2.3.2	Fiber To Electronics Connectors	53	85			5	85	5	44	56	25	69
1.2.2.4	Light-Tight Shell	1	60		10	10	70	10	41	25	10	51
1.2.2.5	Light-Tight Bundle	11	20			11	20	11	20	25	5	25
1.2.2.6	Read-Out System											
1.2.2.6.1	Low Voltage To Preamps	11	80			42	80	42	79	32	25	105
1.2.2.6.2	Low Voltage to Cryostat	11	35		5	3	40	3	21	32	7	27
1.2.2.6.3	Data Cabling	452	50			23	50	23	46	32	15	60
1.2.2.6.4	VLPC/Preamp/Shaper/Disc	54208	720			2277	720	2277	2609	48	1252	3861
1.2.2.6.5	Calibration Interface	11	125			26	125	26	84	32	27	111
1.2.2.6.6	Electronics Assembly	1	50		85	5	135	5	53	32	17	71

FIG. 7.3 Work breakdown structure for the straw-fiber tracking system.

WBS NUMBER	WBS OR ACTIVITY DESCRIPTION	QTY	EN M/D	AD M/D	TEM M/D	$MAJOR(K$)	WBS M/D	WBS MAT (K$	WBSBASE (K$)	CONTING %	CONTING(K$)	WBS TOTAL(K$)
1.2.2.7	Readout Assembly											
1.2.2.7.1	Waveguide Installation	53	80		106	26	186	26	95	38	36	131
1.2.2.7.2	Cryostat Supports	11	30		21	11	51	11	31	18	6	36
1.2.3	SUPPORT STRUCTURE											
1.2.3.1	Segmented Shrouds	24	50		48	120	98	120	157	22	35	192
1.2.3.2	Superlayer Interconnects	10	125		10	10	135	10	71	22	16	86
1.2.3.3	Silicon Tracker Support	1	60		0	60	60	60	88	33	29	117
1.2.3.4	Coil Attachment	46	125		110	23	235	23	114	33	37	151
1.2.3.5	Waveguide Support	20	70		0	10	70	10	42	21	9	51
1.2.3.6	Support Cylinders											
1.2.3.6.1	85 cm Radius	24	15		67	17	82	17	44	32	14	58
1.2.3.6.2	110 cm Radius	31	15		107	22	122	22	61	32	20	80
1.2.3.6.3	135 cm Radius	38	15		320	27	335	27	130	32	42	171
1.2.3.6.4	160 cm Radius	46	15		390	32	405	32	156	32	50	206
1.2.3.6.5	165 cm Radius	47	15		403	33	418	33	161	32	51	212
1.2.3.7	Carbon End Rings											
1.2.3.7.1	85 cm Radius	1	40			20	40	20	38	32	12	51
1.2.3.7.2	110 cm Radius	1	40			26	40	26	44	32	14	58
1.2.3.7.3	135 cm Radius	1	40			32	40	32	50	32	16	66
1.2.3.7.4	160 cm Radius	1	40			38	40	38	56	32	18	74
1.2.3.7.5	165 cm Radius	1	40			39	40	39	57	32	18	76
1.2.4	SUPERLAYER ASSEMBLY											
1.2.4.1	Straw Tube Assembly											
1.2.4.1.1	Gas and HV Connections	415	50		207	4	257	4	89	30	27	116
1.2.4.1.2	Wire Position	106212	50		443	30	493	30	186	50	93	279
1.2.4.1.3	Straw Tube Test Setup	1	65		0	60	65	60	90	50	45	135
1.2.4.1.4	Straw Tube Sub-Assembly	106212	136		2213	106	2349	106	833	35	291	1124
1.2.4.1.4	Straw Tube Placement/Alignment	106212	166		1106	53	1273	53	462	35	162	623
1.2.4.2	SCINTILLATING FIBER ASSEMBLY											
1.2.4.2.1	Axial Ribbon Placement/Alignment	0	0									
1.2.4.2.2	Stereo Ribbon Placement/Alignment	53	200		635	0	835	0	283	30	85	368
1.2.4.2.3	Waveguide/PSF Connection	53	10		53	0	63	0	20	30	6	27
1.2.4.2.4	Shell Placement	1	20		20	0	40	0	15	19	3	18
1.2.4.2.5	Bundle Placement	11	10		21	0	31	0	11	19	2	13
1.2.5	TRACKING SUB-ASSEMBLY											
1.2.5.1	S/L To S/L Assembly	5	25		240		305	0	102	48.00	49	151
1.2.5.2	S/L To S/L Alignment	5	25		160		210	0	71	48.00	34	105
1.2.5.3	Attachment Hardware	5	70			40	110	40	91	30.00	27	118
1.2.6	EQUIPMENT, TOOLING & FIXTURES											
1.2.6.1	Straw Tube Equipment, Tooling & Fixtures											
1.2.6.1.1	Straw Tube Placement Device	1	200		100	175	300	175	297		0	297
1.2.6.1.2	Straw Tube Feed	1	375		0	225	375	225	398	30	119	517
1.2.6.1.3	Wire Insertion Machine	1	250		0	150	250	150	265	30	80	345
1.2.6.2	PSF Equipment, Tooling & Fixtures											
1.2.6.2.1	Ribbon Locating Jig	1	300		40	250	340	250	400	32	128	528

WBS NUMBER	WBS OR ACTIVITY DESCRIPTION	QTY	EN M/D	AD M/D	TEM M/D	$MAJOR(K$)	WBS M/D	WBS MAT (K$)	WBSBASE (K$)	CONTING %	CONTING(K$)	WBS TOTAL(K$)
1.2.6.2.2	Ribbon Handling Fixtures	10	25			5	25	5	17	16	3	19
1.2.6.2.3	Fiber/Fiber Connection Tooling	1	35		25	15	60	15	39	25	10	48
1.2.6.2.4	Light Tight Shell Tooling	1	30			20	30	20	34	24	8	42
1.2.6.2.5	Light Tight Bundle Tooling	11	20			10	20	10	19	24	5	24
1.2.6.2.6	Waveguide Support Tooling	4	20			20	20	20	29	12	4	33
1.2.6.3	Final Assembly Tooling											
1.2.6.3.1	Support/Locating Fixtures	2	250		0	100	250	100	215	16	34	250
1.2.6.3.2	Alignment Verification System	2	250		0	350	250	350	465	32	149	614
1.2.6.3.3	Cylinder Rotator/Indexer	1	375		0	225	375	225	398	20	80	477
1.2.6.4	Cylinder Tooling											
1.2.6.4.1	Support Cylinder Mandrels											
1.2.6.4.1.1	85 cm Radius Mandrel	1	10			215	10	215	220	15	33	253
1.2.6.4.1.2	110 cm Radius Mandrel	1	10			218	10	218	223	15	33	256
1.2.6.4.1.3	135 cm Radius Mandrel	1	10			352	10	352	357	15	54	411
1.2.6.4.1.4	160 cm Radius Mandrel	1	10			474	10	474	478	15	72	550
1.2.6.4.1.5	165 cm Radius Mandrel	1	10			480	10	480	485	15	73	557
1.2.6.4.2	End Ring Tooling											
1.2.6.4.2.1	85 cm Radius	1	20		10	10	30	10	22	15	3	26
1.2.6.4.2.2	110 cm Radius	1	20		10	13	30	13	25	15	4	29
1.2.6.4.2.3	135 cm Radius	1	20		10	16	30	16	28	15	4	32
1.2.6.4.2.4	160 cm Radius	1	20		10	19	30	19	31	15	5	36
1.2.6.4.2.5	165 cm Radius	1	20		10	19	30	19	32	15	5	36
1.2.6.4.3	Cylinder Handling Fixtures	1	35		25	45	60	45	69	24	16	85
1.2.6.5	Superlayer Tooling											
1.2.6.5.1	S/L Support/Locating Fixture	2	200		30	100	230	100	201	35	70	272
1.2.6.5.2	Superlayer Interconnect Tooling	2	60			30	60	30	58	35	20	78
1.2.6.5.3	Shear Panel Fabrication Tooling	24	125		65	3	190	3	80	16	13	93
1.2.6.6	Silicon Tracker Support Fixtures	6	45			12	45	12	33	22	7	40
1.2.6.7	Intermediate Tracker Locator Jigs	1	30			30	30	30	44	18	8	52
1.2.7	**COOLING SYSTEM COMPONENTS**											
1.2.7.1	Manifold	32	125			16	125	16	74	30	22	96
1.2.7.2	Fittings	830	40			1	40	1	19	30	6	25
1.2.7.3	Hoses	415	50			6	50	6	29	30	9	38
1.2.8	**UTILITIES**											
1.2.8.1	Straw Tube Utilities											
1.2.8.1.1	Electronics Cooling System	1	250		50	250	300	250	380	30	114	494
1.2.8.1.2	Drift Gas Supply	1	375		120	250	495	250	459	30	138	596
1.2.8.1.3	Gas Leak Detection System	1	63			50	63	50	79	30	24	103
1.2.8.1.4	Inerting System	1	125			100	125	100	158	30	47	205
1.2.8.2	Fiber Utilities											
1.2.8.2.1	LHe Supply	1	50		20	150	70	150	179	24	43	222
1.2.8.2.2	LHe Distribution System	1	70		35	100	105	100	143	24	34	177
1.2.8.2.3	LHe I&C	1	50		15	60	65	60	88	22	19	107
1.2.9	**WIRE ELECTRONICS**		6490	0	0	4603	6490	4603	7593	29	2167	9761
1.2.10	**PRE-INSTALLATION TEST**											

WBS NUMBER	WBS OR ACTIVITY DESCRIPTION	QTY	EN M/D	AD M/D	TEM M/D	$MAJOR(K$)	WBS M/D	WBS MAT (K$	WBSBASE (K$)	CONTING %	CONTING(K$)	WBS TOTAL(K$)
1.2.10.1	Alignment Test	1	300		500		800	0	288	30	86	375
1.2.10.2	Tracker Functional Test	1	300		500		800	0	288	30	86	375
1.2.11	SHIPPING PROVISIONS						0					
1.2.11.1	Shipping To SSCL		160		65		225	0	93	14	13	106
1.2.11.2	Shipping Containers	1	210		60	125	270	125	240	28	67	307
1.2.11.3	Shipping Atmosphere System	1	55		40	25	95	25	62	28	17	80
1.2.12	INSTALLATION											
1.2.12.1	Installation Tooling	1	200		300	200	500	200	382	22	84	466
1.2.12.2	Installation/Checkout Support		200		200	10	400	10	162	24	39	201
1.2.12.3	Alignment Verification		30		400	10	430	10	144	24	35	178
1.2.13	FACILITIES											
1.2.13.1	Support Assembly											
1.2.13.1.1	Support Assembly Facilities	1	100			200	100	200	246	16	39	285
1.2.13.1.2	Resin Curing Oven	1	100			125	100	125	171	16	27	198
1.2.13.2	Cylinder Assembly											
1.2.13.2.1	Cylinder Assembly Facilities	1	100			250	100	250	296	16	47	343
1.2.13.2.2	Clean Room	1	200			300	200	300	392	16	63	455
1.2.13.2.3	Electronics Assembly	1	100			125	100	125	171	12	21	192
1.2.14	PROGRAM MANAGEMENT											
1.2.14.1	Design Reviews		350	175		35	525	35	237	16	38	275
1.2.14.2	Cost/Schedule		210	105		56	315	56	177	14	25	202
1.2.14.3	Program Reporting		280	140		50	420	50	212	16	34	245
1.2.14.4	Program Coordination		2100	700		75	2800	75	1205	21	253	1458
1.2.14.5	Systems Integration		455	210		60	665	60	318	16	51	369
1.2.14.6	Data Management		1680	700		85	2380	85	1022	16	163	1185
TOTALS			23028	2030	9526	$15,910	34688.8	$15,910	$29,898	29	$8,560	$38,458

support structure is simple and reliable – reducing costs and materials when compared with alternatives; stereo z-measurements are done with fibers, which are much more accommodating to helix mounting than are straw tubes. Also, larger scintillating fibers are utilized which increases the light output to the readouts and reduces the channel count – and consequently the cost. The SFTS represents a simple and reliable system that is affordable and upgradeable. By maintaining development of both straw and fiber technologies, risks are reduced and future growth is assured. The cost of the SFTS meets the requirements of the SDC and the SSC because it relies on one very important key to success - efficiency.

7.4 Shell cost analysis

Recent evaluation of the cylinders used to support the tracking components of the outer tracker has centered around fabrication methods and the cost associated with cylinder production. The basic assumptions for the stable base cylinder are: full length continuous cylinders; 380 μm to 630 μm wall thickness; graphite fiber reinforced epoxy composite; integral end rings with, possibly, intermediate stiffeners; and cylinder support from the ends only. An attempt has been made to produce an accurate cost analysis of the cylinders using these criteria and the dimensions provided for the "baseline" tracker design.

Many cost drivers will affect the estimate for fabrication of the required cylinders. The two principle drivers are cylinder size and required precision. Secondary variables are important, however, because performance requirements could elevate any of them to major importance. A few comments about the secondary variables are in order before discussing the cost estimate in terms of size and precision.

The graphite fiber reinforced epoxy composite material has been chosen because it has a high specific strength and stiffness, low weight, and the material is expected to have little influence on the performance of the detector. There are unknowns associated with this material such as dimensional stability as a result of temperature changes or viscoelastic creep and long term effects of the operational radiation environment.

Within the graphite/epoxy composite itself, the assumption is that the fiber modulus requirement will be less than 55 msi. This assumption is based on preliminary analysis of the strength requirements of the cylinder. Higher modulus fibers are readily available, but these tend to have very low strength and are difficult

to use in high precision fabrication environments. Fibers which are both high in strength and modulus are available for special applications, and will be used if required.

The cylinder wall construction is assumed to be wet wound layup of graphite reinforced epoxy composite material. Additional evaluation and analysis must be performed to determine if this construction will meet mechanical design requirements. If thickness must be increased or the construction method modified, the effect of the presence of the cylinder on detector performance will become increasingly important. The relative effect of another construction method on the cost will be measurable but is not a significant driver at this time.

Cost estimates for the cylinders is presented in terms of cylinder O.D. in Fig. 7.3. Mandrels are assumed to be chrome plated steel. The estimates are based upon informal discussion with mandrel suppliers, winding technology facilities, and potential fabricators. Previous experience at ORNL also was used in the estimates.

The cost estimates are also driven by some hidden considerations. The state of the art in this technology is not advanced sufficiently to build all possibilities without incurring R&D charges. These additional costs are contained in the estimates for the large diameter, high precision cylinders. Conversely, the smaller, less precise cylinders in the upper right quadrant can be produced by several manufacturers without difficulty. Between these regions, there is an increasing amount of sophistication and capability required. For the baseline design, the smaller cylinders will be used for the fiber technology, which requires greater precision for mounting. The larger cylinders will be used for straw tracking which does not require the degree of precision necessary for the fibers. The fiber cylinders would have cylindricity requirements in the 125 μm range, and the straw cylinders in the 250 μm range.

Further evaluation is required to determine the final structural requirements of the cylinder. These requirements will feed directly into the cost estimate and physics performance capabilities of the tracker. These evaluations will continue in concert with the continued refinement of the straw tube and fiber tracking technologies, which will be mounted to the cylinders.

8. Schedule and milestones

8.1. Schedule summary

Scheduling the SFTS is done in a manner similar to the costing. The WBS is used as the backbone of the schedule. Each element is input into the scheduling system, along with its WBS number. An estimate is then made of the time required to complete each phase of the fabrication/assembly. This includes the R&D, design, procurement or fabrication and assembly phases of the element. This continues for all elements in the WBS. Upon completion of the duration input, the items are then placed in a network diagram. At this point, the elements are linked in a logical fashion which depicts the sequence of events necessary to produce the tracker. The start date is defined for the project and the program computes an end date and critical path for the project. To complete the picture, the resource requirements are input for each element, which ultimately provides a project cost profile. The schedule can then be manipulated to level resources and meet other schedule and cost constraints.

An overview of a preliminary SFTS production and installation schedule is presented in Fig. 8.1. This is an outgrowth of a full schedule evaluation carried out using a Gantt chart and network analysis for the Hybrid Central Tracking Collaboration (see Appendix B).

8.2. Critical R&D

<u>Stable-base cylinders</u>

Graphite epoxy based composite cylinders have been in production for many years. The basic construction techniques are very well understood and documented. However, the design requirements of the SDC outer tracker present some challenges, and their associated risks, for the support cylinders.

The proposed construction of the SFTS support cylinders utilizes a sandwich construction of two thin graphite face sheets and a foam core. The large overall cylinder diameter compared with the thin sandwich layup presents the biggest fabrication obstacle. Tolerance control and support cylinder removal from tooling mandrels are areas of concern that will be addressed prior to cylinder production.

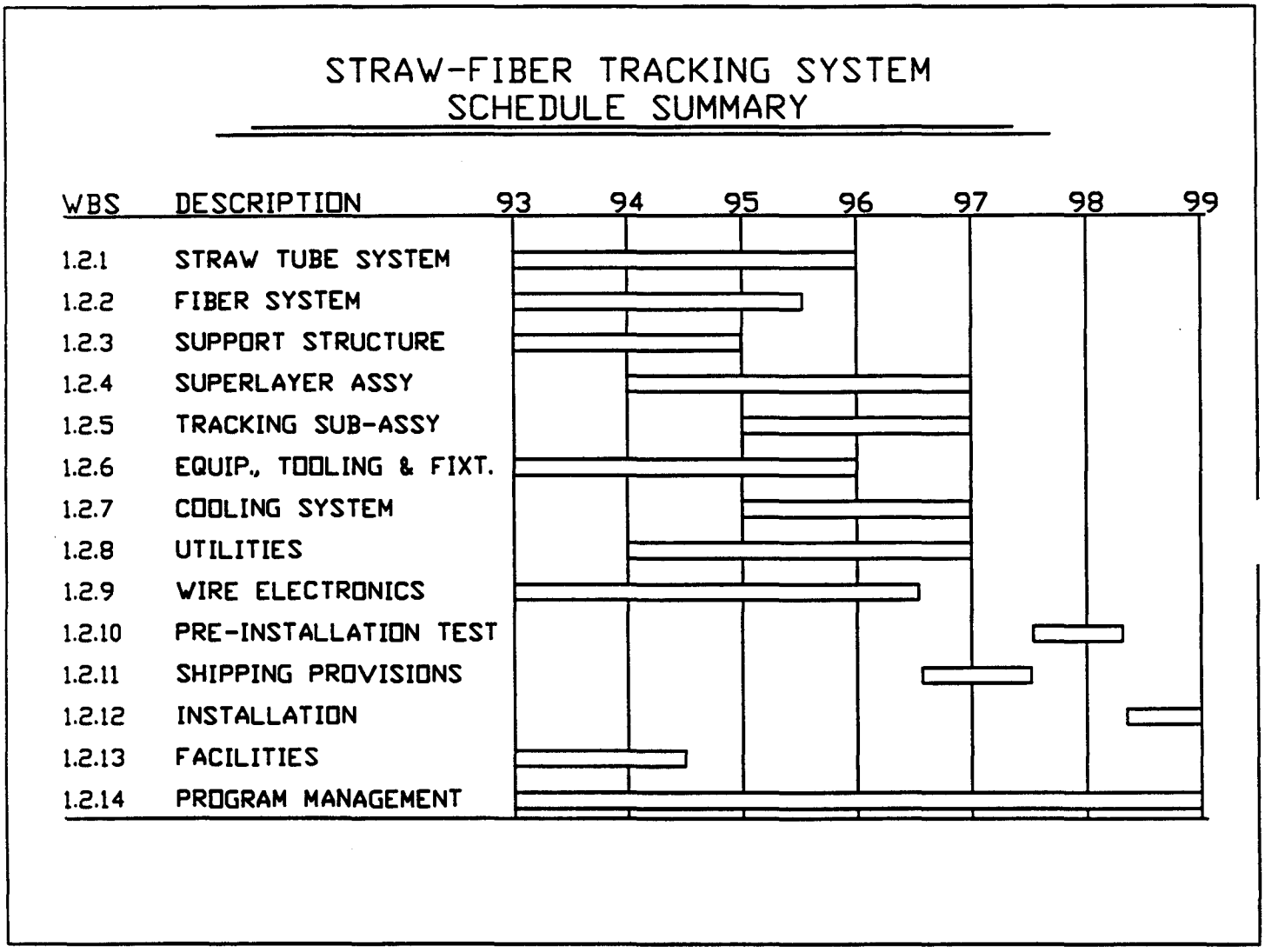

FIG. 8.1. Schedule summary for the straw-fiber tracking system.

Both of these issues have been dealt with in the past for similar items, and have been resolved. There is confidence in the composite community that this will be the case with the SFTS tracker, also.

Straw tube drift cells and superlayers

Straw tube drift cells with 4 mm diameter and length 7 m are operating at Duke University. The attenuation length has been measured to be about 5 m. In addition, straw tube superlayers of length 2.7 m have been operating for the past 18 months, and shown to have a point setting resolution of 120 μm, including both inherent drift cell resolution and straw replacement errors. Tests have been made under simulated SSC background rates (design luminosity with straw 70 cm from the beam), showing that the resolution is not degraded. See Ref. 4 for more details of these R&D results.

The remaining important R&D work falls into three categories.

- Operation of straw tube drift cells at gains of ~2×10^4, using compact, collinear modular electronics: The commercial electronics currently being used for straw tube readout requires operation with gas gains ~10^5. The customized chips to be mounted at the end of the straws (see Section 2.5) will permit operation at lower gains, and thus longer cell lifetime. During FY92 an evaluation of straw tube drift cell performance with this compact, collinear electronics must be made.

- Superlayer construction techniques: There are at least three promising alternatives[4,5] for straw tube superlayer construction in advanced R&D stages. It will be necessary to choose one of these and use it to demonstrate the ability to lay straw tube drift cells in a superlayer semi-automatically to a precision of about 50 μm.

- Radiation resistance of superlayer and electronics: R&D work to date indicates that this should not be a problem. However, after a final superlayer construction scheme is chosen, the assembly will be tested under simulated SSC radiation conditions. Preparations for these tests are being made which will allow operation of the drift cell under radiation conditions (Quantum Research Services, and North Carolina State University).

All the above R&D issues are scheduled to be addressed in FY92.

Scintillating Fibers

Feedback from the high energy physics community to the industrial producers of plastic scintillating fibers has stimulated them to produce brighter and more

radiation resistant fibers. The combination of a 1.5 mm G2 fiber and an APD will provide a high enough detection efficiency over 4 m as shown in Fig. 2.6 (p. 20), and Bicron G2 is certainly not the best product available today. Nevertheless, improvements in light yield and light attenuation characteristics are desirable to give a greater margin in photoelectron statistics. There are several possibilities to achieve this in addition to the basic studies of the combination of base polymer, clad material, and wavelength shifter. So far we have not exploited light reflective coatings on fibers, which could improve the light attenuation. We have not fully optimized the doping concentration of wavelength shifter dyes in terms of the photon yield and light attenuation. We have not studied systematically the effect of the mirror at the far end of the fiber. These are all subject to R&D and optimization. In addition to these studies, we have to finalize our splicing or coupling technique between scintillating fiber and clear wave guide.

Fiber ribbons

A precision requirement in fiber positioning is less necessary in the outer fiber superlayer where the fibers are used to measure z positions of tracks using two stereo double layers. We have measured the average center to center spacing of individual fibers and the average width of fiber ribbons manufactured by Kurary and Bicron. The results were satisfactory and showed that both manufacturers can achieve a fiber center to center tolerance of better than 50 μm.

The relaxed precision requirement and the fact that the fiber manufacturers have developed the necessary techniques to manufacture ribbons have prompted us to plan to purchase fiber ribbons from the fiber manufacturers rather than fabricating the ribbons by ourselves. Our effort will be devoted to verifying the quality of fiber ribbons delivered by the manufacturers. One of the fiber manufacturers has quoted a price on such a fiber ribbon made of 1,024 fibers (see Appendix A). The outer fiber super layer consists of 54k fibers corresponding to 53 ribbons, which is not overwhelming, but is large enough to justify an automated system to measure the quality of fiber ribbons in terms of the photon detector characteristics and dimensional stability of fibers.

Photo detectors

In this tracking system we are not pushing the technology of photon detection to the limit since there will be enough photons because of the 1.5 mm fiber diameter.

The large fiber diameter contributes not only to a larger number of photons generated by ionizing particles but also to a longer attenuation length. Therefore, we could use either VLPC's or APD's as the photon detector. We have assumed the VLPC to be the photodetector of the system in our cost estimate. This should give an upper limit cost estimate since the VLPC is considered to be a more expensive device than the APD. Knowledge of the VLPC performance is limited (especially so since the true VLPC device does not yet exist) and we will restrict ourselves to a discussion of APD R&D.

We have been using APD's in the Geiger mode because of the simplicity of operation. There are two difficulties in this mode. One is its long recovery time, typically on the order of a few hundred ns. We have achieved a minimum recovery time of ~150 ns by a passive quench circuit. But improving this limit has become an increasingly difficult task. Another difficulty in running the APD in Geiger mode is that the surface area of the device must be kept small enough to suppress dark counts. To date we have limited our R&D to the 0.5 mm APD. The combination of a 1.5 mm fiber and 0.5 mm APD necessitates an effective and small light collector as the coupler between the fiber and the APD.

The sub-Geiger mode operation of the APD has been suggested as an alternative to a fast quench circuit in order to reduce the recovery time of the APD. The work on this mode of operation has been delayed because of work on the fast quench circuit. However, a dead time of 15 ns has been reported using this mode. A low-noise amplifier and a low k or Slik detector are required for a single photon detection efficiency of 30-40%. This mode also allows the use of large area APD's and that simplifies problems with the coupling between the fiber and the APD.

The manufacturer of the APD (EG&G) has demonstrated an ability to fabricate APD's in arrays. The device they have so far provided is a 4-channel array of APD's which exhibits negligible cross-talk characteristics. We shall determine the most effective approach to packaging arrays of APD's, together with appropriate electronics, which can then be easily coupled to or decoupled from the plastic scintillating fiber ribbons.

Radiation hardness of fibers

Relatively high gamma-ray and neutron levels will be present in the central tracking region. The green emitting fibers we are currently evaluating provide for

appropriate radiation resistance. But the dependence of scintillator radiation hardness on many variables (for example, temperature, gas atmosphere, base polymer, clad material, UV exposure, dose, delivery rate, etc.) requires further studies. We intend to continue to investigate the interplay of the many variables that affect scintillator radiation hardness. The fibers will be obtained from several sources. We shall study intensively a few of the more promising fibers in the later stage. The primary emphasis will be on mixed field (neutron-photon) irradiations. However, some strictly gamma-ray exposure and some strictly neutron exposures will be included in order to isolate neutron and photon effects. We shall also investigate spectral effects by using shields, filters, and conditioners.

8.3. Risk considerations

The major *perceived* risks associated with the SFTS appear to be the following:

- the cost associated with co-developing two technologies (straws and fibers) will necessarily be too high
- straw occupancy is too high at small radii
- fibers of 4 m length may have insufficient light output

Those of us who have been working for two years with the straw-fiber concept of melding two good but not perfect technologies see the major risks as the following:

- VLPC technology may not be developed at the per channel costs now being suggested
- operation of straw tube drift cells at gas gains of ~2×10^4 with compact, colinear electronics
- unsuspected radiation effects associated with extended mixed-field exposures may affect performance of straws or fibers
- the construction of superlayer of radius up to 1.6 m and length up to 8 m; element placement precision and long term stability.

We will briefly comment on each of these items below.

<u>Cost</u>

The presumption that a straw-fiber tracker must cost more than an all-straw or an all-fiber tracker fails to account for several cost-saving factors. As discussed in more detail in section 7, the cost of structural support must be paid for only once in the SFTS because straws and fibers are both supported by identical stable-base

cylinders. Also, compared to the all-straw modular approach we save the significant costs of engineering supports for stereo straws and the costs of designing, constructing, and connecting the modules; compared to the all-fiber approach we save the costs associated with large channel numbers and with quarter-fiber overlapping techniques. Thus, since we use the appropriate technology for each superlayer and since we share a common support architecture, we save the engineering costs associated with the difficulties of each technology.

Straw occupancy

In the straw-fiber tracks, all straw tubes are outside a radius of 85 cm. At a design luminosity of 10^{33} $cm^{-2}s^{-1}$, the occupancy of all superlayers for a Higgs production event plus minimum bias background is less than 15%. This rises by about a factor of 2 when the luminosity increases by a factor of 5 (most of the hits come from the Higgs event itself, and therefore the occupancy does not scale linearly with luminosity). The fact that the SFTS measures 32 r-ϕ points/track keeps the track finding efficiency high up to a luminosity of 5×10^{33} $cm^{-2}s^{-1}$ (high P_t tracks are found with an efficiency greater than 95%). Above 5×10^{33} $cm^{-2}s^{-1}$ the SFTS requires an upgrade by the addition of an inner scintillating fiber vector superlayer.

Long fibers

Several workers have now shown that existing scintillating fibers of diameter ~1 mm and length up to 4 m have a large enough light yield and long enough attenuation length to provide efficient detector elements when solid-state readout devices are used. We have concentrated our efforts on Bicron G2 fibers of different diameter even though both Bicron and Kurary have recently produced fibers of better quality. As a readout device, we have extensive experience with the EG&G avalanche photodiode. According to its specified characteristics, the Rockwell VOLPC should be a better – if more expensive and more complicated – device than the APD. Certainly the VLPC predecessor, the SSPM is an excellent photodetector.

Nevertheless, the combination of 4 m long 1.5 mm diameter Bicron G2 fiber plus Geiger-mode APD gives a tracking element which has an efficiency that is never less than 96%. This should be adequate for the SFTS outer stereo superlayer.

VLCP and APD cost

As noted above the VLPC should be a better photodetector than the APD. Since the APD has been a commercially available device for 15 years and the VLPC does

not yet exist, it is easier to evaluate the APD characteristics and to obtain reliable cost estimates. The APD is a room-temperature device; the VLPC operating temperature is ~7k. The VLPC will probably cost more per channel than the APD. Curiously, current cost estimates do not indicate this.

Whatever the relative advantages of the two devices and whatever their eventual cost, it is certainly advantageous to have the two alternatives available for fiber readout.

Operation of straw drift cells at gains of ~2×10^4 with modular electronics

The University of Pennsylvania, University of Colorado and Oak Ridge National Laboratory are designing the front end logic chips and modular electronics for the straw tube superlayers. These will be tested on straw tube superlayers at Duke and Indiana University. This R&D work will be completed in FY92.

Radiation effects

Most research to date indicates that current materials are sufficiently rad-hard for central tracking purposes. However, neither straw electronics modules nor VLPC's have yet been tested and low-dose-rate testing of integrated systems has not taken place, although the effect is not extremely large. Recent work[16] has shown that damage to scintillating fibers is more severe if the dose is administered slowly as opposed to very quickly, although the effect is not extreme Other long-term or interactive effects may also exhibit themselves and so we feel that further radiation studies of integrated subsystems under SSC-like radiation conditions is warranted. Even so, we do not anticipate that any unexpected difficulties, if encountered, cannot be overcome.

Stable-base cylinders and element placement

The ultimate precision of the SFTS will likely be determined by the uncertainty of the detection element placement. The stable-base cylinder support must be developed for all outer barrel tracker options. The SFTS relies predominantly on straw tube superlayers for the high precision measurements. for these there are three options for superlayer construction. The fiber superlayers do not require elegant 1/4 fiber alignment methods. SFTS minimizes the risk associated with large-volume barrel tracker construction.

9. Conclusions

This Conceptual Design Report (CDR) describes a straw-fiber tracking system (SFTS) covering the Solenoidal Detector tracking volume outside the silicon tracker (radius greater than 50 cm) and interfacing with the intermediate tracker at pseudorapidity of about 1.6. The SFTS is composed of six superlayers with the structure shown in Fig. 1.1 (p. 2) and described in Table 1.1 (p. 3). High momentum tracks within $|\eta| < 1.6$ will be measured by 32 points in the r-ϕ plane and vector track segments localized in r-ϕ-z at radii of 60 and 160 cm. This draft CDR describes the fabrication of the SFTS, required readout and trigger electronics, physics performance, and cost and schedule analyses based upon a scenario which stages the inner scintillating fiber superlayer.

The major conclusions of this study are summarized in the following tables, divided into issues related to construction of the barrel tracker, electronics and trigger, physics performance, cost and schedule. These show that the SFTS, used in conjunction with the descoped silicon tracker and a preliminary version of the intermediate gas microstrip tracker, provides a promising solution to the SDC tracking requirements.

TABLE 9.1

Barrel tracker construction issues

Item	Comments
1. Maturity of design	Design results from ~2 year optimization process
2. Flexibility of design	Straw/fiber mix yields full range of options. Three options available for straw-tube superlayer construction. Several fiber readout alternatives.
3. Integration	Coordination needed to integrate with intermediate tracker. No radial integration problems.
4. Amount of material (% X_0 at $\eta = 0, 1.5$)	3.0% (5.2% with staged superlayer) at $\eta = 0$ ~6.5% (13% with staged superlayer) at $\eta = 1.5$
5. Radiation resistance	Fiber rad hardness still being evaluated. Initial results indicate suitable fibers will be available. Fiber readout devices neutron sensitive, must be located outside calorimeter. Straw tubes: good performance obtained using CF_4-isobutane gas, copper/mylar cell walls, gold plated tungsten wires; electronics to be evaluated.
6. Survivability	Goal is 100 years at 10^{33} $cm^{-2}s^{-1}$; see 5.
7. Ease of alignment	Large-scale alignment techniques need to be developed.
8. Access requirements	~1 m access needed at end of barrel; minimal access space between calorimeter and muon system.
9. Failure mode management	Assume minimal superlayer maintenance requirements. All electronics modular and accessible.
10. Safety	Not yet fully evaluated. Issues involve straw tube gas, high voltage supplies and possible cryogenics.
11. Upgrade and staging	Staging necessary for operation above 5×10^{33} $cm^{-2}s^{-1}$. Mechanical structure is designed to accommodate high luminosity inner superlayer. Third straw superlayer electronics upgradable for high luminosity trigger.

TABLE 9.2

Electronics and trigger issues

Item	Comments
1. Straw tube readout	Development work to be completed in FY92.
2. Fiber readout	APD adequate for initial SFTS. APD and/or VLPC development work needed for staged superlayers.
3. Placement of straw tube electronics	Modular, removable and located at superlayer ends.
4. Placement of fiber electronics	Located in access space between calorimeter and muon system.
5. Trigger (levels 1 and 2)	Uses outer two straw superlayers which have been optimized for the trigger algorithm. Third superlayer can be easily upgraded (from 6 to 8 layers) for high luminosity trigger algorithm.
6. Access requirements	Straw electronics needs 1 m access at end of barrel tracker. Fiber electronics needs modest access space between calorimeter and muon system (no cryogenics).

TABLE 9.3

Physics performance

Item	Comments
1. Simulation procedure	Operating within SDC shell. Inner and outer tracker simulation advanced. Intermediate tracker not yet included. Staged portion of outer tracker not yet included.
2. Reconstruction procedure	Uses 32 r-ϕ points plus outer r-ϕ-z vector at R = 160 cm. Staged layer will give additional r-ϕ-z vector at R = 60 cm.
3. Reconstruction efficiency versus luminosity	>99% at 10^{33} $cm^{-2}s^{-1}$ >95% at $5x10^{33}$ $cm^{-2}s^{-1}$
4. Single track resolution	~50 μm per straw tube superlayer
5. Two track resolution	~750 μm for outer fibers ~500 μm for inner fibers
6. Momentum resolution versus luminosity (σ_{P_t}/P_t^2)	0.13 TeV^{-1} at 10^{33} $cm^{-2}s^{-1}$ 0.23 TeV^{-1} at $5x10^{33}$ $cm^{-2}s^{-1}$
7. Position resolution at calorimeter Position resolution at muon system	~3 mm in z Not yet evaluated
8. Mass resolution of 300 GeV/c $H^\circ \rightarrow$ 4 leptons	~17 GeV/c^2
9. High luminosity performance	Initial SFTS (superlayers 2-6) acceptable up to luminosity ~ $5x10^{33}$ $cm^{-2}s^{-1}$. Staging (superlayers 1-6) needed for higher luminosity.

TABLE 9.4

Cost

Item	Comments
1. Number of straw-tube channels	106,200
2. Number of fiber channels	54,200
3. Number of support cylinders	5
4. Total cost plus contingency including all electronics	$38.5M
5. Total cost plus contingency without straw tube electronics	$28.7M
6. Total cost plus contingency without straw and fiber electronics	$24.3M
7. Average contingency	29%
8. Number of staged fiber channels	62,100

TABLE 9.5

Schedule, risk, feasibility issues

Item	Comments
1. Schedule	Comfortable
2. Feasibility – Support cylinders – Straw tubes – Scintillating fibers	 All proof-of-principle issues have been addressed Some critical R&D remains
3. Critical R&D – Mechanical – Straw tube – Fibers	 Precision and stability of detector elements Evaluation of compact low gain electronics modules Evaluation and choice of readout device
4. Risk items	Straw tube and fiber readout electronics
5. Impact on electronics	Fiber readout options; possibility of room temperature operation
6. Impact on calorimeter	Fiber readout same as for shower maximum detector
7. Impact on muon system	Modest access requirements for fiber electronics

10. References

1. Koltick, D., and D. Vandergriff, Scintillating Fiber Tracker Baseline Costing/Schedule and Construction Concepts, Purdue University, July 31, 1991.
2. Letter of Intent by the Solenoidal Detector Collaboration, SDC-90-00151, 30 November 1990.
3. Cental and Forward Tracking Collaboration Progress Report for FY1991, SDC-000104.
4. Hybrid Central Tracking Chamber Collaboration Progress Report for FY1991, September 1991.
5. Straw Tube Superlayer Design Concepts (SDC Tracker Review), May 20, 1991.
6. Williams, H., et al., SDC Straw Tracking Electronics, Preliminary Conceptual Design Report, October 31, 1991.
7. Blake, S., and J. Paulos, Front-End Electronics for the HCTC: Summary Report, North Carolina State University, August 1991.
8. Blocker, C., et al., Front End Electronics Development for SSC Detectors, UPR-0208E, pp. 92-96, September 15, 1991.
9. Paetroff & Staplebroek
10. Progress Report for the Trigger for a Fast Solenoidal SSC Detector, SSC Subsystem Report, Chicago and Michigan, October 1991.
11. Smith, W., et al., SDC Trigger Preliminary Conceptual Design, August 1991.
12. Chapman, J., and J. Mann, Triggering in the SDC Using Mean Timer Synchoronizers with Straw Drift Tubes, *Conference on Electronics for Future Colliders*, LeCroy Corporation, May 1991.
13. Kondo, T., SDC Task Force Report on the Effects of a Non-uniform Field, KEK, 1991.
14. Chapman, J., Drift Tube Synchronizers, University of Michigan Preprint, UM-IIE-89-10, June 1989.
15. Groom, D.E., Radiation Levels in SSC Detectors, SSC-201, January 1990.
16. Kross, B., S. Majewski, R. Wojcik, and C. Zorn, Results of Low Dose Rate Irradiation of Selected Plastic Scintillating Fibers, contained in Ref. 4.
17. Dunn, W.L, T.S. Elleman, A.T. Goshaw, S.H. Oh, W.J. Robertson, A. Grimes, I. Leedom, and S. Reucroft, Radiation Damage Studies of Straw Tube and Scintillating Fiber Elements, *Proc. Symp. Det. R&D for SSC*, pp. 669-71, Fort Worth, TX, October 15-18, 1990.

18. Zhou, B., D. Warner, J. Rohlf, D. Osborne, A. Marin, W.W. Lu, G. Hopkins, T. Coan, J. Beatty, and S. Ahlen, Performance of Small-Radius Thin-Wall Drift Tubes in an SSC Radiation Environment at the MIT Research Reactor, BUHEP-90-2, December 27, 1989.

Appendix A

BICRON FAX

TO: NORTHEASTERN UNIVERSITY, PHYSICS DEPARTMENT
ATTN: DR. S. REUCROFT
FROM: CHUCK HURLBUT
DATED: 29 AUGUST 1991

SUBJECT: FIBER RIBBON BUDGETARY PRICING

Steve,

Confirming our conversation of last evening, here are the budgetary estimates for the fiber ribbons that you requested.

DESCRIPTION:
Precision scintillating fiber ribbons consisting of two nested layers of parallel round fibers of diameters as stated below and four meters long. The fibers would be parallel and uniformly spaced at about 1.02 times the nominal fiber diameter. The second layer would lie in the valleys of the first.

Each ribbon would contain 1024 fibers, 512 per layer.

The fiber type quoted in the examples below is BCF-12 with an emission peak at 434 nm and a principal decay time of 3.4 ns.

Fiber location would be guaranteed to a precision of fifty microns or better referenced to one edge of the ribbon.

The ends of the fibers would be even and diamond milled flat and perpendicular to the fiber axes and ribbon plane to assure good optical coupling to optical waveguides. Both ends would be clamped in precision metal frames providing permanent positioning of the fiber ends and easy attachment and alignment to similar waveguide assemblies. The frames would be curved to match the curvature of the barrel frame over which the ribbons would be wound.

PRICING ESTIMATES:
The following prices apply to quantities of twenty arrays.

A. FIBER DIAMETER: 1.0 MM Unit Price: $5,300

The raw fiber is priced at 36 cents per meter.

B. FIBER DIAMETER: 1.5 MM Unit Price: $6,800

The raw fiber is priced as 69 cents per meter.

Charles R. Hurlbut

Appendix B

HYBRID TRACKING CHAMBER
PROJECT: C:\projsch\files\hyb

CURRENT DATE: 03/24/91
AS OF DATE: 03/04/91

Job#	WBS	OBS	Name
1	01	a	R&D
2	02		Conceptual Design
3	02.1		Cost Estimating
4	03	b	Detail Design
5	04	c	Procurement
6	05	d	Assembly
7	06		Test & Check Out
8	1.2	1	Central Tracker
9	1.2	a	Design & Fab - Straw/Fibe
11	1.2.1	1	SUPPORT STRUCTURE
12	1.2.1.1	1	Support Attachment
13	1.2.1.1	a	R&D
14	1.2.1.1	b	Design
15	1.2.1.1	c	Proc or Fab
16	1.2.1.1	d	Assy
17	1.2.1.2	1	Support Stringers
18	1.2.1.2	a	R&D
19	1.2.1.2	b	Design
20	1.2.1.2	c	Proc or Fab
21	1.2.1.2	d	Assy
22	1.2.1.3	1	Silicon Tracker Support
23	1.2.1.3	a	R&D
24	1.2.1.3	b	Design
25	1.2.1.3	c	Proc or Fab
26	1.2.1.3	d	Assy
27	1.2.1.4	1	Coil Attachment
28	1.2.1.4	a	R&D
29	1.2.1.4	b	DESIGN
30	1.2.1.4	c	PROC OR FAB
31	1.2.1.4	d	ASSY
32	1.2.1.5	1	Waveguide Support
33	1.2.1.5	a	R&D
34	1.2.1.5	b	DESIGN
35	1.2.1.5	c	PROC OR FAB
36	1.2.1.5	d	ASSY
37	1.2.1.6	1	Intermediate Tracker Supp
38	1.2.1.6	a	R&D
39	1.2.1.6	b	DESIGN
40	1.2.1.6	c	PROC OR FAB
41	1.2.1.6	d	ASSY
42	1.2.1.7	1	Final Assembly Tooling
43	1.2.1.7	a	R&D
44	1.2.1.7	b	DESIGN
45	1.2.1.7	c	PROC OR FAB
46	1.2.1.7	d	ASSY
47	[illegible].1.8	1	Support/Locating Fixtures

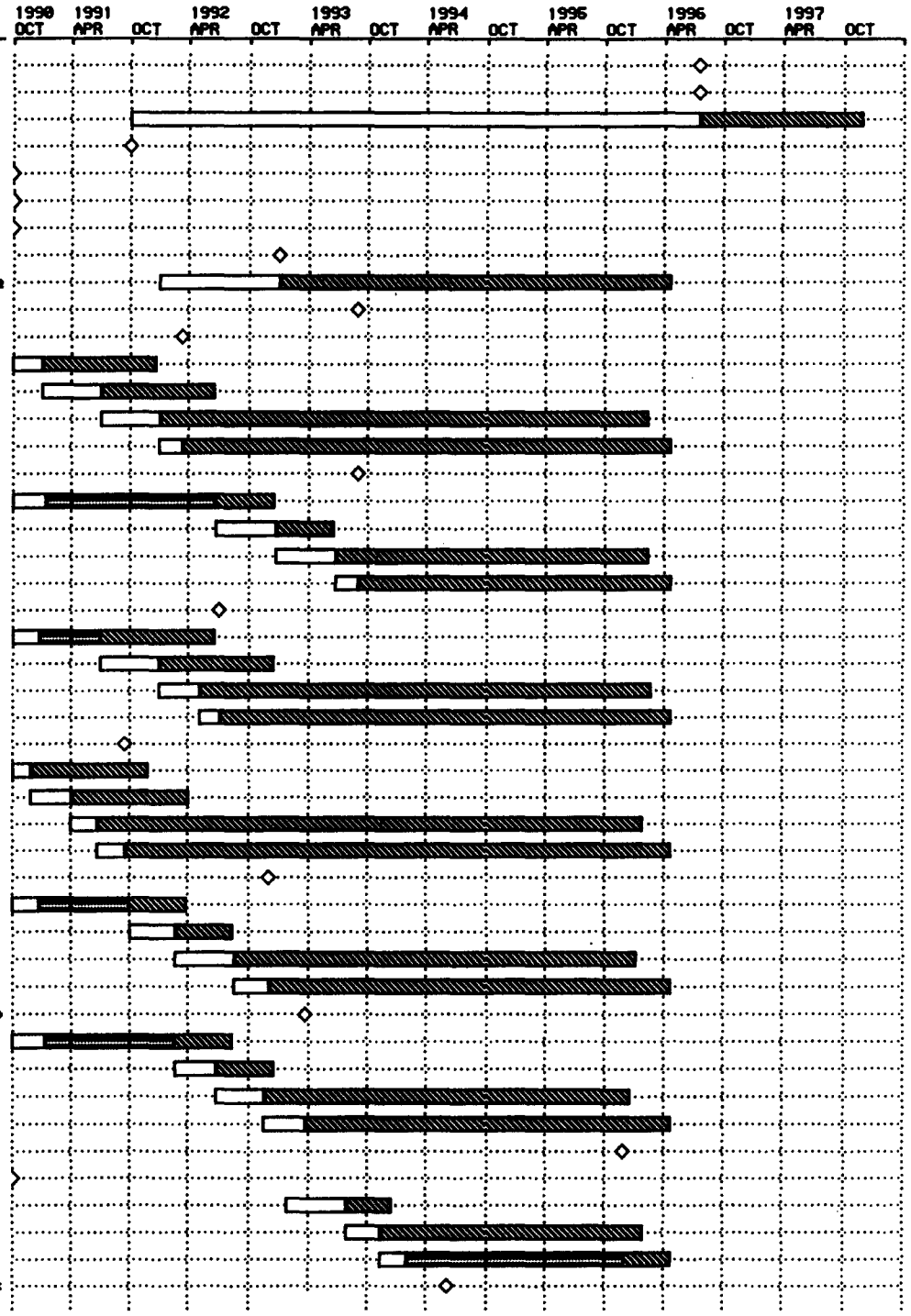

Job#	WBS	OBS	Name
48	1.2.1.8	a	R&D
49	1.2.1.8	b	DESIGN
50	1.2.1.8	c	PROC OR FAB
51	1.2.1.8	d	ASSY
52	1.2.1.9	1	Alignment Fixtures
53	1.2.1.9	a	R&D
54	1.2.1.9	b	DESIGN
55	1.2.1.9	c	PROC OR FAB
56	1.2.1.9	d	ASSY
57	1.2.1.10	1	Inspection/Test Equipment
58	1.2.1.10	a	R&D
59	1.2.1.10	b	DESIGN
60	1.2.1.10	c	PROC OR FAB
61	1.2.1.10	d	ASSY
62	1.2.2	1	STABLE BASE CYLINDERS
63	1.2.2	a	Prototype Alum. Composite
64	1.2.2.1	1	Straw Tube Cylinders
65	1.2.2.1	a	Prototype Carbon Cylinder
66	1.2.2.1	b	DESIGN
67	1.2.2.1	c	PROC OR FAB
68	1.2.2.1	d	ASSY
69	1.2.2.2	1	Scintillating Fiber Cylin
70	1.2.2.2	a	R&D
71	1.2.2.2	b	DESIGN
72	1.2.2.2	c	PROC OR FAB
73	1.2.2.2	d	ASSY
74	1.2.2.3	1	Cylinder Handling Fixture
75	1.2.2.3	a	R&D
76	1.2.2.3	b	DESIGN
77	1.2.2.3	c	PROC OR FAB
78	1.2.2.3	d	ASSY
79	1.2.3	1	STRAW TUBE SYSTEM
80	1.2.3	a	Straw Tube R&D
81	1.2.3	a.1	Resolution Test @SSC Rate
82	1.2.3	a.2	Mid-Termination of 6 M Tu
83	1.2.3	a.3	Install Straws on Cyl. Pr
84	1.2.3	a.4	Superlayer Assy and Test
85	1.2.3.1	1	End Plate Assy
86	1.2.3.1	a	R&D
87	1.2.3.1	b	DESIGN
88	1.2.3.1	c	PROC OR FAB
89	1.2.3.1	d	ASSY
90	1.2.3.1.1	1	Carbon End Ring
91	1.2.3.1.1	a	Prototype Carbon End Ring
92	1.2.3.1.1	b	DESIGN
93	1.2.3.1.1	c	PROC OR FAB

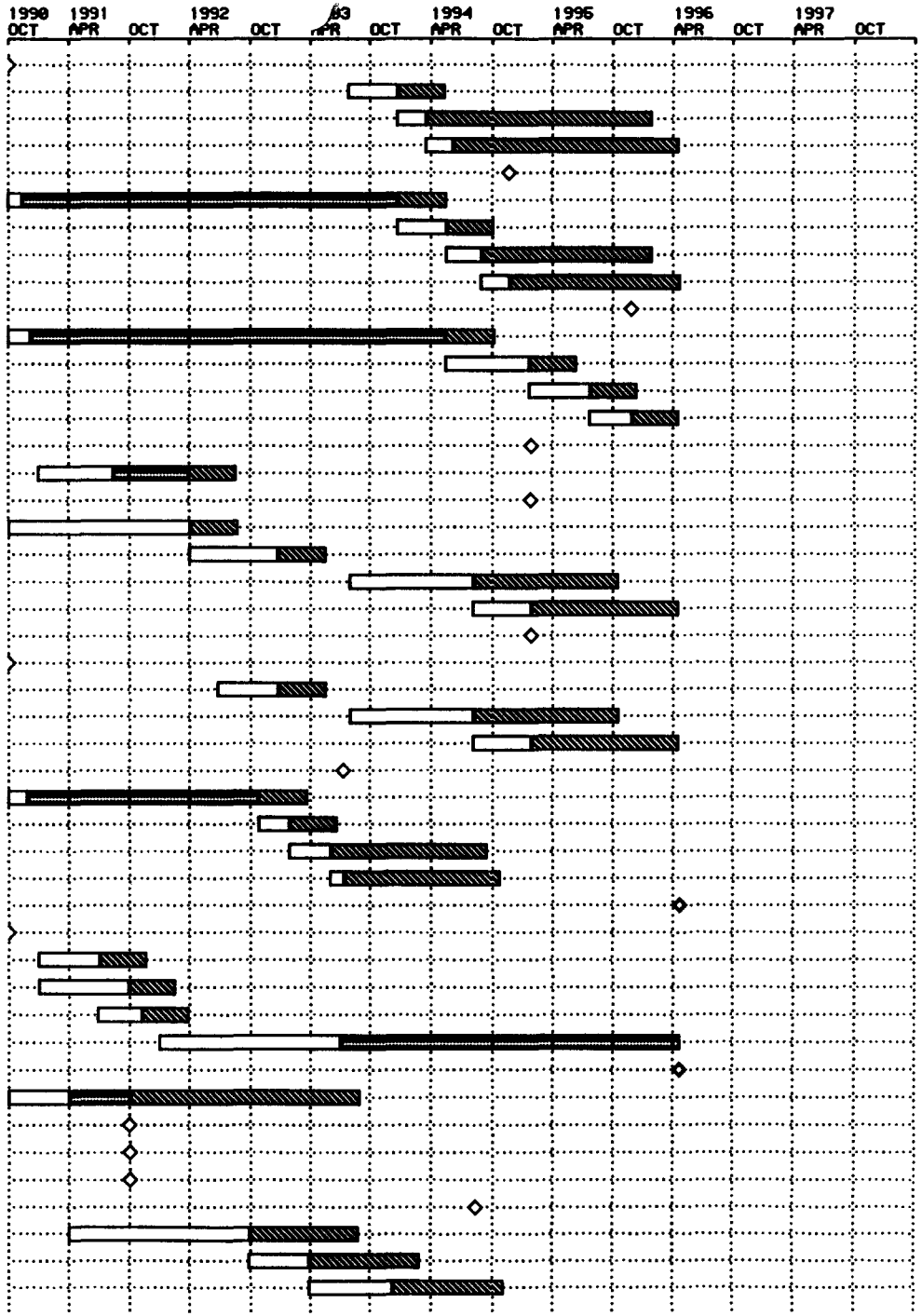

Job#	WBS	OBS	Name
94	1.2.3.1.1	d	ASSY
95	1.2.3.1.2	1	PC Board Attachment
96	1.2.3.1.2	a	R&D
97	1.2.3.1.2	b	DESIGN
98	1.2.3.1.2	c	PROC OR FAB
99	1.2.3.1.2	d	ASSY
100	1.2.3.1.3	1	Grounding
101	1.2.3.1.3	a	R&D
102	1.2.3.1.3	b	DESIGN
103	1.2.3.1.3	c	PROC OR FAB
104	1.2.3.1.3	d	ASSY
105	1.2.3.2	1	Straw Tube Assembly
106	1.2.3.2	a	R&D
107	1.2.3.2	b	DESIGN
108	1.2.3.2	c	PROC OR FAB
109	1.2.3.2	d	ASSY
110	1.2.3.2.2	1	Straw Tube Placement Tool
111	1.2.3.2.2	a	Prototype Tube Placing Ma
112	1.2.3.2.2	b	DESIGN
113	1.2.3.2.2	c	PROC OR FAB
114	1.2.3.2.2	d	ASSY
115	1.2.3.2.3	1	Wire Insertion Machine
116	1.2.3.2.3	a	R&D
117	1.2.3.2.3	b	DESIGN
118	1.2.3.2.3	c	PROC OR FAB
119	1.2.3.2.3	d	ASSY
120	1.2.4	1	SCINTILLATING FIBER SYSTE
121	1.2.4.1	1	End Plate
122	1.2.4.1	a	R&D
123	1.2.4.1	b	DESIGN
124	1.2.4.1	c	PROC OR FAB
125	1.2.4.1	d	ASSY
126	1.2.4.2	1	Solfi Electronics
127	1.2.4.2	a	R&D
128	1.2.4.2	b	DESIGN
129	1.2.4.2	c	PROC OR FAB
130	1.2.4.2	d	ASSY
131	1.2.4.3	1	Fibers
132	1.2.4.3	a	R&D
133	1.2.4.3	b	DESIGN
134	1.2.4.3	c	PROC OR FAB
135	1.2.4.3	d	ASSY
136	1.2.4.4	1	Ribbon Fabrication
137	1.2.4.4	a	R&D
1[illegible]	1.4	b	DESIGN
1[illegible]	1.4	c	PROC OR FAB

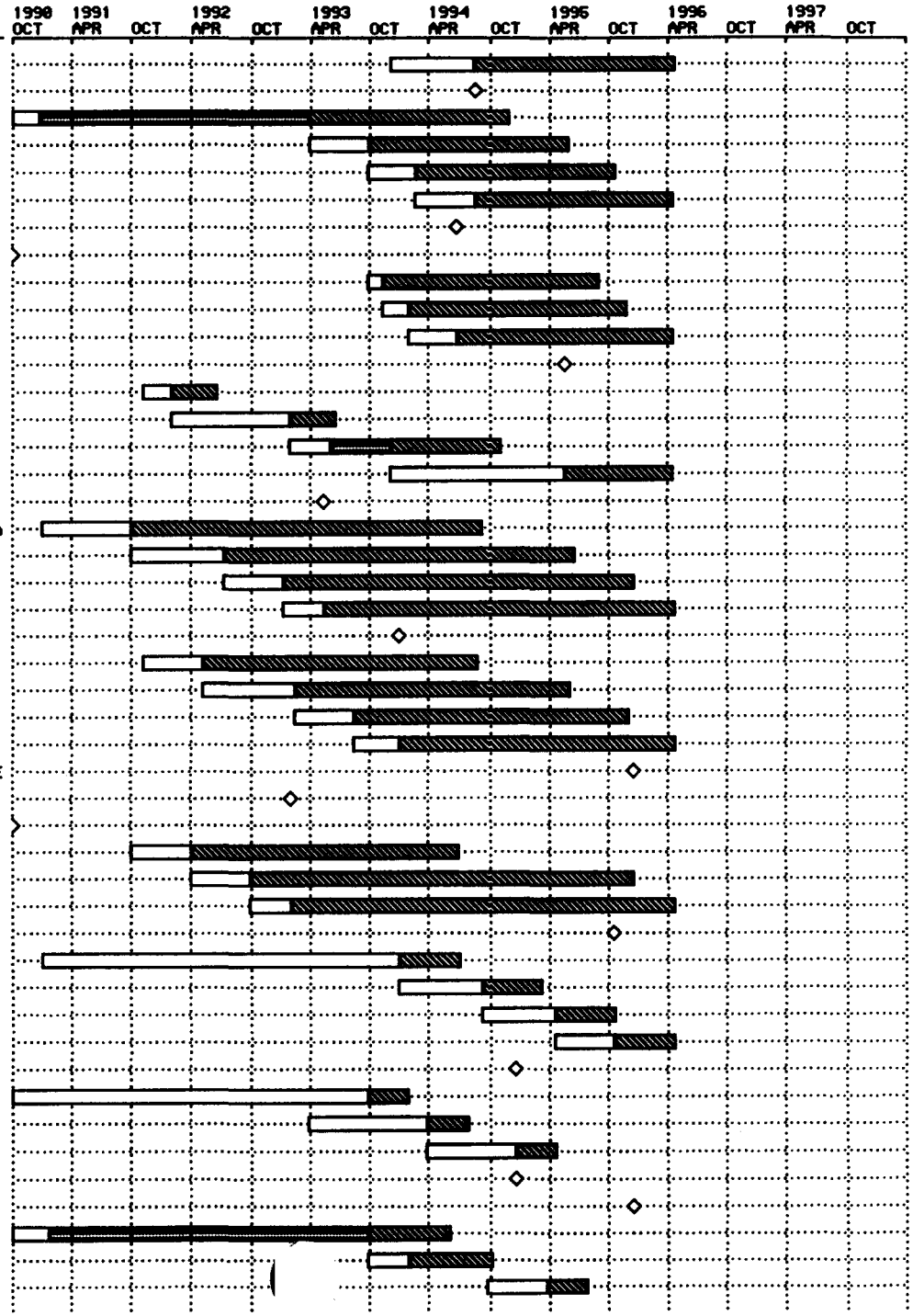

Job#	WBS	OBS	Name
140	1.2.4.4	d	ASSY
141	1.2.4.5	1	Fiber Placement Tooling
142	1.2.4.5	a	R&D
143	1.2.4.5	b	DESIGN
144	1.2.4.5	c	PROC OR FAB
145	1.2.4.5	d	ASSY
146	1.2.4.6	1	Light-Tight Shell
147	1.2.4.6	a	R&D
148	1.2.4.6	b	DESIGN
149	1.2.4.6	c	PROC OR FAB
150	1.2.4.6	d	ASSY
151	1.2.4.7	1	Light-Tight Bundle
152	1.2.4.7	a	R&D
153	1.2.4.7	b	DESIGN
154	1.2.4.7	c	PROC OR FAB
155	1.2.4.7	d	ASSY
156	1.2.4.8	1	Readout Assembly
157	1.2.4.8	a	R&D
158	1.2.4.8	b	DESIGN
159	1.2.4.8	c	PROC OR FAB
160	1.2.4.8	d	ASSY
161	1.2.4.8.2	1	Fiber Interface
162	1.2.4.8.2	a	R&D
163	1.2.4.8.2	b	DESIGN
164	1.2.4.8.2	c	PROC OR FAB
165	1.2.4.8.2	d	ASSY
166	1.2.4.8.3	1	Data Output Interface
167	1.2.4.8.3	a	R&D
168	1.2.4.8.3	b	DESIGN
169	1.2.4.8.3	c	PROC OR FAB
170	1.2.4.8.3	d	ASSY
171	1.2.4.8.4	1	Supports
172	1.2.4.8.4	a	R&D
173	1.2.4.8.4	b	DESIGN
174	1.2.4.8.4	c	PROC OR FAB
175	1.2.4.8.4	d	ASSY
176	1.2.4.9	1	SCIFI Utilities
177	1.2.4.9	a	R&D
178	1.2.4.9	b	DESIGN
179	1.2.4.9	c	PROC OR FAB
180	1.2.4.9	d	ASSY
181	1.2.4.91	1	Splicing
182	1.2.4.91	a	R&D
183	1.2.4.91	b	DESIGN
184	1.2.4.91	c	PROC OR FAB
185	1.2.4.91	d	ASSY

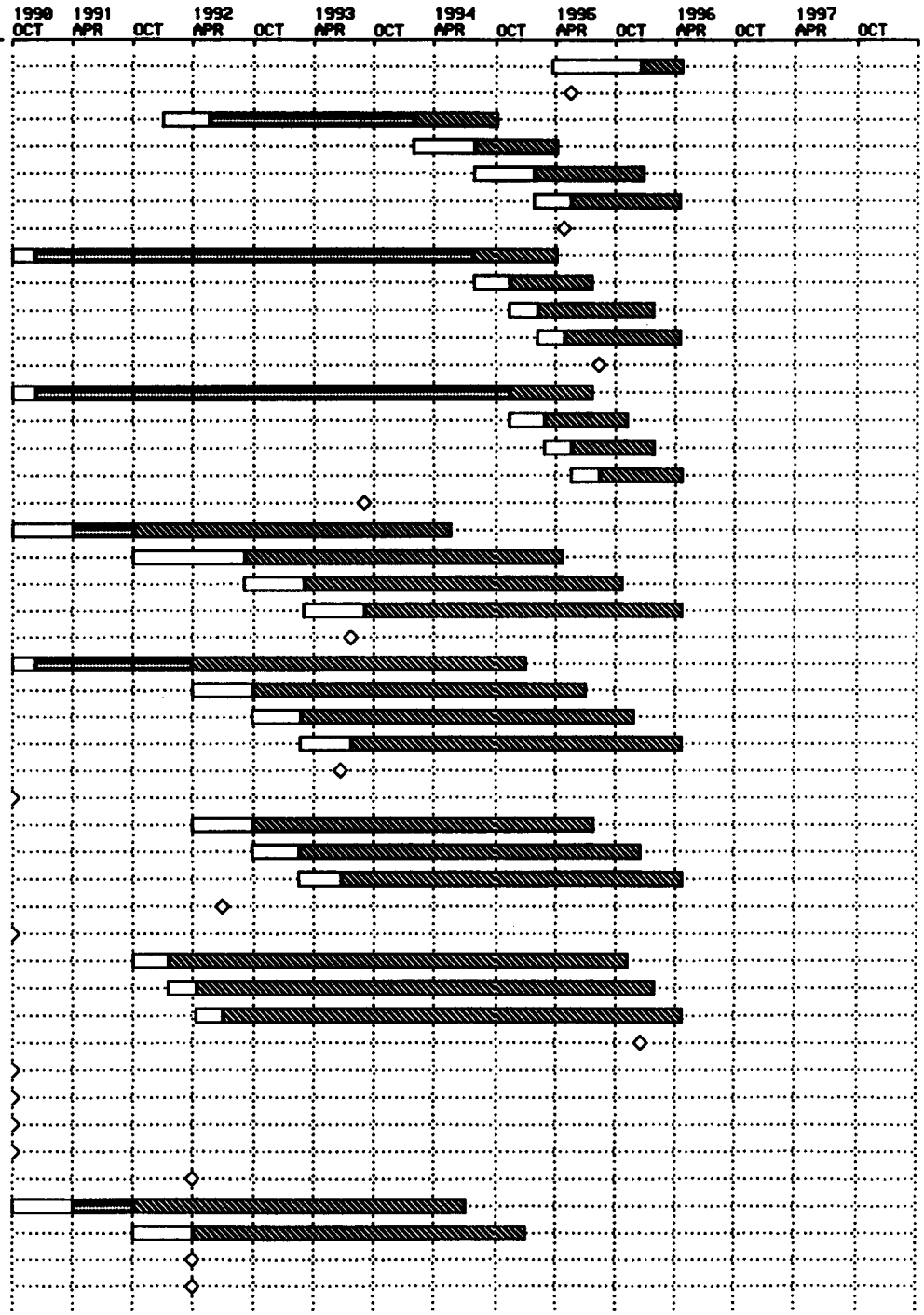

Job#	WBS	OBS	Name
186	1.2.5	1	COOLING ASSEMBLY
187	1.2.5	a	R&D
188	1.2.5	b	DESIGN
189	1.2.5	c	PROC OR FAB
190	1.2.5	d	ASSY
191	1.2.6	1	UTILITIES
192	1.2.6	a	R&D
193	1.2.6	b	DESIGN
194	1.2.6	c	PROC OR FAB
195	1.2.6	d	ASSY
196	1.2.6.1	1	Electronics Cooling Syste
197	1.2.6.1	a	R&D
198	1.2.6.1	b	DESIGN
199	1.2.6.1	c	PROC OR FAB
200	1.2.6.1	d	ASSY
201	1.2.6.2	1	Drift Gas Supply
202	1.2.6.2	a	R&D
203	1.2.6.2	b	DESIGN
204	1.2.6.2	c	PROC OR FAB
205	1.2.6.2	d	ASSY
206	1.2.6.3	1	Gas Leak Detection System
208	1.2.6.3	b	DESIGN
209	1.2.6.3	c	PROC OR FAB
210	1.2.6.3	d	ASSY
211	1.2.6.4	1	INERTING SYSTEM
213	1.2.6.4	b	DESIGN
214	1.2.6.4	c	PROC OR FAB
215	1.2.6.4	d	ASSY
216	1.2.7	1	FINAL FACTORY TESTING
217	1.2.7	a	R&D
218	1.2.7	b	DESIGN
219	1.2.7	c	PROC OR FAB
220	1.2.7	d	ASSY
221	1.2.7.1	1	Test Equipment
222	1.2.7.1	a	R&D
223	1.2.7.1	b	DESIGN
224	1.2.7.1	c	PROC OR FAB
225	1.2.7.1	d	ASSY
226	1.2.7.2	1	Tracker Functional Test
227	1.2.7.2	b	Functional Test Procedure
228	1.2.8	1	SHIP TO SITE
229	1.2.8.1	1	Shipping Support
230	1.2.8.1	b	DESIGN
231	[illegible].8.1	c	PROC OR FAB
23[illegible]	[illegible].1	d	ASSY
23[illegible]	[illegible].2	1	Shipping Containers

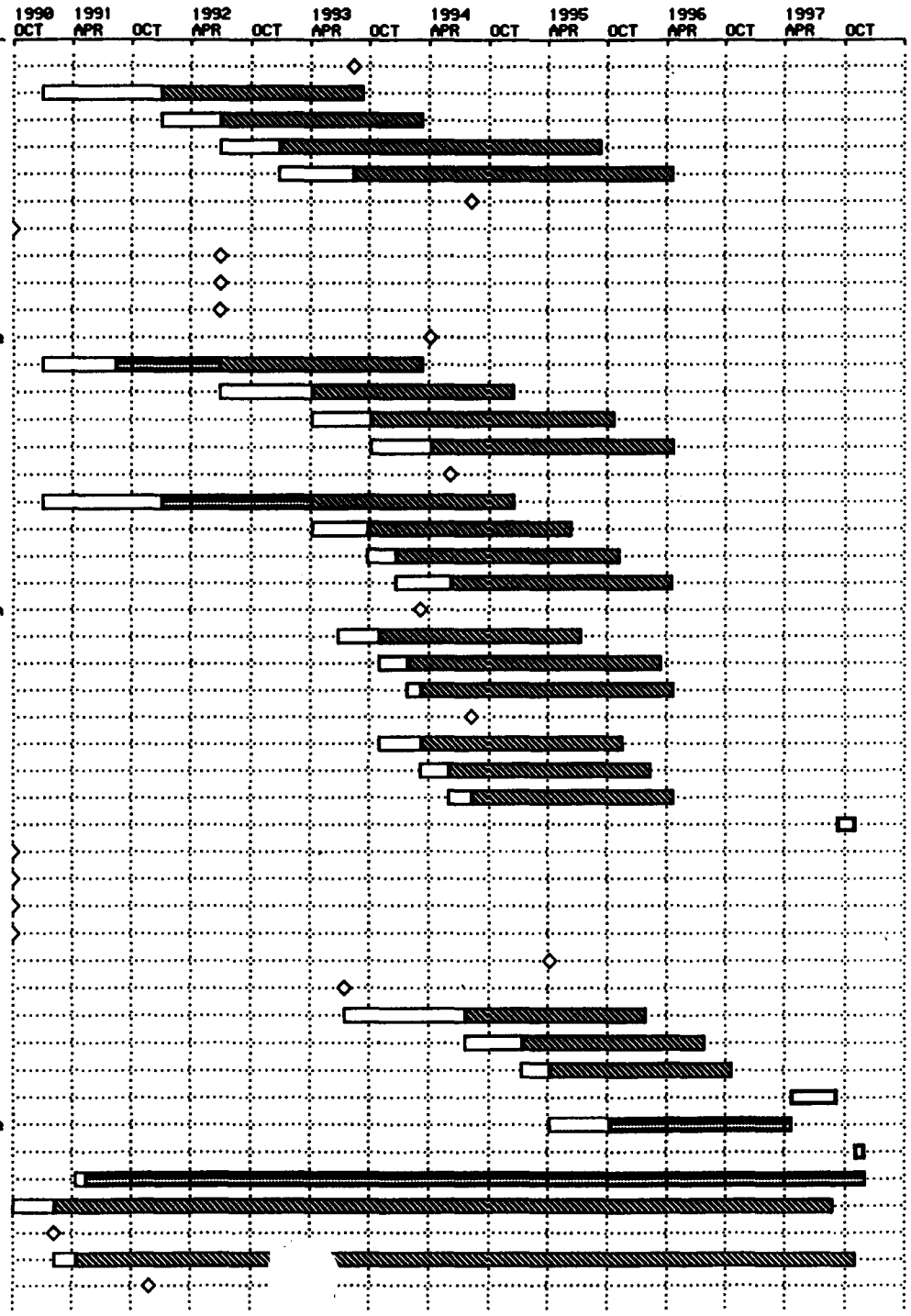

Job#	WBS	OBS	Name
234	1.2.8.2	a	R&D
235	1.2.8.2	b	DESIGN
236	1.2.8.2	c	PROC OR FAB
237	1.2.8.2	d	ASSY
238	1.2.8.3	1	Shipping Atmosphere Syste
239	1.2.8.3	a	R&D
240	1.2.8.3	b	DESIGN
241	1.2.8.3	c	PROC OR FAB
242	1.2.8.3	d	ASSY
243	1.2.9	1	Arrive at SSCL
244	1.2.9.1	1	Installation Tooling
245	1.2.9.1	a	R&D
246	1.2.9.1	b	DESIGN
247	1.2.9.1	c	PROC OR FAB
248	1.2.9.1	d	ASSY
249	1.2.9.2	1	Installation/Checkout Sup
250	1.2.9.2	a	R&D
251	1.2.9.2	b	DESIGN
252	1.2.9.2	c	PROC OR FAB
253	1.2.9.2	d	ASSY
254	1.2.a	1	WIRE ELECTRONICS ASSEMBLY
256	1.2.91	a.1	Test of Penn&KEK ASD/S-la
257	1.2.91	a.2	Test of TMC/TVC Chip
258	1.2.91	a.3	TMC/TVC & ASD Chip Evalua
259	1.2.91	a.4	Proto Fab and Test
260	1.2.91	a.5	LSI Proto Fab and Test
261	1.2.91	b	DESIGN
262	1.2.91	c	PROC OR FAB
263	1.2.91	d	ASSY
264	1.2.91.1	1	LV Supplies
265	1.2.91.1	a	R&D
266	1.2.91.1	b	LV Supplies Design
267	1.2.91.1	c	PROC OR FAB
268	1.2.91.1	d	ASSY
269	1.2.91.2	1	LV Distribution to Detect
270	1.2.91.2	a	R&D
271	1.2.91.2	b	LV Distribution Design
272	1.2.91.2	c	PROC OR FAB
273	1.2.91.2	d	ASSY
274	1.2.91.3	1	LV Distribution on Detect
275	1.2.91.3	a	R&D
276	1.2.91.3	b	LV Distribution Design
277	1.2.91.3	c	PROC OR FAB
278	1.2.91.3	d	ASSY
279	1.2.91.4	1	HV Supplies
280	1.2.91.4	a	R&D

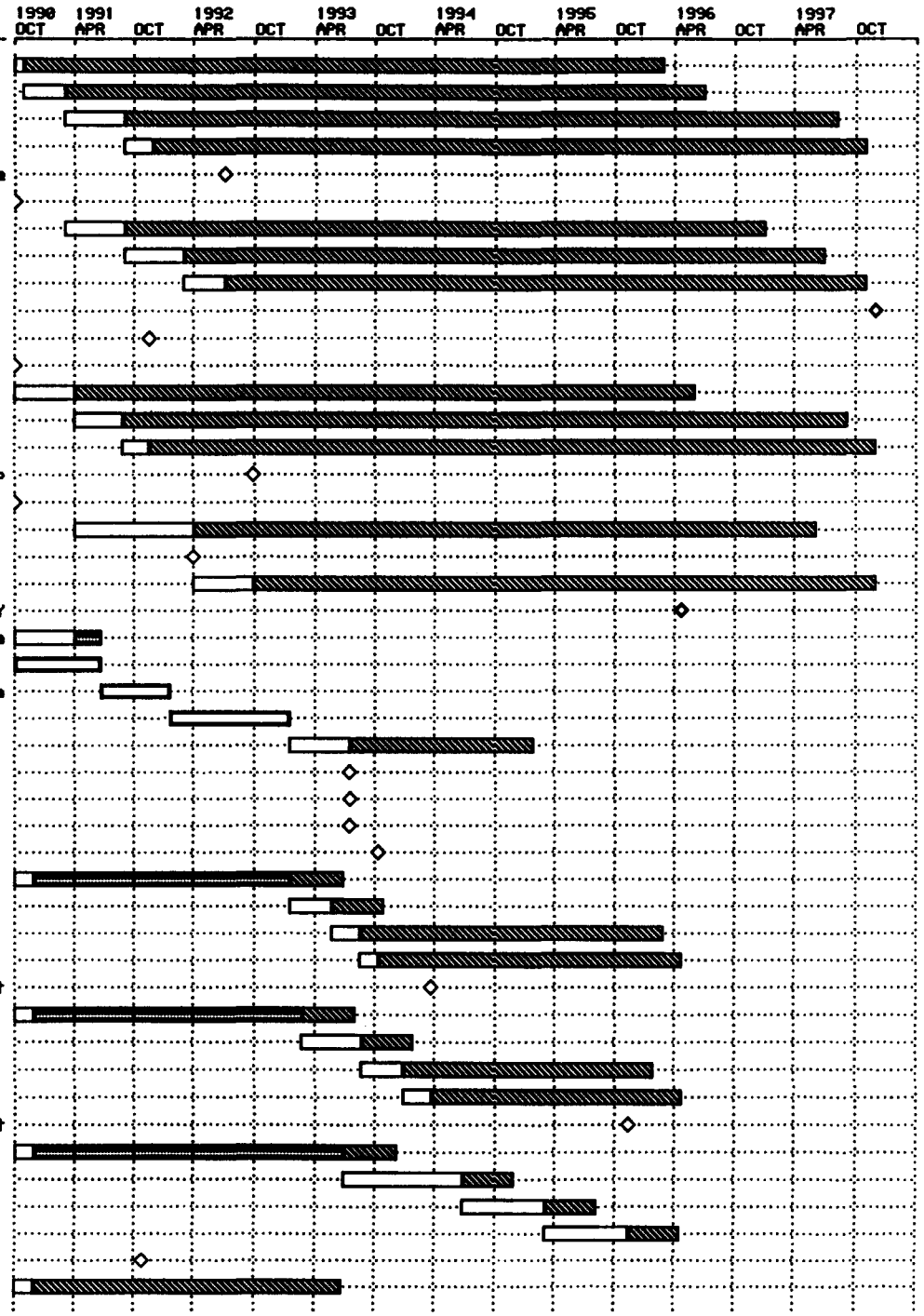
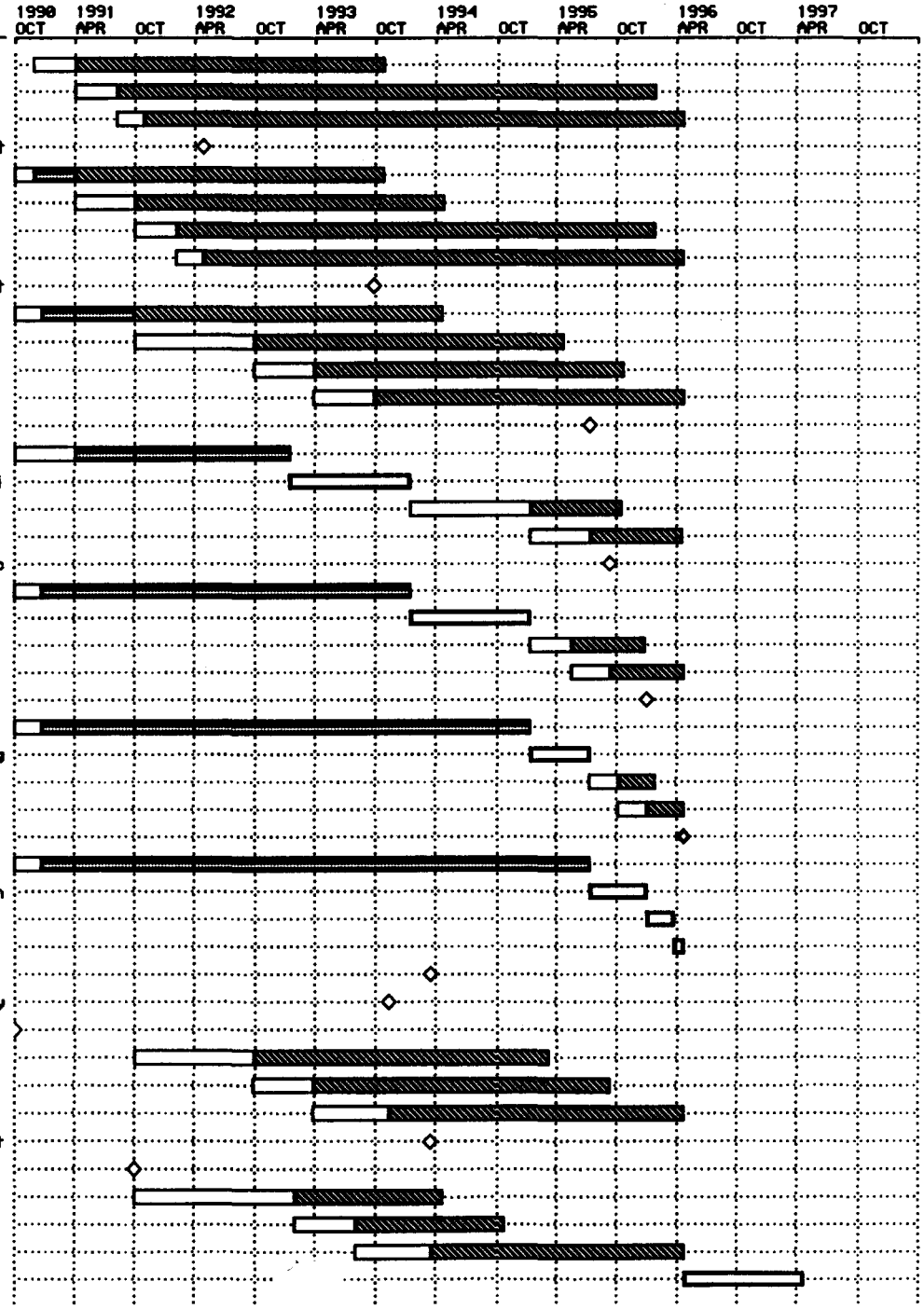
Job#	WBS	OBS	Name
281	1.2.91.4	b	HV Supplies Design
282	1.2.91.4	c	PROC OR FAB
283	1.2.91.4	d	ASSY
284	1.2.91.5	1	HV Distribution to Detect
285	1.2.91.5	a	R&D
286	1.2.91.5	b	HV Distribution Design
287	1.2.91.5	c	PROC OR FAB
288	1.2.91.5	d	ASSY
289	1.2.91.6	1	HV Distribution on Detect
290	1.2.91.6	a	R&D
291	1.2.91.6	b	DESIGN
292	1.2.91.6	c	PROC OR FAB
293	1.2.91.6	d	ASSY
294	1.2.91.7	1	Front End Electronics
295	1.2.91.7	a	R&D
296	1.2.91.7	b	Front End Electronic Desi
297	1.2.91.7	c	PROC OR FAB
298	1.2.91.7	d	ASSY
299	1.2.91.8	1	Data Acquisition Interfac
300	1.2.91.8	a	R&D
301	1.2.91.8	b	DAQ Design
302	1.2.91.8	c	PROC OR FAB
303	1.2.91.8	d	ASSY
304	1.2.91.9	1	Trigger Signal Interface
305	1.2.91.9	a	R&D
306	1.2.91.9	b	Trigger Signal Int. Desig
307	1.2.91.9	c	PROC OR FAB
308	1.2.91.9	d	ASSY
309	1.2.91.91	1	Calibration System
310	1.2.91.91	a	R&D
311	1.2.91.91	b	Calibration System Design
312	1.2.91.91	c	PROC OR FAB
313	1.2.91.91	d	ASSY
314	1.2.11	1	FACILITIES
315	1.2.11.1	1	Support Assembly Facility
316	1.2.11.1	a	R&D
317	1.2.11.1	b	DESIGN
318	1.2.11.1	c	PROC OR FAB
319	1.2.11.1	d	ASSY
320	1.2.11.2	1	Cylinder Assembly Facilit
321	1.2.11.2	a	R&D
322	1.2.11.2	b	DESIGN
323	1.2.11.2	c	PROC OR FAB
324	1 2.11.2	d	Assembly
32		1	FINAL ASSEMBLY